Characterization of Atmospheric Aerosols over the Southern Ocean and Coastal East
Antarctica

by

Guojie Xu

A Dissertation submitted to the

Graduate School - Newark

Rutgers, The State University of New Jersey

in partial fulfillment of the requirements

for the degree of

Doctor of Philosophy

Graduate Program in

Environmental Science

Written under the direction of

Dr. Yuan Gao

and approved by

_____

_____

_____

_____

Newark, New Jersey

January 2015

ABSTRACT OF THE DISSERTATION

Characterization of Atmospheric Aerosols over the Southern Ocean and Coastal East
Antarctica

By Guojie Xu

Dissertation Director:

Dr. Yuan Gao

Marine aerosols can directly and indirectly influence climate. To characterize the

chemical and physical properties of marine aerosols over the Southern Ocean and coastal

Antarctica, bulk and size-segregated aerosol samples were collected during a cruise from

November 2010 to March 2011. Results showed that sea salt was the major component of

the aerosol mass, accounting for 72% over the Southern Ocean and 56% over coastal East

Antarctica. Aerosol mass had a bimodal size distribution over coastal East Antarctica,

peaking at 0.32-0.56 μm and 3.2-5.6 μm, respectively. nss-SO_4^{2-}, MSA and oxalate were

mainly enriched in the fine mode, contributing to chloride depletion. Na, Mg and K were

accumulated in the coarse mode, and Al, Fe and Mn displayed a bimodal size

distribution. Based on particle-size distributions, enrichment factors and correlation

analysis, Na, Mg and K mainly came from the marine source, while Al, Fe and Mn were

contributed by the crustal source. High enrichment factors were associated with Ni, Cd

and Se, indicating mixed sources from the Antarctic continent, long-range transport,

marine biogenic emissions and anthropogenic emissions.

As a comparison, aerosols collected over Asian marginal seas, South Indian Ocean and Australian coast during the same cruise showed that sea salt and nss-SO_4^{2-} were the main components in aerosols. MSA concentrations and MSA/nss-SO_4^{2-} ratios increased southward. Sea salt and NO_3^- were accumulated in the coarse mode, while nss-SO_4^{2-} and NH_4^+ mainly peaked in the fine mode. Oxalate displayed a bimodal size distribution in both fine and coarse modes. A good relationship was found between total dissolved iron and nss-SO_4^{2-}, indicating that acid processing during long-range transport could affect fractional iron solubility in aerosols.

Results from this study fill in the data gap and serve for better understanding aerosols over the Southern Ocean and coastal Antarctic regions. Aerosol chemical composition and size distributions obtained from this study in these regions can be used to improve atmospheric model simulations, better interpret ocean biogeochemical cycles and evaluate aerosols' climate effects.

ACKNOWLEDGEMENTS

assistance and the friendship.

Finally, I am indebted to my parents for their love and constant support during this journey. I would also like to thank all my friends for their encouragement and support.

TABLE OF CONTENTS

LIST OF TABLES

LIST OF FIGURES

Chapter 1: Introduction

1.1 Overview

Marine aerosols play an important role in global climate change, both directly and indirectly, with the oceans covering more than 70% of the earth's surface [*Anttila and Kerminen*, 2002; *Fitzgerald*, 1991; *Murphy et al.*, 1998; *Myriokefalitakis et al.*, 2011; *D O'Dowd and de Leeuw*, 2007; *Yum et al.*, 1998]. Chemical compositions and size distributions are important properties of marine aerosols, affecting their transport, transformation, removal and extent of aerosol radiative forcing [*Cruz and Pandis*, 1997; *Fu et al.*, 2011; *Lapina et al.*, 2011; *Ovadnevaite et al.*, 2011; *Saxena et al.*, 1995; *Seinfeld and Pandis*, 2006; *Vallina et al.*, 2006; *Whitby*, 1978]. Marine aerosols are made up of a variety of individual species, including water-soluble inorganic and organic species, such as sea salt, sulfate, MSA and oxalate etc. and trace elements, such as Al, Fe, Zn etc. The concentrations and size distributions properties of these species in the atmosphere are of great importance.

First, water-soluble inorganic aerosol species, such as sea salt and sulfate aerosols are the two dominant inorganic aerosol components in the marine atmosphere [*Bates et al.*, 2008; *Read et al.*, 2008; *Rempillo et al.*, 2011; *Yang et al.*, 2011]. Other water-soluble inorganic aerosol species include nitrate, which is mainly formed by the reaction of HNO_3 with sea-salt particles over remote oceans and predominately accumulated in the aerosol coarse fraction [*Andreae et al.*, 1999; *Koçak et al.*, 2007; *Zhuang et al.*, 1999]. Ammonium (NH_4^+) is also an important inorganic aerosol compound affecting the acidity of the marine atmosphere, which is a secondary product of NH_3 through gas-phase and

aqueous-phase reactions with acidic species (e.g., H_2SO_4) [*Zhang et al.*, 2008].

Second, besides inorganic aerosol species, marine aerosols also contain a variety of water- soluble organic compounds (WSOCs). Among these organic species, methane sulfonate (MSA) is a species known to be mainly produced by the oxidation of dimethylsulfide (DMS) from marine phytoplankton, and thus MSA has been proposed as a tracer of marine biogenic production to separate sulfate of marine biogenic origin from other sources [*Bates et al.*, 2001; *Davis et al.*, 1999; *Legrand et al.*, 1991; *Minikin et al.*, 1998; *Read et al.*, 2008]. Other water-soluble organic species include a group of carboxylic acids, mainly monocarboxylic acids (formic (C1) and acetic (C2)) and dicarboxylic acids (oxalic (C2), malonic (C3), and succinic (C4)) [*Abbatt et al.*, 2005; *Kawamura et al.*, 1996a; *Vallina et al.*, 2006; *Wang et al.*, 2010]. Oxalic acid ($H_2C_2O_4$) is the most abundant dicarboxylic acid associated with tropospheric aerosols [*Kerminen et al.*, 1999], with its concentration being about a few ng m^{-3} over remote oceans [*Kerminen et al.*, 1999; *Warneck*, 2003]. Since these organic acidic aerosol species are highly water-soluble, they can modify the hygroscopic properties of aerosol particles in the marine atmosphere [*Hara et al.*, 2002; *Yu*, 2000].

Third, trace elements are the important aerosol species over many oceanic regions, which is also an important contributor to deep-sea sediments [*Hesse*, 1994; *Rea*, 1994]. The aerosol particles are produced from multi-sources, i.e., natural sources, such as rock, soil dusts and ocean primary emissions through bubble bursting processes or anthropogenic activities, such as human activities on Antarctic scientific stations, fossil fuel

combustions, ship emissions and even long range transport from Northern Hemisphere. Therefore, several trace elements distribution characteristics in aerosols may represent the anthropogenic impacts on the Antarctic atmosphere. On the other side, in the mineral dust, iron is believed to be a limiting micronutrient over many remote oceanic regions [*de, Baar et al.*, 1995; *Jickells et al.*, 2005]. The concentrations of the total Fe and its interactions with acidic aerosol species including S-containing species have been suggested to affect Fe solubility [*Sholkovitz et al.*, 2012; *Gao et al., 2013*], in particular in the marine atmosphere affected by anthropogenic emissions [*Baker and Croot*, 2010; Hsu et al., 2010; Buck et al., 2013]; Other elements associated with dust could also play an important role in the biogeochemistry of the oceans. It is widely documented that transition trace metals, such as Mn, Co, Zn, Cu, and Ni are essential nutrients to marine biota [*Bruland et al.*, 1991; *Butler*, 1998; *Whitfield*, 2001], which also mean bioactive elements. In the remote oceans, particularly in the high nutrient, low-chlorophyll (HNLC) areas of the open oceans, atmospheric depositions are a vital source of bioavailable Fe and bring about biological stimulation [*Bishop et al.*, 2002; *Jickells et al.*, 2005]. Recent field measurements have shown that the enhancement in nitrogen fixation and biological blooms in the remote oceans corresponds to the episodic supply by atmospheric deposition [*Baker et al.*, 2003; *Yuan and Zhang*, 2006].

Chemical compositions and size distributions of aerosol water soluble compounds and their role as CCN during the cloud formation processes over remote ocean areas remain unclear, especially the water-soluble organic compounds are still poorly understood; Information on aerosol trace elements components over the Southern Ocean and coastal

East Antarctica is very important for better understanding of biogeochemical cycles in these regions, however, it has not been in investigated simultaneously yet; Chemical composition, size distributions and iron solubility of marine aerosols and precipitation over Asian marginal seas, South Indian Ocean and Australian coast remain limited. The purpose of this study is to fill in theses gaps and to better understand the characteristics of aerosols over the remote and coastal oceanic regions. The results can be used to assist scientists to evaluate the model results compared with field observation results and then to improve atmospheric model simulations.

1.2 Research Objectives

The primary goal of this thesis is to quantify the chemical and physical properties of atmospheric aerosol over remote and costal oceanic regions. Within this content, several specific objectives are listed as follows:

(1) Quantify the mass and chemical concentrations, size distributions and spatial distributions of water-soluble inorganic and organic species, evaluate the possible sources for these species;

(2) Quantify the chemical concentrations, size distributions and spatial distributions of trace elements, explore their possible sources and implicate their potential for phytoplankton utilization;

(3) Quantify the chemical concentrations, size distributions, spatial distributions and iron solubility of marine aerosols and precipitation over Asian marginal seas, South Indian Ocean and Australian coast.

Chapter 2: Characteristics of Water-Soluble Inorganic and Organic Ions in Aerosols over the Southern Ocean and Coastal East Antarctica during Austral Summer[1]

Abstract

To characterize the concentrations and size distributions of water-soluble organic and inorganic aerosol species, including Na^+, non-sea-salt sulfate ($nss\text{-}SO_4^{2-}$), methane sulfonate (MSA), oxalate and succinate, over the Southern Ocean (SO) and coastal East Antarctica (CEA), bulk and size-segregated aerosols were collected from 40°S, 100°E to 69°S, 76°E and between 69°S, 76°E and 66°S, 110°E during a cruise from November 2010 to March 2011. Results show that sea salt was the major component of the total aerosol mass, accounting for 72% over the SO and 56% over CEA. The average concentrations of $nss\text{-}SO_4^{2-}$ varied from 420 ng m^{-3} over the SO to 480 ng m^{-3} over CEA. The concentrations of MSA ranged from 63 to 87 ng m^{-3} over the SO and from 46 to 170 ng m^{-3} in CEA. The average concentrations of oxalate were 3.8ng m^{-3} over the SO and 2.2ng m^{-3} over CEA. The concentrations of formate, acetate, and succinate were lower than those of oxalate. A bimodal size distribution of aerosol mass existed over CEA, peaking at 0.32-0.56 μm and 3.2-5.6 μm. MSA was accumulated in particles of 0.32-0.56 μm over CEA. High chloride depletion was associated with fine-mode particles enriched with $nss\text{-}SO_4^{2-}$, MSA and oxalate. Higher cation-to-anion and $NH_4^+/nss\text{-}SO_4^{2-}$ ratios in

aerosols over CEA compared to that over the SO imply the higher neutralization capacity of the marine atmosphere over CEA.

Keywords: Water-Soluble ions; Southern Ocean; Coastal East Antarctica; Size distribution; Sources.

2.1 Introduction

Marine aerosols play an important role in global climate change, both directly and indirectly [*O'Dowd and de Leeuw*, 2007]. Chemical composition and size distributions are important properties of marine aerosols, affecting their transport, transformation, removal and extent of aerosol radiative forcing [*Seinfeld and Pandis*, 2006]. Water soluble aerosol species, particularly those in the fine mode, could be an important source of cloud condensation nuclei (CCN) (size range 0.04-0.3 μm), affecting cloud microphysics and consequently climate [*Ayers and Gras*, 1991; *Liss and Lovelock*, 2007]. However, the information on certain aerosol species and their climate effects is limited in several under-sampled oceanic regions, such as the Southern Ocean, due to the difficulties in conducting field measurements.

The Southern Ocean plays an important role in global carbon cycles and thus climate change [*Sarmiento et al.*, 1998]. Previous studies showed the importance of CCN and sulfur-containing species over the Southern Ocean, which interact with incoming solar radiation and affect cloud albedo, impacting the Southern Ocean biogeochemistry cycle [*Ayers and Gras*, 1991; *Liss and Lovelock*, 2007]. Significant progress in characterization

of aerosols and trace gases over the Antarctica was made through several large field measurements, including: The Sulfur Chemistry in the Antarctic Troposphere Experiment [*Berresheim and Eisele*, 1998; *Minikin et al.*, 1998], Investigation of Sulfur Chemistry in the Antarctic Troposphere (ISCAT) [*Arimoto et al.*, 2001; *Davis et al.*, 2004], and Antarctic Tropospheric Chemistry Investigation (ANTCI) [*Arimoto et al.*, 2008; *Eisele et al.*, 2008]. Measurements of sulfur aerosols were also conducted at several coastal Antarctic stations, Dumont d'Urville (66.7^{o}S, 140°E) [*Legrand et al.*, 1998], Mawson (67.6^{o}S, 62.5^{o}E) [*Savoie et al.*, 1992] and Neumayer (70.7°S, 8.3^{o}W) [*Savoie et al.*, 1993; *Wagenbach*, 1996; *Wolff et al.*, 1998]. However, few efforts have been made to study water-soluble organic compounds (WSOCs) in aerosols over the Southern Ocean and coastal Antarctica. The properties of these aerosol species, in particular the mass-size distributions and their relationships with other aerosol species, are largely unknown in these regions.

To characterize water-soluble inorganic and organic species over the Southern Ocean and coastal East Antarctica, shipboard aerosol measurements were conducted in the regions between November, 2010 and March, 2011. In this paper, we report the new results from this shipboard experiment on the concentration distributions of ten water soluble inorganic and organic species in aerosols and their particle size distributions. Possible sources and factors affecting their properties are discussed. We also explore the potential implications of the observed aerosol properties for chlorine depletion in aerosols and cloud formation. We hope that our results from this work may fill the gaps of and enrich the database for the Southern Ocean and coastal Antarctica. The new data set can also be

used to improve and test the parameterizations of aerosol properties used in global climate models.

2.2 Methods and Materials

2.2.1 Sampling

Shipboard sampling was carried out on the Chinese icebreaker, R/V Xuelong, during the cruise from November 2010 to March 2011. Aerosol sample collections were made in the Southern Ocean on the legs between Fremantle, Australia (32^oS, 115^oE) and the Chinese Zhongshan Station (69°22'S, 76°22'E) in East Antarctica (Figure 2.1). Aerosol sampling was also made on the legs between the Chinese Zhongshan Station and the Australian Casey Station (66^o17'S, 110^o32'E). In this study, the Southern Ocean is defined as the region between 40^oS and 65^oS, and coastal East Antarctica is defined as the region between 65^oS-69^oS; the data discussions in Section 3 were based on two distinct sets of results from these two regions. This treatment of data was decided for two reasons. One reason was that the air mass origins and wind patterns in the Southern Ocean and coastal East Antarctica were different. The origins of air masses affecting samples collected over the Southern Ocean were mainly originated over the Southern Ocean based on 7-day air mass back trajectories, while samples collected in coastal East Antarctica were mainly impacted by air masses from the Antarctic continent. This feature was also seen by wind patterns: the Southern Ocean was under westerly winds, but coastal East Antarctica was largely effected by Katabatic winds down the slopes of the Antarctic continent. Another reason was that the extent of sea ice coverage was different in these two regions that may impact marine primary productivity [*Nicol et al.*, 2000; *Smith and Comiso*, 2008],

consequently affecting the production of marine biogenic aerosols. In austral summer, large areas between 40°S and 65°S were ice-free, while the region of 65°S-69°S was often covered with pack ice and experienced substantial sea ice melting, and higher emissions of dimethyl sulfide (DMS) from seawater were observed in the coastal Antarctic sea ice zone compared with those in the Southern Ocean [*Trevena and Jones*, 2006].

Air samplers were installed on a 3×6 m^2 platform on the ship's 8th floor front deck about 25 meters above the sea surface. To attain size-segregated aerosol samples, two aerosol sizing samplers were used. One was a High-Volume (H-V) cascade impactor (CI) for sampling in the Southern Ocean, with a flow rate of $\sim$1m^3 min^{-1} (Graseby, Smyrna, GA) and Whatman 41 cellulose filters (Whatman International Ltd., England) as the sampling media based on the procedures by *Gao* [2002]. The sampling duration with the CI sampler was $\sim$ 4 days. The aerodynamic diameter cutoff sizes of the CI sampler were 0.49, 0.95, 1.5, 3.0, and 7.2 μm. In this study, the particle size 1.5 μm was used as a cutoff size to separate the fine and coarse mode particles for this sampler. Another sampler was a 10-stage micro-orifice uniform deposit impactor (MOUDI, MSP Corp., Shoreview, MN) with a flow rate of 30 L min^{-1} and sampling duration of $\sim$4 days, which was used for sampling in coastal East Antarctica. Teflon filters (Pall Corp., 47mm diameter, 1.0 μm pore size) were used as sampling substrates for MOUDI. The 50% cut-off sizes of the MOUDI were 0.056, 0.10, 0.18, 0.32, 0.56, 1.0, 1.8, 3.2, 5.6, 10 and 18 μm in aerodynamic diameter. The particle size 1.8 μm was used as a cutoff size to separate the fine and coarse fractions for MOUDI samples [*Zhao and Gao*, 2008a]. Bulk aerosols or total suspended particles (TSP) were collected on Whatman-41 filters by a

High-Volume sampler (Aquaero Tech, Miami, FL) for aerosol composition, which operated with a flow rate of ~1 m^3 min^{-1} and sampling duration of ~ 2 days [*Xia and Gao*, 2010]. A Low-Volume (L-V) ChemComb cartridge (Thermo Scientific, MA, USA) was used to collect bulk aerosol particles for aerosol mass determination, which operated at a flow rate of 15 L min^{-1}, with sampling duration of ~48-72 hours and Teflon filters as sampling media (Pall Corp., 47mm diameter, 1.0 μm). To avoid contamination from the ship, all sampling instruments were controlled with a wind speed and direction system installed on the same sampling platform, which operated sampling only when the wind was from a sector 90° left and right on the center line of the ship's path and at wind velocities > 2 m s^{-1}.

During sampling, loading and unloading of the filters were conducted in a 100-class laminar flow clean-room hood in the ship's chemical laboratory, following clean-room operation procedures. After sampling, sample filters with field blanks were stored in the refrigerator at 4°C aboard the R/V XueLong. A total of 17 H-V bulk aerosol samples, 17 L-V bulk aerosol samples, 4 H-V CI samples, and 2 MOUDI samples were collected during this cruise. Detailed sampling information is given in Table 2.1. For aerosol gravimetric mass, teflon sample filters from the L-V ChemComb cartridge and MOUDI were pre- and post-weighed by a microbalance (Model MT-5, Metter Toledo) in a weighing chamber where relative humidity and temperature were kept at 32% and 20°C, respectively, at Rutgers University [*Song and Gao*, 2011].

2.2.2 Chemical Analyses

 A Dionex ICS-2500 ion chromatograph (IC) was used to analyze aerosol samples for water soluble ions (Na^+, NH_4^+, acetate, formate, MSA, Cl^-, NO_3^-, succinate, SO_4^{2-}, oxalate). The cations were analyzed with a CS12A analytical column and a CG12A guard column, and the anions were analyzed with an AS18 analytical column and an AG18 guard column. Experimental methods, similar to *Zhao and Gao* [2008a], were as follows: a portion of each filter was placed in 15 mL of deionized water, ultrasonicated for 40 minutes and leached overnight. Then the sample solutions were injected into the IC system through 0.22 μm filters. The detection limits were 0.40 ng m^{-3} for chloride, 0.13 ng m^{-3} for sulfate, and 0.29 ng m^{-3} for nitrate for H-V samples. The detection limits for water soluble organic species in H-V samples were 0.02 ng m^{-3} for acetate, 0.029 ng m^{-3} for formate, 0.13 ng m^{-3} for succinate, 0.095 ng m^{-3} for oxalate, and 0.016 ng m^{-3} for MSA. The concentrations of these organic species in H-V samples were 47-82% higher than their blank values, and their concentrations in H-V CI samples were from 70% to >100% higher than their blank values. The concentrations of these organics in MOUDI samples were from 60% to >100% higher than the values in their blanks. Final concentrations of these species were obtained after correction with field blanks, and their standard deviations were below 0.001. The precision of the analytical procedures based on seven spiked samples was <5%.

2.2.3 Data Analysis

In this study, sea salt aerosol concentrations were calculated using the equation: Sea salt = Cl^- +1.47×Na^+, where 1.47 is the mass ratio of (Na^+ + K^+ + Mg^{2+} + Ca^{2+} + SO_4^{2-} + HCO_3^-) to Na^+ in seawater [*Bates et al.*, 2001]. nss-SO_4^{2-} was calculated based on the

equation of nss-SO_4^{2-} = $[SO_4^{2-}]_{Total}$ - $[Na^+] \times 0.25$, where 0.25 is the value of SO_4^{2-}/Na^+ in

seawater [*Millero and Sohn*, 1992]. Chloride depletion was calculated with the equation:

% Chloride Depletion = $(1.81 \times [Na^+] - [Cl^-])/(1.81 \times [Na^+] \times 100$, assuming all Na^+ in

aerosol was from sea water in which the average ratio of Cl^- to Na^+ equals to 1.81

[*Finlayson-Pitts and Pitts*, 2000; *Zhao and Gao*, 2008b]. Relevant meteorological

parameters measured in the ship (Wind speed, direction, relative humidity, air

temperature and pressure) are in Table 2.1. In addition, the positive matrix factorization

(PMF) method was applied to the aerosol mass data obtained by one set of MOUDI

samples to create a general aerosol mass-size distribution [*Kim et al.*, 2003], and this

method gave the resolved size distribution data with lognormal distribution functions.

2.3 Results and Discussions

2.3.1 Spatial Concentration Distributions by Bulk Aerosols

2.3.1.1 Aerosol Mass and Inorganic Species

Figure 2.2(a) shows the latitudinal distributions of aerosol mass based on bulk aerosol

samples collected on Teflon filters by the L-V sampler. The average mass concentrations

of bulk aerosols were 6.5±5.0 µg m^{-3} (n=6) over the Southern Ocean and 4.6±3.8 µg m^{-3}

(n=11) over coastal East Antarctica. The average mass concentration of bulk aerosols

over the Southern Ocean was 1.6 times higher than that in coastal East Antarctica. The

sea-salt aerosols in bulk samples contributed to ~72% of the mass over the Southern

Ocean and ~56% in coastal East Antarctica.

Sea-Salt Aerosol: Figure 2.2(b) shows the latitudinal distribution of sea salt aerosol

represented by the Na^+ concentrations. The average concentration of sea salt aerosol in bulk samples was 5900 ± 5600 ng m^{-3} over the Southern Ocean, more than two times higher than that observed over coastal East Antarctica (2600 ± 2300 ng m^{-3}). The higher sea salt aerosol concentrations over the Southern Ocean is clearly a result of strong westerly winds in that region, as the ship encountered several cyclones during the sampling period, while the average wind speeds often exceeded 13 m s^{-1} with whitecaps being present, generating a tremendous amount of sea salt aerosol particles in the marine atmosphere. *Jourdain and Legrand* [2002] also found that sea salt particles contributed substantially to the total marine aerosol mass relative to other aerosol species in coastal Antarctica.

nss-Sulfate: The latitudinal distribution of nss-SO_4^{2-} is shown in Figure 2.2(c). Over the Southern Ocean, the average concentration of nss-SO_4^{2-} was 420 ± 150 ng m^{-3}, ranging from 230 ng m^{-3} to 600 ng m^{-3}. Over coastal East Antarctica, the average concentration of nss-SO_4^{2-} was 480 ± 290 ng m^{-3}, with a range of 230-1200 ng m^{-3}. High DMS emissions from marine phytoplankton were observed around coastal Antarctica [*Berresheim et al.*, 1998], which could contribute to the observed high nss-sulfate concentrations observed in this region. The results from this study were consistent with those in several Antarctic coastal stations. *Minikin et al.* [1998] reported that the mean concentrations of aerosol nss-SO_4^{2-} in austral summer were 250 ng m^{-3} at Neumayer, ~300 ng m^{-3} at Dumont d'Urville, and ~100 ng m^{-3} at Halley (75°S, 26°W). These summer-time concentrations of nss-SO_4^{2-} were significantly higher than the annual average concentrations also reported by *Minikin et al.* [1998], indicating high marine biogenic emissions in austral summer.

Nitrate: The average concentrations of nitrate were 41 ± 8.0 ng m^{-3} over the Southern Ocean and 50 ± 20 ng m^{-3} over coastal Antarctica (Figure 2.2(d)). The observed aerosol nitrate could come from several sources. The long-range transport of substances from the mid-latitude continents was suggested as the primary source of nitrate in aerosols observed at Mawson Station in East Antarctica [*Savoie et al.*, 1992]. However, the impact of continental sources on aerosol samples collected during this study was low based on the air mass back-trajectory analyses, and this result is consistent with the finding by *Wagenbach et al.* [1998] that the continental source for nitrate at coastal Antarctica was relatively unimportant. Higher concentrations of aerosol nitrate observed at coastal Antarctica compared with those over the Southern Ocean during this study suggests additional sources. One such source could be the release of NO_x from the Antarctic snowpack into the atmosphere, which could undergo photochemical reactions to form nitric acid that consequently reacted with alkaline sea salt and dust particles to form aerosol nitrate [*Seinfeld and Pandis*, 2006]. Based on the measurements at German Neumayer Station during austral summer 1999, *Jones et al.* [2001] estimated that an annual NO_x emission from the snowpack was in the order of 0.0076 Tg N over Antarctica. *Wolff* [1995] suggested that the dominant contribution of nitrate in Antarctica snow was natural sources that included the production of NO_x by lightning in the troposphere and the entrainment of NO_x into the troposphere that was produced through the oxidation of N_2O in the lower stratosphere. Nitrate derived from reactions involving NO_x in the troposphere was deposited onto Antarctic snow and ice and undergone post-deposition photolysis, resulting the formation of NO_x in the Antarctic snowpack [*Honrath*

et al., 1999; *Zatko, et al.*, 2013]. Other sources of nitrate over coastal Antarctica may include human activities, such as the emissions from vehicles used at research bases, in particular during the austral summer, the peak season for conducting research at many Antarctic stations. *Mazzera et al.* [2001a] utilized the chemical mass balance model to study the aerosol source apportionment at McMurdo Station in Antarctica and found that nitrate aerosol at this site in austral summer was mainly originated from local vehicles and power plant emissions.

Ammonium: The average NH_4^+ concentration over the Southern Ocean was 42 ± 31 ng m^{-3}, while its average concentration over coastal East Antarctica was 96 ± 43 ng m^{-3} (Figure 2.2(e)). The observed NH_4^+ values from this study are consistent with the observed NH_4^+ concentrations of 37- 47 ng m^{-3} near Vanda Station (77°32'S, 161°38'E) during November and December 1980 [*Gras*, 1983] and 61 ng m^{-3} at Mawson Station (67°36'S, 62°30'E) [*Savoie et al.*, 1992]. The highest concentration of NH_4^+, 160 ng m^{-3}, was observed at 69°S, 77°E, suggesting potential local sources for NH_4^+ in austral summer. A seasonal variation of NH_4^+ was observed at Dumont D'Urville with the maxima in spring and summer and minima in winter [*Legrand et al.*, 1998]. In addition to possible impact of solar radiation intensity on the NH_4^+ production, the seasonal variation of NH_4^+ may be linked to the presence of a large Adélie penguin population in the region. *Legrand et al.* [2012] showed that at Dumont d'Urville the high levels of ammonia (NH_3) in the air were found in the area where guano decomposition in the large penguin colonies was present. *Zhu et al.* [2011] collected penguin guano and ornithogenic soils from four penguin colonies and seal colony soils in coastal Antarctica and found that the NH_3

emissions fluxes were 7.66 ± 4.33 mg NH_3 kg^{-1} h^{-1} from emperor penguin guano and

1.31 ± 0.64 mg NH_3 kg^{-1} h^{-1} from Adélie penguin guano. The importance of NH_3

emissions from sea birds has been recognized by recent studies [*Legrand et al.*, 1998 and

2012; *Blackall et al.* 2007]. *Blackall et al.* [2007] conducted ammonium emission

observations from seabird colonies, suggesting that seabird colonies could stand for the

largest point sources of ammonia in the region south of 45°S. These observations suggest

that the emissions of NH_3 from sea birds and animals and ornithogenic soils could be an

important sources of NH_3 in coastal Antarctica, contributing to the high concentration of

NH_4^+ in aerosols in the Antarctic coastal marine atmosphere observed during this study.

The importance of air-sea exchange of NH_3 gas to the formation of marine aerosols and

its climate feedback has long been recognized [*Liss and Galloway*, 1993]. Recently,

Jickells et al. [2003] utilized the isotopic signatures of ammonium to identify the

existence of marine sources for aerosol ammonium. *Johnson and Bell* [2008] proposed

that the DMS emissions from the ocean indirectly controlled the flux of NH_3 from the

ocean through neutralization processes involving acidic DMS oxidation products.

Legrand et al. [1998] reported that ~5 millions Adélie penguin inhabitations around

Antarctica contributed to 2.5×10^{-4} megatonne (Mt) of NH_3-N emissions during the austral

summer, while the marine biogenic emissions of ammonia were estimated to be up to 640

$\times 10^{-4}$ Mt of NH_3-N in summer in the oceanic regions south of 50°S. Thus, the NH_3

emissions from the Adélie penguins source could account for ~0.4% of the total oceanic

NH_3 emissions during austral summer. However, this percentage may represent the lower

end of the range of the total NH_3 emissions from all seabirds and sea animals as other

seabirds beside Adélie penguins and sea animals were not included in the calculation. *Möller* [2010] calculated NH_3 emission fluxes with models and suggested that the best estimates of the NH_3 emissions from the global oceans were in the range of 10-15 Tg N yr^{-1}. *Riddick et al.* [2012] studied the global NH_3 emissions from seabird colonies and suggested an estimate of 0.27 Tg NH_3-N yr^{-1} of NH_3 emissions from seabird colonies; thereby the NH_3 emissions from seabirds can explain for 1.8-2.7 % of oceanic emissions. The uncertainties, such as temperature dependence of NH_3 emission, seasonal changes in biological productivity, variation in air/sea exchange rates and breeding colony populations, exist in estimating the relative contribution of seabird colony emissions in the ammonia production budget [*Legrand et al.*, 1998 and *Riddick et al.*, 2012].

2.3.1.2 Organic Aerosol Species

Methane sulfonate: The concentrations of MSA did not vary dramatically over the Southern Ocean, ranging from 63 to 87ng m^{-3} (average concentration: 77±8.7 ng m^{-3}). However, the concentrations of MSA over coastal East Antarctica showed more variations, ranging from 46 to 170 ng m^{-3} (average concentration: 86 ± 40 ng m^{-3}) (Figure 2.3(a)). The two highest MSA values, 140 ng m^{-3} and 170 ng m^{-3} were found at 69°S, 75°E-64°S, 102°E and ~69°S, 77°E. The higher concentrations of MSA observed in coastal East Antarctica compared to those over the Southern Ocean could be attributed to higher DMS emissions of marine biogenic sources in coastal Antarctica than those in the Southern Ocean. The observed average DMS concentration in seawater in the Southern Ocean (Indian sector) was 1.87±2.11 nmol L^{-1} during Jan. 2006, Jan. 2008 and Feb. 2008, with the highest concentration of ~10 nmol L^{-1} at 63.4°S, 71.2°E and the lowest one of

0.41 nmol L^{-1} at 53.3^{o}S, 98.3^{o}E (*Nobue Kasamatsu*, 2006-2008, unpublished data, http://saga.pmel.noaa.gov/dms/select.php). This spatial pattern of DMS distributions in seawater was consistent with that of aerosol MSA observed in this study. *Trevena and Jones* [2012] conducted observations of seawater DMS in the Antarctic sea ice zone of East Antarctica and found that the areas with substantial ice melting could release a large amount of DMS gases in austral summer. Thus, we could infer that high MSA concentrations in the marine atmosphere over coastal Antarctica observed during this study could be linked to high DMS emissions in seawater. Year-round observations of MSA in coastal Antarctica revealed that the maximum MSA existed in austral summer annually [*Jourdain and Legrand*, 2002; *Weller and Wagenbach*, 2007]. These results are consistent with previous studies on the spatial and temporal characteristics of MSA in coastal and inland Antarctica [*Savoie et al.*, 1992; *Rankin and Wolff*, 2003; *Weller and Wagenbach*, 2007]. As the MSA is considered to be of marine biogenic origin, many factors and processes associated with the marine primary production could impact the distributions of MSA in the marine atmosphere, including the marine ecosystem dynamics and spatial variability of phytoplankton species in the water column, air-sea exchange rates of DMS, and different oxidation pathways of DMS [*O'Dowd et al.*, 1997]. In addition, different physical factors and environmental conditions may also affect the MSA properties, such as the temperature variations, solar radiation intensity, precipitation patterns, sea-ice conditions, winds and ocean currents [*O'Dowd et al.*, 1997].

Oxalate: The concentrations of oxalate as well as other organic acids were low and their presence was detected in only a portion of samples collected during this study (Figure 2.3(b)). The average concentrations of oxalate were 3.8 ± 3.8 ng m^{-3} (range: 0 to 9.1 ng m^{-3}) over the Southern Ocean and 2.2 ± 1.5 ng m^{-3} (range: 0 to 4.6 ng m^{-3}) over coastal Antarctica. These results are consistent with recent studies carried out at several locations in the regions. *Virkkula et al.* [2006a] reported that the concentrations of oxalate were 0.6-1.4 ng m^{-3} over the Southern Ocean and 2.1 ± 5.1 ng m^{-3} at Aboa Station (73°03'S, 13°25'W) in coastal Antarctica. *Wang et al.* [2006] reported that oxalate concentrations ranged from 1.4 - 4.2 ng m^{-3} in the region of $>50^{o}$S, 130°-150°E. Oxalic acid ($H_2C_2O_4$) was among the dominant dicarboxylic acids (DCAs), accounting for up to 50% of the total atmospheric DCAs in remote marine atmospheres [*Martinelango et al.*, 2007]. Isoprene produced by marine photosynthetic organisms is considered to be the major source of oxalic acid in the marine atmosphere [*Kawamura and Ikushima*, 1993]; it could be oxidized into pyruvic acid and methylglyoxal, acting as intermediates in the in-cloud formation of oxalic acid [*Ervens et al., 2004*]. On the other hand, *Legrand et al.* [2012] observed an enrichment of oxalate in aerosols at Dumont d'Urville Station that was associated with the high levels of NH_3 in the air, and this may suggest that sea birds and animals at coastal Antarctica could also be sources for aerosol oxalate observed during this study.

Formate, Acetate and Succinate: The average concentration of formate was 0.23 ± 0.45 ng m^{-3} (range: 0-1.1 ng m^{-3} over the Southern Ocean (Figure 2.3(c)). In coastal Antarctica, its concentrations ranged from 0 to 1.7 ng m^{-3}. Acetate was detected in only a

few samples over coastal East Antarctica, and ranged from 0-7.8 ng m^{-3} (Figure 2.3(d)).

The succinate concentrations observed during this study ranged from 0 to 2.9 ng m^{-3} over

the Southern Ocean and from 0 to 0.95 ng m^{-3} in coastal East Antarctica (Figure 2.3(e)).

Formic acid (HCOOH) and acetic acids (CH$_3$COOH) exists in liquid, aerosol, and vapor

phases [*Keene and Galloway,* 1988]. Based on the year-round investigation at Dumont

d'Urville, *Legrand et al.* [2004] showed that both formic and acetic acids are mainly

(99%) present in the gas phase with their concentrations ranging from <0.5 ppt in winter

to 3 ppt in summer, and they concluded that these low-C compounds were mainly

produced by photochemical production of alkenes released by phytoplankton, and their

variations follow the annual cycle of sea ice extent and solar radiation.

2.3.2 Aerosol Particle-Size Distributions

2.3.2.1 General Size Distribution

Figure 2.4 shows the mass distribution of size-segregated particulate matter based on one

set of MOUDI sample collected over coastal East Antarctica, while the ambient relative

humidity (RH) was on average 69% (range: 46-98%). A general mass-size distribution of

particulate matter existed in a bimodal pattern (curve (a) in Figure 2.4) with one peak at

aerodynamic diameter at 0.32-0.56 μm (accumulation mode, curve (b) in Figure 2.4),

accounting for 28% of the total mass, and the other peak at 3.2-5.6 μm (coarse mode,

curve (c) in Figure 2.4), constituting ~52% of the total mass. The highest mass

concentration, 1100 ng m^{-3}, was associated with the size of 3.2-5.6 μm, while the lowest

mass concentration was 370 ng m^{-3} with the size of 0.056-0.1 μm. The observed size

distributions were contributed by individual aerosol species, as sea salt particles had a

major contribution to the coarse mode particles, while nss-SO_4^{2-}, MSA and oxalate

contributed to the fine mode particles significantly, which will be discussed in the later

sections. *Teinilä et al.* [2000] found that the measured ions (major inorganic ions, MSA,

and dicarboxylates) contributed on average one third of the total mass in fine mode

particles (diameter < 2 μm) at Aboa Station in Antactica.

2.3.2.2 Inorganic Aerosol Species

Sea Salt: Over the Southern Ocean, sea salt aerosol mainly existed in the coarse mode,

peaking at >3.0 μm (Figure 2.5(a)), strongly impacted by westerly winds. This result is

consistent with the earlier finding that during high wind speeds over the ocean, there are

always significant amounts of sea-salt particles with diameter >10 μm [*O'Dowd et al.*,

1997]. *Quinn et al.* [1996] reported that submicron and supermicron sea-salt aerosols

contributed ~10% and 80% of the total marine aerosol mass, respectively. Over coastal

Antarctica, the size of sea salt aerosol peaked at 5.6-10 μm with the corresponding

concentration of 1800±1800 ng m^{-3} (n=2) (Figure 2.6(a)).

nss-Sulfate: Figure 2.5(b) shows that the concentrations of nss-SO_4^{2-} increased as the

particle size decreased over the Southern Ocean. Aerosol nss-SO_4^{2-} was mainly

accumulated in the fine mode, peaking at <0.49 μm with the corresponding concentration

of ~110±57 ng m^{-3} (n=4). Over coastal East Antarctica, the nss-SO_4^{2-} was also

accumulated in the fine-mode, and peaked at 0.10-0.18 μm and 0.32-0.56 μm size ranges,

plus a small portion accumulated in the size range 5.6-10 μm (Figure 2.6(b)). High nss-

SO_4^{2-} concentrations in the fine mode particles could be attributed to the gas-to-particle

conversion of S-containing gas-phase species from marine phytoplankton emissions and in-cloud heterogeneous oxidation of SO_2 through phase reaction with H_2O_2 and O_3 [*Harris et al.*, 2013]. On the other hand, the existence of nss-SO_4^{2-} in the coarse mode indicates its interactions with sea salt [*Zhuang et al.,* 1999]. The heterogeneous oxidation of SO_2 in freshly formed coarse sea salt by O_3 has been suggested to be the major pathway for the formation of coarse-mode nss-sulfate in the marine boundary layer (MBL) [*Sievering et al.*, 1991]. Other formation mechanisms of nss-sulfate in the coarse mode include the aqueous-phase oxidation of SO_2 in cloud droplets [*McInnes et al.*, 1994; *Kerminen et al.*, 1997] and the interactions between H_2SO_4 gas and NaCl, leading to the formation of coarse mode nss-sulfate; however, the contribution from the latter is less important as the gas-phase H_2SO_4 concentration is low in clean marine environments [*Zhuang, et al.*, 1999]. Interestingly, some of the nss-SO_4^{2-} concentrations observed in this study were below zero when the particle size was larger than 3.0 μm. This could be attributed to the definition of the nss-SO_4^{2-} concentration that was derived by subtracting the sea-salt sulfate from the total sulfate, using the weight ratio of SO_4^{2-}/Na^+ in seawater (0.25) [*Wolff et al.*, 2006]. Recent studies reported that sea ice existed in the surface of the Southern Ocean and Antarctic coastal seawater, and highly saline frost flowers were the main source of sea salt, with sulfate being depleted strongly relative to sodium [*Rankin et al.*, 2002]. Therefore utilizing the common SO_4^{2-}/Na^+ ratio in seawater for calculating nss-sulfate in the Southern Ocean may have resulted in the lower nss-SO_4^{2-} concentrations found in this study.

Nitrate: A bimodal size distribution of aerosol NO_3^- was observed during this study. Over

the Southern Ocean, the NO_3^- concentrations peaked at 0.95-1.5 μm (corresponding

concentration: 15 ± 8.8 ng m^{-3}) and at 3.0-7.2 μm (concentration: 21±13 ng m^{-3}) (Figure

2.5(c)). The NO_3^- concentration in the coarse mode was larger than that in the fine mode,

and high sea salt concentrations could contribute to the production of NO_3^- in the coarse

mode. The NO_3^- in the coarse mode was mainly produced in the surface of sea salt

aerosol through the reactions below [*Seinfeld and Pandis, 2006*]:

$$NH_3\ (g)+HNO_3\ (g)→NH_4NO_3 \qquad (1)$$

$$HNO_3\ (g)+ NaCl→NaNO_3+HCl(g) \quad (2)$$
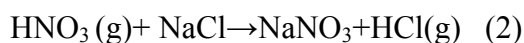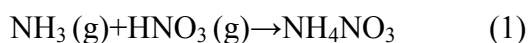
Reaction (2) was the main production process over remote oceans, which may also cause

chloride depletion. However, over coastal Antarctica, the NO_3^- concentrations peaked at

0.1-0.18 μm (average: 50±19 ng m^{-3}) and at 1.0 -1.8 μm (average: 46±12 ng m^{-3}), mainly

accumulated in the fine mode (Figure 2.6(c)). Two pathways may explain the formation

of NO_3^- in the fine mode: In-cloud processes and condensation of its precursors onto

preexisting particles [*Herner et al.,* 2006]. A good correlation, defined as Pearson value

>0.5, p<0.05, between NO_3^- and nss-SO_4^{2-} in the fine mode was observed in this study

(Table 2.2(a)), inferring that nitrate in the fine mode could be produced through the in-

cloud processes [*Zhao and Gao,* 2008a]. In addition, there was a good correlation

between NO_3^- and NH_4^+ in the fine mode, and a large amount of NH_4^+ in the same size

range as that of NO_3^- makes the presence of NH_4NO_3 possible. Based on simple

stoichiometric calculations, ~20 % of NO_3^- in the fine mode existed as NH_4NO_3 over

coastal East Antarctica. The fine-mode NO_3^- could be produced by co-condensation of

gaseous NH_3 and HNO_3 as shown in Reaction (1), consistent with the work by *Zhao and*

Gao [2008a] and *Bardouki et al.* [2003].

Ammonium: The size distributions of NH_4^+ peaked at 0.95-1.5 μm with the average

concentration of 8.4 ± 5.7 ng m^{-3} over the Southern Ocean (Figure 2.5(d)). Over coastal

East Antarctica, however, the NH_4^+ concentration peaked at 0.10-0.32 μm with the

average concentration of 24 ± 7.9 ng m^{-3} (Figure 2.6(d)), which was about three times

higher than that in the Southern Ocean. The enrichment of NH_4^+ in the fine mode

particles was similar to that of nss-SO_4^{2-} observed in this study. The formation of NH_4^+ in

the fine mode was affected by the SO_4^{2-} abundance and related to its gaseous precursor

NH_3 through gas-phase and aqueous-phase reactions with acidic species (e.g., H_2SO_4)

[*Zhang et al.,* 2008]. Based on the equivalent ratios of [NH_4^+] to [NO_3^-] and [NH_4^+] to

[SO_4^{2-}], most NH_4^+ in the fine-mode particles was produced through the reactions

preferentially first with H_2SO_4 as $(NH_4)_2SO_4$ and then with HNO_3 as NH_4NO_3. Previous

studies indicated that the concentration of ammonium was relatively stable in coastal

Antarctica, and the mass size distribution of NH_4^+ had a shape similar to that of nss-SO_4^{2-}

[*Legrand et al.*, 1998; *Teinilä et al.*, 2000].

2.3.2.3 Organic Aerosol Species

Methane sulfonate: Figure 2.7(a) showed that the MSA concentrations increased with

decreasing size for the size range of <3.0 μm, peaking at 0.32-0.56 μm over the Southern

Ocean. About 72% of the total MSA was enriched in the accumulation mode, and only a

small portion of MSA was in the coarse mode of 3.0-7.2 μm that could be produced

through the condensation of gas-phase methane sulfonic acid on the surface of pre-

existing sea salt aerosol particles [*O'Dowd et al.*, 1997]. Over coastal Antarctica,

although the concentrations of MSA ranged from 1.9 to 42 ng m^{-3} for all particle sizes, its concentration peak was at 0.32-0.56 μm (Figure 2.8(a)). This size distribution feature observed over coastal East Antarctica during this study was consistent with earlier studies conducted over West Antarctica [*Read et al.*, 2008] and other coastal regions, including Florida coast and the Gulf of Mexico [*Saltzman et al.*, 1983], Washington coast [*Quinn et al.*, 1993] and the China Sea [*Gao et. al.*, 1996], which reflected the MSA production mechanism through the gas-to-particle conversion and oxidation of S-containing species in the marine atmosphere.

Oxalate: The size distributions of oxalate over the Southern Ocean are shown in Figure 2.7(b), peaking at <0.49μm with the corresponding concentration of 3.1±0.93 ng m^{-3} and at 0.95-1.5 μm with the concentration of 1.8 ± 0.80 ng m^{-3}. Over coastal East Antarctica, the particle size of oxalate peaked at 0.56-1.8 μm (Figure 2.8(b)), with the concentration of 1.6 ± 0.70 ng m^{-3}. Thus, oxalate was mainly accumulated in the fine-mode particles over both the Southern Ocean and coastal East Antarctica.

Formate, Acetate and Succinate: Figure 2.7(c) shows two peaks in the size distributions of formate over the Southern Ocean, <0.49 and 0.95 -1.5 μm, and this species mainly existed in the fine mode. The size distributions of formate over coastal East Antarctica (Figure 2.8(c)) also had two peaks, 0.10-0.18 μm and 1.0-1.8 μm. This result demonstrated that formate in aerosols mainly existed in the fine mode both over the Southern Ocean and coastal East Antarctica. Over the Southern Ocean, acetate peaked at 3.0-7.2 μm in the coarse mode, accounting for 42% of the total acetate combined in all

size ranges (Figure 2.7(d)). However, a large portion of acetate over coastal Antarctica

was dominated by fine-mode particles, particularly in the sizes of 0.1-0.18 μm and 1.0-

1.8 μm (Figure 2.8(d)). The fine-mode feature with acetate observed in coastal Antarctica

in this study could have resulted from gas-to-particle conversion processes. *Legrand et al*

[2004] reported that acetate was mainly derived from the photochemistry of propene

emitted by photo-degradation of dissolved organic matter (DOM) in the ocean. Thus, the

DOM-rich waters in some of the Antarctic coastal seas might be the source of propene

and then of acetate in marine aerosols in this region. The particle sizes of succinate over

the Southern Ocean showed a bi-model distribution (Figure 2.7(e)), peaked at <0.49 μm

and at 3.0-7.2 μm. A similar bi-model size distribution of succinate also existed over

coastal East Antarctica where the size peaks of succinate were at 0.10-0.18 μm and at 3.2-

5.6 μm observed in early December during this study (Figure 2.8(e)). Recent studies

reported that free radicals and oxidants generated by photochemical processes could

greatly control the chemistry of organic compounds like succinate in the atmosphere

[*Limbeck et al.*, 2003; *Neu et al.*, 2007].

2.3.3 MSA and MSA/nss-SO$_4^{2-}$ Ratios

The concentrations of aerosol MSA in high-latitude oceanic regions may reflect the level

of the marine biogenic production, and MSA/nss-SO$_4^{2-}$ ratios could be used to evaluate

the relative contributions of marine biogenic and other sources to the sulfur budget

[*Saltzman, et al.*, 2006]. The average MSA/nss-SO$_4^{2-}$ ratio derived from bulk aerosol

samples from this study was 0.18 over the Southern Ocean and 0.21 over coastal East

Antarctica, and a high ratio 0.32 appeared at coastal East Antarctica when the MSA

concentration was high (110 ng m^{-3}). These results are consistent with those at Mawson, Antarctica (67°36'S, 62°30'E) from February 1987 to October 1989 by *Prospero et al.* [1991] who showed that the MSA/nss-SO$_4^{2-}$ ratio was about 0.31. However, the highest ratio was not always associated with the highest MSA concentration observed in this study, suggesting that other factors may affect the concentrations of either MSA or nss-SO$_4^{2-}$.

Temperature was among the factors that may affect MSA production [*Bates et al.*, 1992; *Arsene et al.*, 1999]. Previous studies found that the oxidation rate of marine biogenic DMS at low temperatures could contribute to the high yield of MSA, resulting in high ratios of MSA/nss-SO$_4^{2-}$ near coastal Antarctica [*Turnipseed et al.*, 1996; *Barnes et al.*, 2006]. However, in this study, the correlation between MSA and ambient air temperature (T) was weak ($R^2 = 0.005$); the same was found for the MSA/nss-SO$_4^{2-}$ correlation ($R^2 = 0.003$) (Figure 2.9). The three highest MSA values (170 ng m^{-3}, 140 ng m^{-3} and 110 ng m^{-3}) were not associated with the lowest temperature, suggesting that the temperature was not the sole condition affecting the MSA production and the MSA/nss-SO$_4^{2-}$ ratios. *Wagenbach* [1996] observed abrupt changes in the MSA/nss-SO$_4^{2-}$ ratio during summer but with no concomitant changes in temperature in coastal Antarctica. With the fact that the air masses affecting samples collected during this study mainly originated from either the Southern Ocean or Antarctica, the effects of long-range transport from the continents on the observed nss-SO$_4^{2-}$ should be negligible. On the other hand, local emissions from power generation and vehicle operations at some Antarctic stations generated SO$_2$ [*Mazzera et al.*, 2001b], which could affect the MSA/nss-SO$_4^{2-}$ ratios. However, the high

MSA concentrations (140 ng m^{-3} and 110 ng m^{-3}) corresponded to high MSA/nss-SO$_4$$^{2-}$ ratios (0.31 and 0.32), suggesting that MSA plays an important role in shaping the spatial variation in MSA/nss-SO$_4$$^{2-}$ in the southern hemisphere, consistent with the results by *Arimoto et al.*[2001] who found that it is MSA more than sulfate that drives the spatial differences in this ratio.

2.3.4 Cl$^-$ Depletion and Cation to Anion Ratios

Chloride depletion in marine aerosols occurs due to reactions of sea salt with acidic compounds, such as sulfuric acid, nitric acid and certain organic acids including MSA, resulting in the loss of Cl$^-$ in the form of HCl gas [*Pakkanen*, 1996; *Kerminen et al.*, 1997; *Virkkula et al.*, 2006b]. Based on the calculation by the Equation in Section 2.3, the average chloride depletion over the Southern Ocean was 5.8%, while it was ~10% over coastal Antarctica, consistent with the results of previous studies, that the average loss of chloride was ~10-20% over coastal Antarctica during austral summer [*Jourdain and Legrand*, 2002; *Rankin and Wolff*, 2003]. The percentage losses of Cl$^-$ as a function of aerosol particle sizes are shown in Figure 2.10. High Cl$^-$ depletion mainly occurred on particles in the size range <1.5 μm, and the extent of depletion in aerosols over coastal Antarctica was higher than that over the Southern Ocean. Over the Southern Ocean, ~92%-98% of nss-SO$_4$$^{2-}$ and 69%-74% of MSA mass concentrations observed in this study were accumulated in the fine mode particles, which were associated with chloride depletion in particles of <1.5 μm in diameter. Over coastal East Antarctica, ~61%-84% of nss-SO$_4$$^{2-}$, 83-88% of NO$_3$$^-$, 90%-94% of MSA, and 62%-72% of oxalate mass concentrations were accumulated in particles of <1.8 μm. Thus, the enrichment of more

acidic species in fine particles over coastal East Antarctica may explain the higher

chloride depletion observed in this region. This result suggests that acidic water-soluble

inorganic and organic species had high potential to substitute for sea salt chloride,

particularly sulfate, nitrate and MSA, in the marine atmosphere over coastal East

Antarctica.

To further explore the role of these acidic aerosol species in Cl^- depletion, aerosol acidity

was estimated by calculating the measured cation-to-anion ratios in charge equivalents

(Figure 2.11). In the fine mode, the average ratios were 0.70 over the Southern Ocean and

0.74 in coastal Antarctica. The minimum cation-to-anion ratio was associated with

particles of <0.5 μm in diameter, suggesting that fine mode particles were more acidic

due to the accumulation of several acidic species on the particles. This result is consistent

with the results obtained by *Kerminen et al.* [2001] who observed that the measured

cation-to-anion ratios vary with particle sizes and particles in accumulation mode were

more acidic, probably due to the cloud processing of aerosols. A similar feature was also

observed by *Virkkula et al.* [2006b] at 40°S and in the Antarctic region. In the coarse

mode, however, the average cation-to-anion ratios increased to 0.86 over the Southern

Ocean and 1.08 in coastal Antarctica, indicating that coarse aerosols were more

neutralized over coastal East Antarctica than over the Southern Ocean. Results of aerosol

dissolvable Fe size distributions from samples collected on the same cruise showed a

small peak in the coarse mode with possible contributions of dust from sources in

Antarctica [*Gao et al.,* 2013]. This may partially explain a relatively high cation-to-anion

ratio over coastal East Antarctica found in this study, as dust is rich in alkaline material

and can neutralize acidic aerosols [*Rastogi and Sarin*, 2006].

On the other hand, the average molar ratios of NH_4^+/nss-SO_4^{2-} in fine mode particles that dominated the total concentrations of NH_4^+ and nss-SO_4^{2-} observed during this study were 0.26 over the Southern Ocean and 0.93 over coastal East Antarctica. Higher NH_4^+/nss-SO_4^{2-} ratio over coastal East Antarctica compared with that over the Southern Ocean may suggest a higher neutralization capacity of the marine atmosphere over the Antarctic coast. The NH_4^+/nss-SO_4^{2-} ratios from this study fitted in the latitudinal pattern of the NH_4^+/nss-SO_4^{2-} ratios observed by *Virkkula et al*. [2006a] who reported that the NH_4^+/nss-SO_4^{2-} ratios in submicron particles decreased from 2 in the North Atlantic to below 1 in coastal Antarctica. These results reveal an inter-hemisphere difference with respect to the spatial distributions of NH_4^+/nss-SO_4^{2-} ratios in the global marine atmosphere, with the lower end of this ratio being present in high latitudes of the Southern Hemisphere. Factors affecting this ratio in aerosols may include seawater pH, temperature and wind speeds, which controlled the air-to-sea fluxes of ammonia [*Johnson and Bell* [2008]. On the other hand, the "hot spots" of NH_3 gas emissions from seabird colonies during Austral summer [*Legrand et al*., 1998 and 2012] could also explain the high ratio in aerosols observed over coastal Antarctica in this study.

To explore the possible sources-particle size distribution relationships and their impacts on Cl⁻ depletion, results from both Cascade Impactor and MOUDI samples were divided into fine and coarse modes (CI samples <1.5 μm, MOUDI samples <1.8 μm as fine mode; CI samples >1.5 μm, MOUDI samples >1.8 μm as coarse mode). The correlation

results of major water-soluble species in both modes are shown in 2.2. In fine mode

particles (Table 2.2(a)), NO_3^-, nss-SO_4^{2-} and NH_4^+ had significant correlations with each

other (Pearson value >0.9, p<0.01), suggesting similar sources of these species. They

were also in good correlation with acetate, formate, and succinate, while only NO_3^- had

relatively significant correlation with oxalate. These secondary organic aerosols could be

produced by photochemical oxidation of biogenic volatile organic compounds (VOCs)

emitted from the ocean and the gas-to-particle conversion processes that resulted in their

formation in the fine mode. However, in the coarse mode (Table 2.2(b)), formate, acetate,

and oxalate had no significant correlation with each other except for the correlation of

formate with succinate (Pearson value >0.8, p<0.05), suggesting they were produced by

different means. On the other hand, all these organic species had no significant

correlation with NO_3^-, nss-SO_4^{2-} and NH_4^+ except for succinate, which had significant

correlations with nss-SO_4^{2-} and NH_4^+ (Pearson value >0.6, p<0.01). Although there was

good correlation between MSA and secondary inorganic species (NO_3^-, NH_4^+ and nss-

SO_4^{2-}) in fine mode particles (Pearson value >0.8, p<0.05), MSA had no significant

correlation with the above species in the coarse mode, suggesting a unique feature of

MSA production different from those secondary inorganic species in the coarse mode. As

good correlations were found between MSA and Na^+ and Cl^- (Pearson value >0.8,

p<0.05) (Table 2.2(b)), the formation of MSA in the coarse mode could be through the

interactions with sea salt that may affect Cl^- depletion.

2.4 Implications for Aerosol-Clouds-Marine-Ecosystem Interactions.

The WSOCs observed in this study provide the evidence of their existence over the

Southern Ocean and coastal East Antarctica during austral summer. The WSOCs are part of secondary organic aerosol (SOA), produced by certain gas-phase precursors, including propene, isoprene, iodomethanes, amines, and monoterpenes in the remote marine atmosphere [*Simó*, 2011]. These precursors are natural VOCs produced by plankton and photochemical reactions over the ocean [*Dachs et al.*, 2005; *Simó*, 2011]. One process that could be involved in the production of the WSOCs is sea spray. The surface of sea spray droplets is enriched with organic matter. *Kawamura et al.* [1996a and 1996b] attributed the origin of low molecular weight (LMW) acids to the atmospheric degradation of biogenic organic matter transferred in the atmosphere within sea spray. Thus, sea salt aerosol could be involved in the production process of monocarboxylic and dicarboxylic acids observed in this study. These low molecular-weight WSOCs can also be formed in clouds and aerosols through the aqueous phase reactions of SOA [*Blando and Turpin*, 2000; *Ervens et al.*, 2011]. Thus, the observed WSOCs during this study may be formed through either gas/particle partitioning or aqueous phase processes, affecting aerosol hygroscopic properties and then CCN activation. *Yu* [2000] reviewed the role for the organic compounds (mainly formic, acetic, pyruvic and oxalic acids) in the formation of CCN, and their results showed that although most (98–99%) of these volatile organic acids are present in the gas phase, their concentrations in the aerosol particles are sufficient to make them a good candidate for CCN.

One unique feature of aerosols observed for the first time over the Southern Ocean and East Antarctica from this study is that the particle size distributions of MSA plus several organic species (oxalate, formate, acetate, succinate) peaked at the fine mode of <1.0 μm,

similar to that of nss-SO$_4^{2-}$, largely in the size spectrum of CCN. This result implies that these organic and inorganic aerosols of marine biogenic origins could function as CCN, enhancing the development of clouds over the Southern Ocean and coastal Antarctica. One way that WSOCs may affect cloud formation is through their interactions with sea salt aerosol [*Kawamura et al.*, 1996a and 1996b; *Fuentes et al.*, 2010]. Sea salt aerosol produced by bubbles bursting on the sea surface could be the source of certain organic substances in the coarse mode particles, including MSA, oxalate, formate, acetate and succinate observed during this study. This process could be particularly important in the regions with relatively low marine productivity. *Murphy et al.* [1998] reported that over 90% of aerosol particles larger than 0.13 μm diameter contain sea-salt in low biological activity areas. Thus, the interactions of submicron sea-salt and WSOCs particles could contribute to the modification of marine aerosol properties, affecting cloud properties.

The composition and size distributions of marine aerosols play important roles in CCN formation and the radiation budget, which remain poorly understood over the Southern Ocean and Antarctica. Extensive clouds exist in summer over Antarctica [*Van Den Broeke et al.*, 2006], and this phenomenon might be connected with high production of biogenic aerosols in austral summer in the region. *Quinn and Bates* [2011] suggested that sea spray emissions of sea salt and organics constituted the main sources of CCN in the remote MBL. It is important at present to study their connections and roles in affecting cloud formation, particularly in the under-sampled remote oceanic regions, in order to better understand the climate forcing by the aerosol-cloud-marine ecosystem interactions.

Table 2.1 Sampling information*.

Sample Type	No.	Sampling Date	Location	WS (m/s)	AT (°C)	RH (%)	AP (hPa)
	B1	11/25/10-11/27/10	34°S, 109°E-41°S, 100°E	14.1	8.8	68.4	1026
	B2	11/27/10-11/30/10	42°S, 100°E-56°S, 94°E	6.9	13.1	78.2	1014
	B3	11/30/10-12/02/10	56°S, 94°E-62°S, 81°E	14.5	0.7	94.5	995
	B4	12/03/10-12/04/10	65°S, 78°E-69°S, 94°E	13.4	-3.4	79.5	985
	B5	12/05/10-12/07/10	69°S, 76°E-69°S, 76°E	4.2	-2	55.9	996
	B6	01/11/11-01/19/11	69°S, 75°E-64°S, 102°E	5.8	0.5	83.3	997
	B7	01/19/11	64°S, 103°E-66°S, 110°E	5.9	0.7	76.2	999
	B8	01/26/11-01/28/11	66°S, 110°E-65°S, 87°E	8.1	0.1	73.5	988
Bulk(B)	B9	01/28/11-01/30/11	64°S, 84°E-69°S, 76°E	6.3	-0.6	78.3	996
	B10	02/10/11-02/11/11	69°S, 78°E	6	-4.3	45.3	986
	B11	02/12/11	69°S, 78°E-69°S, 77°E	7.7	-5.4	38	982
	B12	02/12/11-02/15/11	69°S, 77°E	7.8	-4.4	48	992
	B13	02/15/11-02/18/11	69°S, 77°E-69°S, 78°E	11.7	-3.6	47.8	995
	B14	02/26/11-03/01/11	69°S, 76°E-57°S, 76°E	10.6	-1.9	82.3	983
	B15	03/02/11-03/04/11	58°S, 81°E-44°S, 96°E	9.4	8.6	70.1	1018
	B16	03/04/11-03/06/11	44°S, 96°E-36°S, 102°E	7.7	13.7	67.5	1023
	B17	03/06/11-03/08/11	35°S, 102°E-32°S, 115°E	13.8	20	59.9	1019
MOUDI (M)	M1	12/05/10-12/09/10	69°S, 76°E	5.2	-2.2	61.8	991
	M2	01/11/11-01/19/11	69°S, 75°E-66°S, 110°E	5.8	0.5	82.7	997
	CI1	11/25/10-11/30/11	34°S,109°E-56°S, 94°E	11.3	9.9	74.1	1019
Cascade Impactor (CI)	CI2	11/30/10-12/04/10	56°S, 94°E-69°S, 76°E	16.1	-1.2	89.2	988
	CI3	02/26/11-03/02/11	69°S, 76°E-52°S, 84°E	11.3	-0.3	85.4	987
	CI4	03/03/11-03/07/11	48°S, 89°E-33°S, 110°E	9.3	14.3	63.6	1023

*WS stands for wind speed; AT stands for air temperature; RH stands for relative humidity; AP

stands for air pressure.

Table 2.2 (a) Correlations between water-soluble ions concentrations (N=6) of fine particles.

Ions	Acetate	Formate	MSA	Succinate	Oxalate	NO_3^-	$nss\text{-}SO_4^{2-}$	Cl^-	Na^+	NH_4^+	K^+	Mg^{2+}	Ca^{2+}
Acetate	1	0.93**	0.70	0.87*	0.70	0.92*	0.92**	-0.46	-0.04	0.90*	-0.30	0.72	0.72
Formate		1	0.79	0.93**	0.87*	0.97**	0.90*	-0.72	-0.38	0.95**	-0.53	0.51	0.79
MSA			1	0.96**	0.62	0.88*	0.86*	-0.81	-0.52	0.90*	-0.18	0.61	0.88*
Succinate				1	0.73	0.97**	0.93**	-0.78	-0.44	0.98**	-0.34	0.64	0.90*
Oxalate					1	0.82*	0.75	-0.64	-0.47	0.76	-0.60	0.15	0.47
NO_3^-						1	0.95**	-0.71	-0.36	0.99**	-0.45	0.57	0.79
$nss\text{-}SO_4^{2-}$							1	-0.53	-0.15	0.93**	-0.19	0.72	0.71
Cl^-								1	0.89*	-0.75	0.57	-0.16	-0.83*
Na^+									1	-0.39	0.57	0.25	-0.53
NH_4^+										1	-0.45	0.58	0.84*
K^+											1	0.40	-0.24
Mg^{2+}												1	0.65
Ca^{2+}													1

Table 2.2 (b) Correlations between water-soluble ions concentrations (N=6) of coarse particles.

Ions	Acetate	Formate	MSA	Succinate	Oxalate	NO_3^-	$nss\text{-}SO_4^{2-}$	Cl^-	Na^+	NH_4^+	K^+	Mg^{2+}	Ca^{2+}
Acetate	1	0.01	0.22	0.34	0.45	-0.46	0.42	-0.09	-0.08	-0.48	-0.40	-0.03	0.34
Formate		1	-0.89*	0.88*	0.21	0.01	0.75	-0.95**	-0.96**	-0.73	-0.72	-0.79	-0.79
MSA			1	-0.70	0.08	-0.25	-0.70	0.86*	0.87*	0.44	0.37	0.87*	0.79
Succinate				1	0.55	0.14	0.93**	-0.96**	-0.95**	-0.93**	-0.80	-0.60	-0.49
Oxalate					1	0.21	0.45	-0.36	-0.35	-0.79	-0.71	0.33	0.36
NO_3^-						1	0.24	-0.22	-0.22	-0.04	0.23	0.11	0.10
$nss\text{-}SO_4^{2-}$							1	-0.89*	-0.89*	-0.81*	-0.57	-0.64	-0.36
Cl^-								1	1.00*	0.81	0.69	0.73	0.67
Na^+									1	0.80	0.68	0.73	0.67
NH_4^+										1	0.91*	0.31	0.22
K^+											1	0.24	0.26
Mg^{2+}												1	0.84*
Ca^{2+}													1

* Correlation is significant at the 0.05 level (2-tailed); ** Correlation is significant at the 0.01 level (2-tailed).
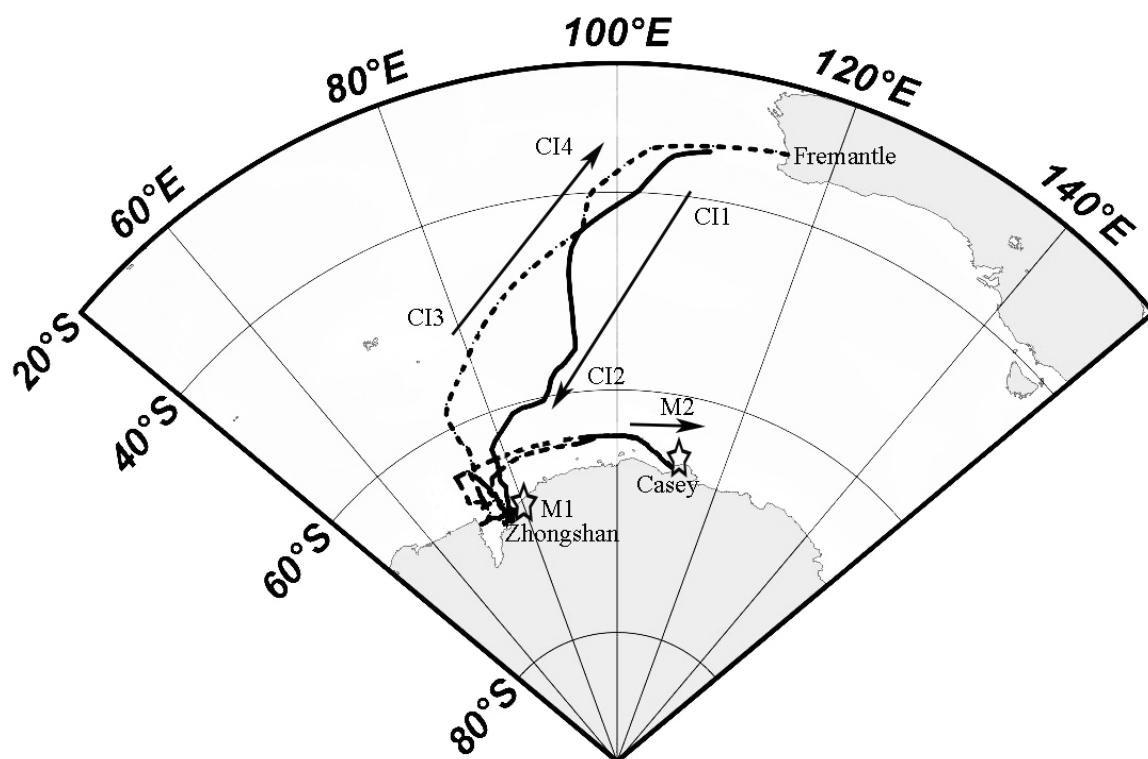
Figure 2.1 Cruise tracks and sampling locations. The solid line represents the legs from Fremantle, Australia to Chinese Antarctic Zhongshan Station (CI1, CI2); the dashed line represents the legs between Zhongshan Station and Australia Antarctic Casey Station (M1, M2); the dash-dot line represents the legs from Zhongshan Station to Fremantle (CI3, CI4).
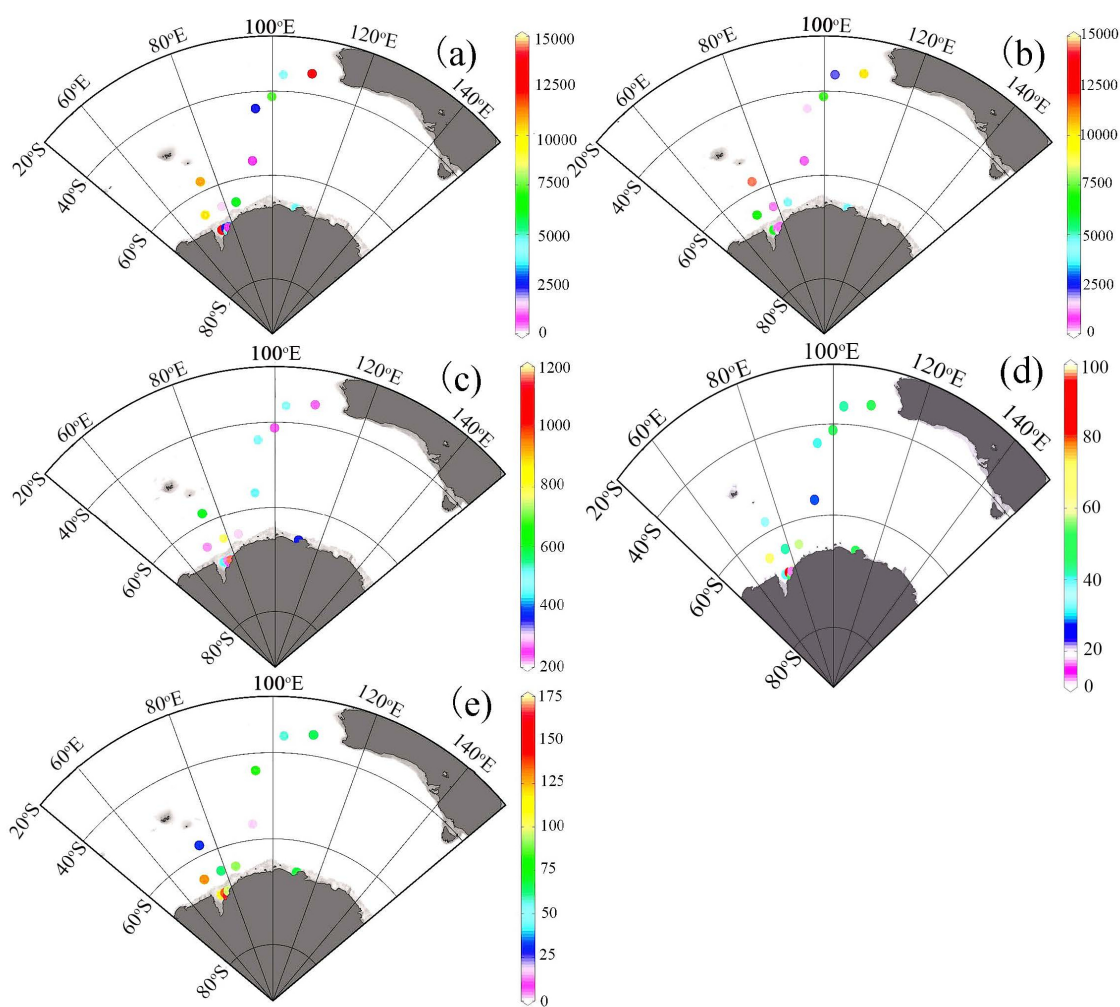
Figure 2.2 Latitudinal concentration distributions of aerosol mass and selected water-soluble inorganic aerosol species: (a) mass, (b) sea salt, (c) nss-SO_4^{2-}, (d) NO_3^-, and (e) NH_4^+ (unit: ng m^{-3}).
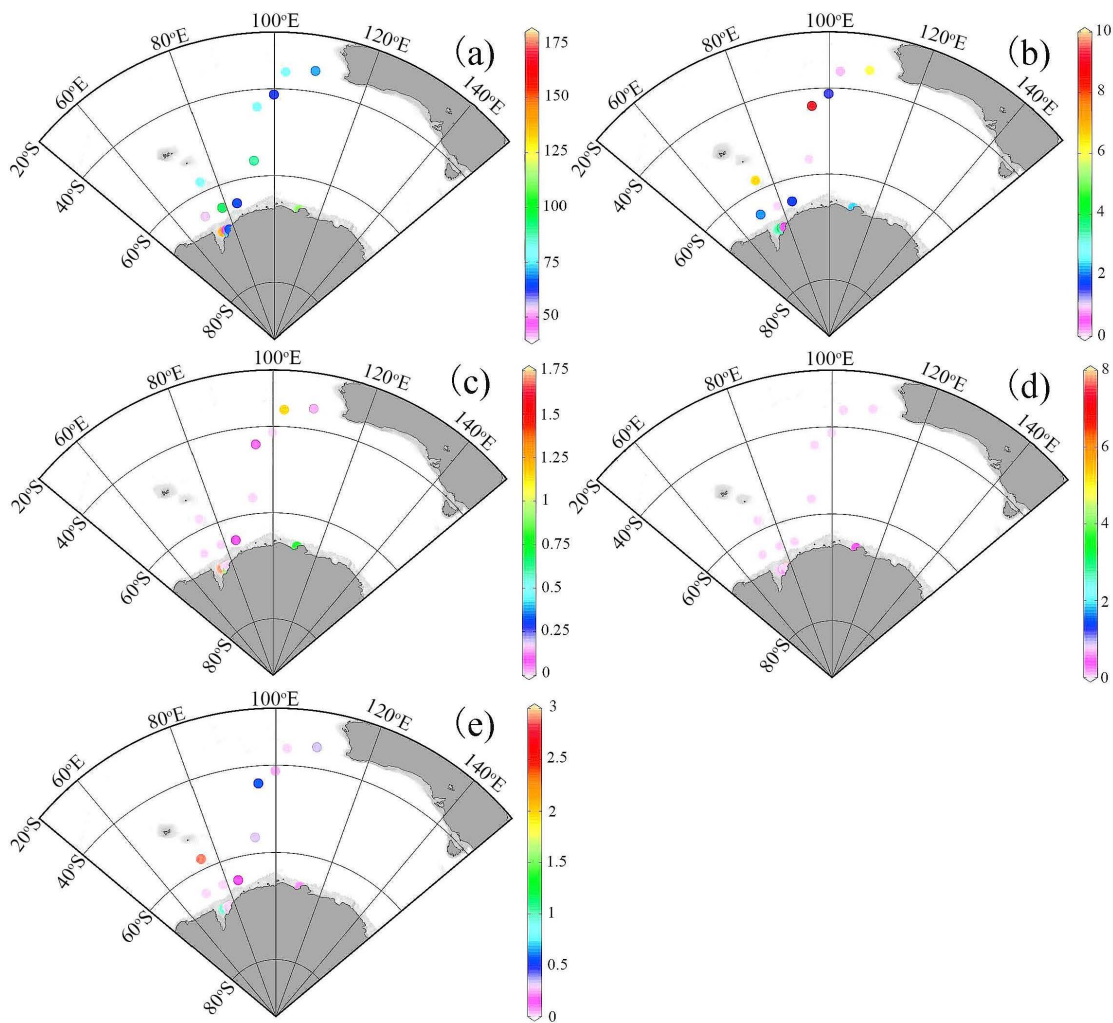
Figure 2.3 Latitudinal concentration distributions of aerosol mass and selected water-soluble organic aerosol species: (a) MSA, (b) oxalate, (c) formate, (d) acetate, and (e) succinate (unit: ng m^{-3}).
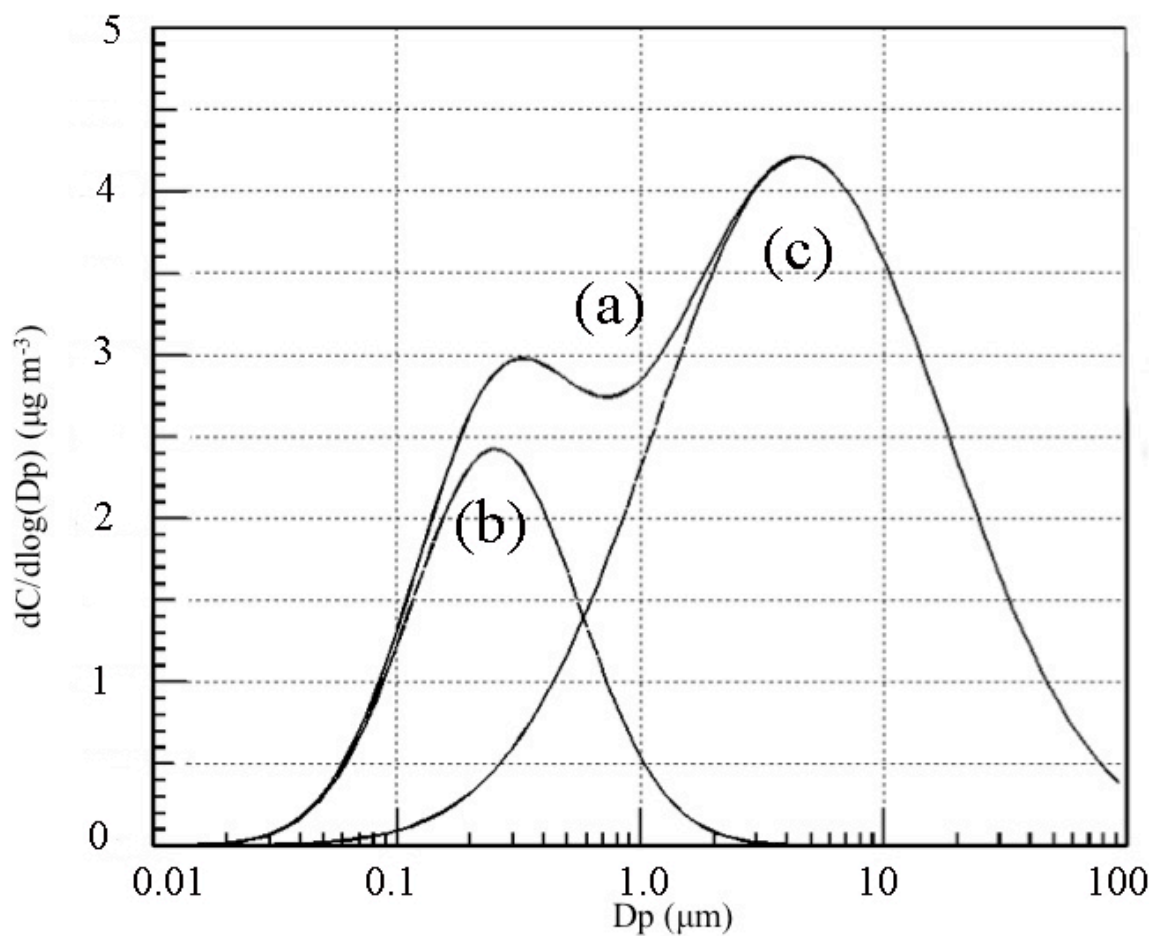
Figure 2.4 Aerosol mass-size distributions over coastal Antarctica by utilizing positive matrix factorization (PMF) - resolved size distribution data with lognormal distribution functions using DISFIT software (TSI, USA). The curve (a) is a general mass size distribution; the curve (b) is the size distribution of the resolved accumulation mode particles; the curve (c) is the size distribution of the resolved coarse mode particles.
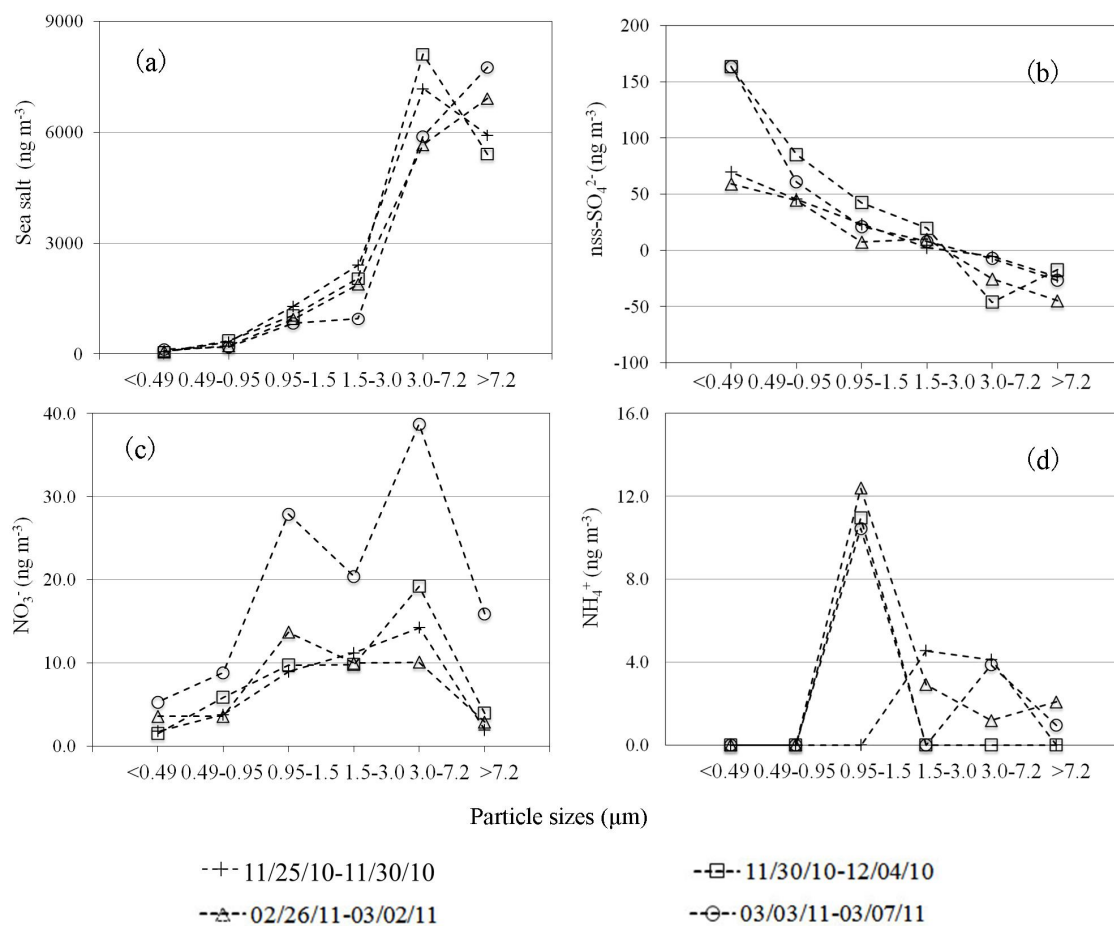
Figure 2.5 Size distributions of water-soluble inorganic compounds in aerosols over the Southern Ocean: (a) sea salt, (b) nss-SO_4^{2-}, (c) NO_3^-, and (d) NH_4^+.
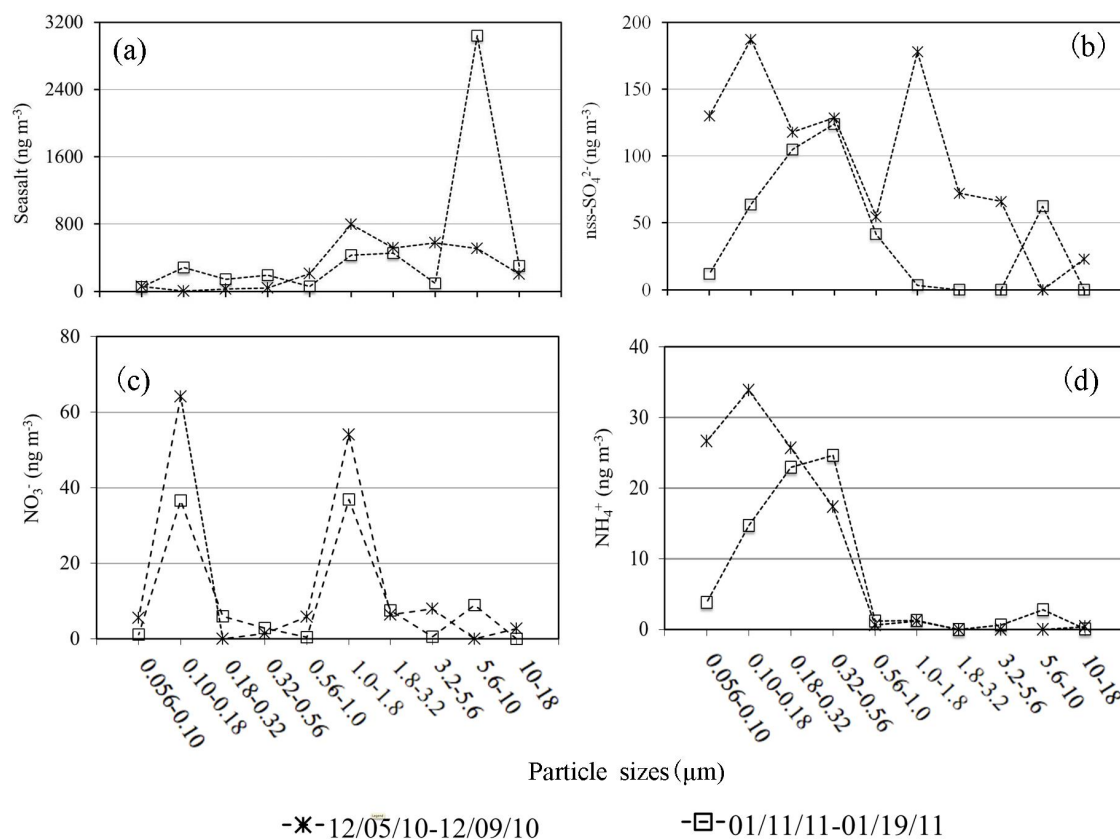
Figure 2.6 Size distributions of aerosol water-soluble inorganic compounds over coastal East Antarctica: (a) sea salt, (b) nss-SO_4^{2-}, (c) NO_3^-, and (d) NH_4^+.
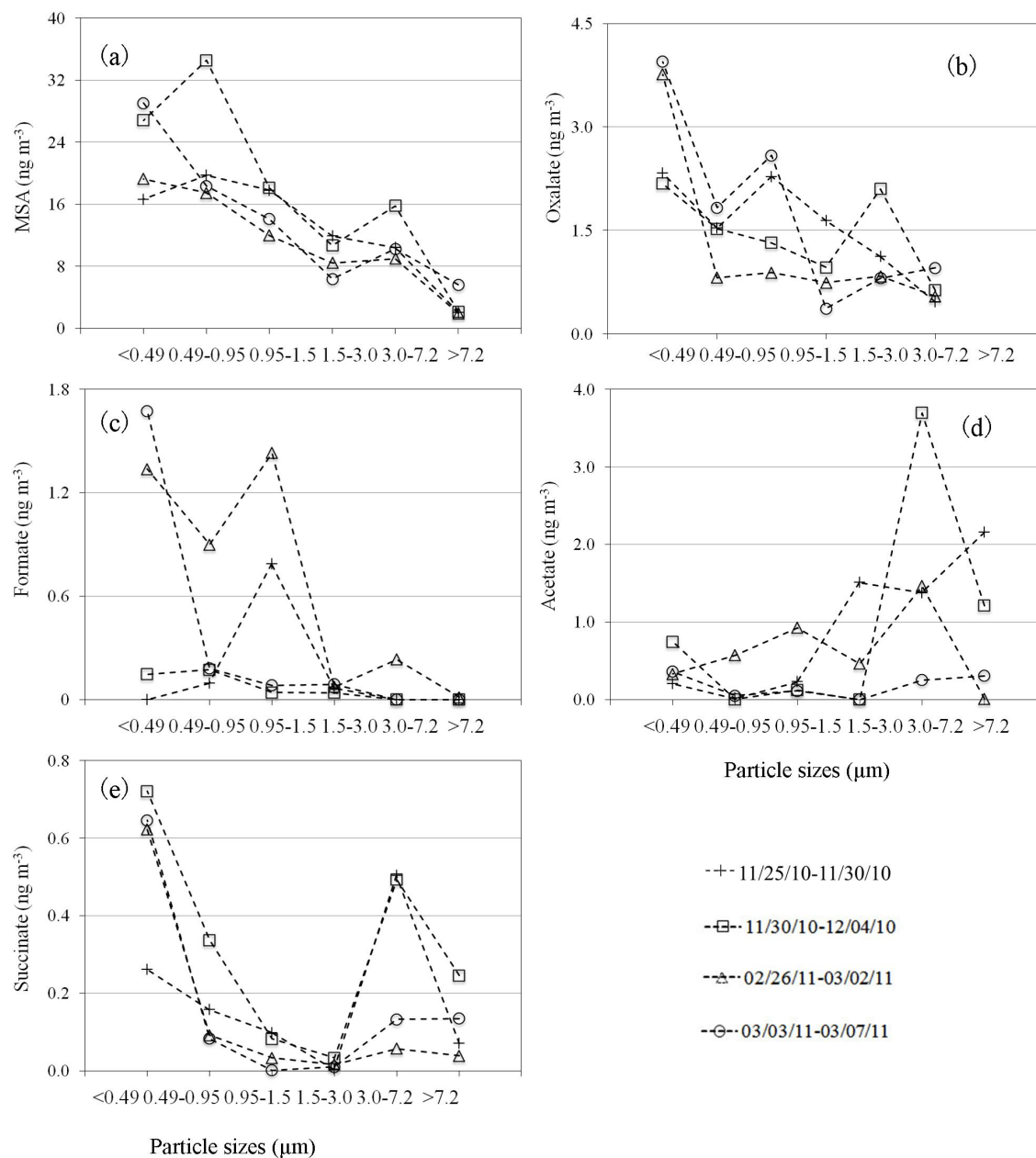
Figure 2.7 Size distributions of aerosol water-soluble organic compounds over the Southern Ocean: (a) MSA, (b) oxalate, (c) formate, (d) acetate, and (e) succinate.
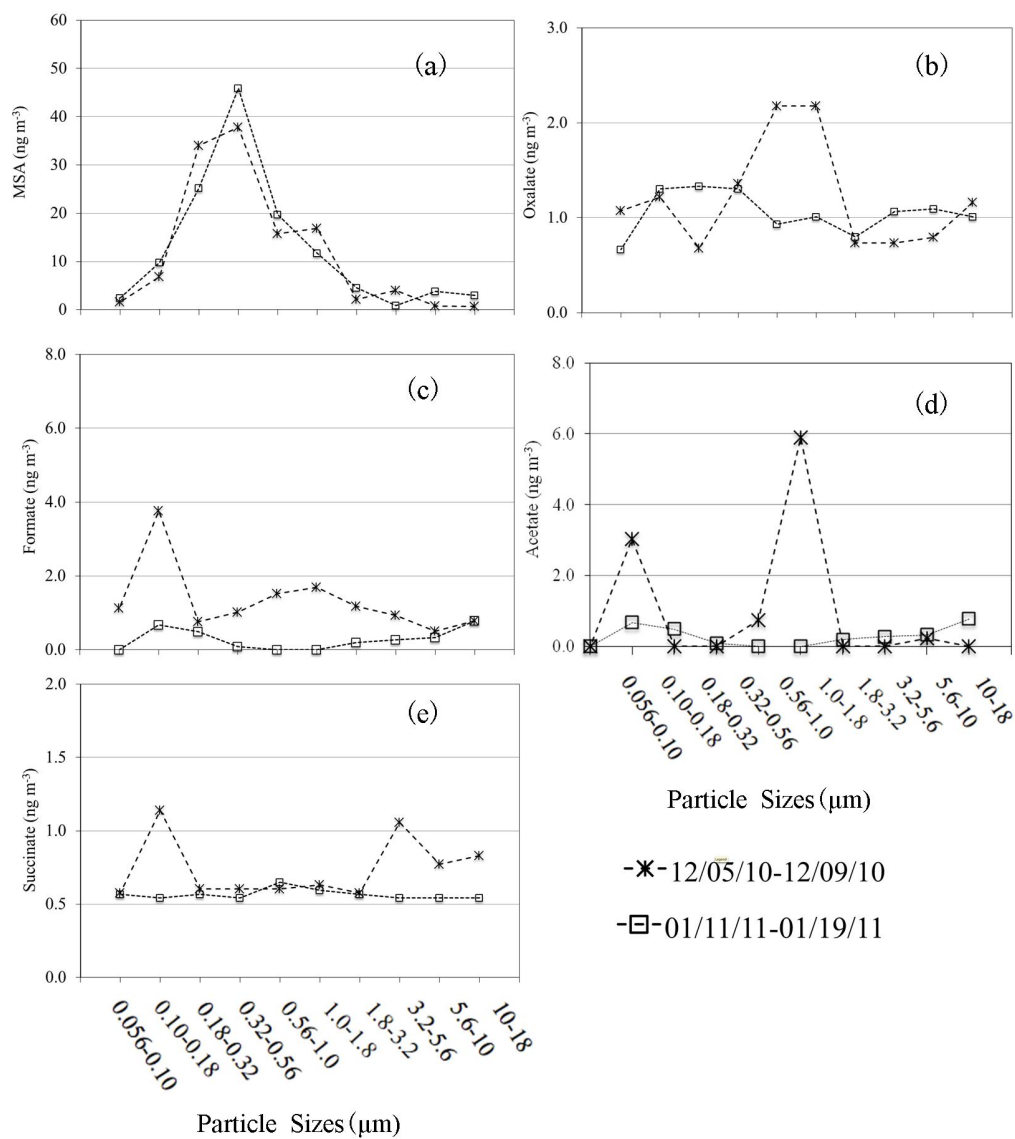
Figure 2.8 Size distributions of aerosol water-soluble organic compounds over coastal East Antarctica: (a) MSA, (b) oxalate, (c) formate, (d) acetate, and (e) succinate.
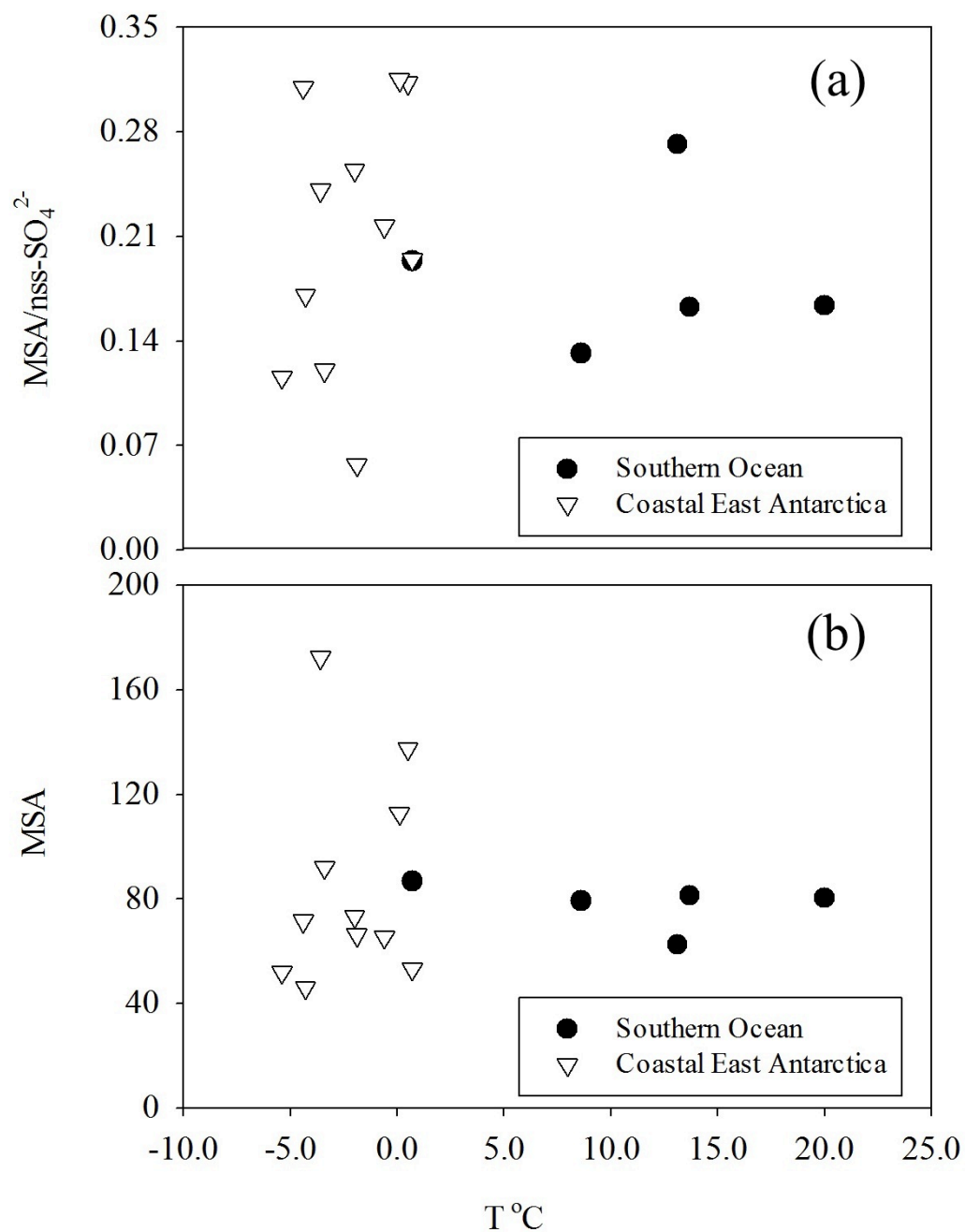
Figure 2.9 (a) Correlations between MSA and T, and (b) correlations between MSA/nss- SO_4^{2-} and T over the Southern Ocean and coastal East Antarctica.
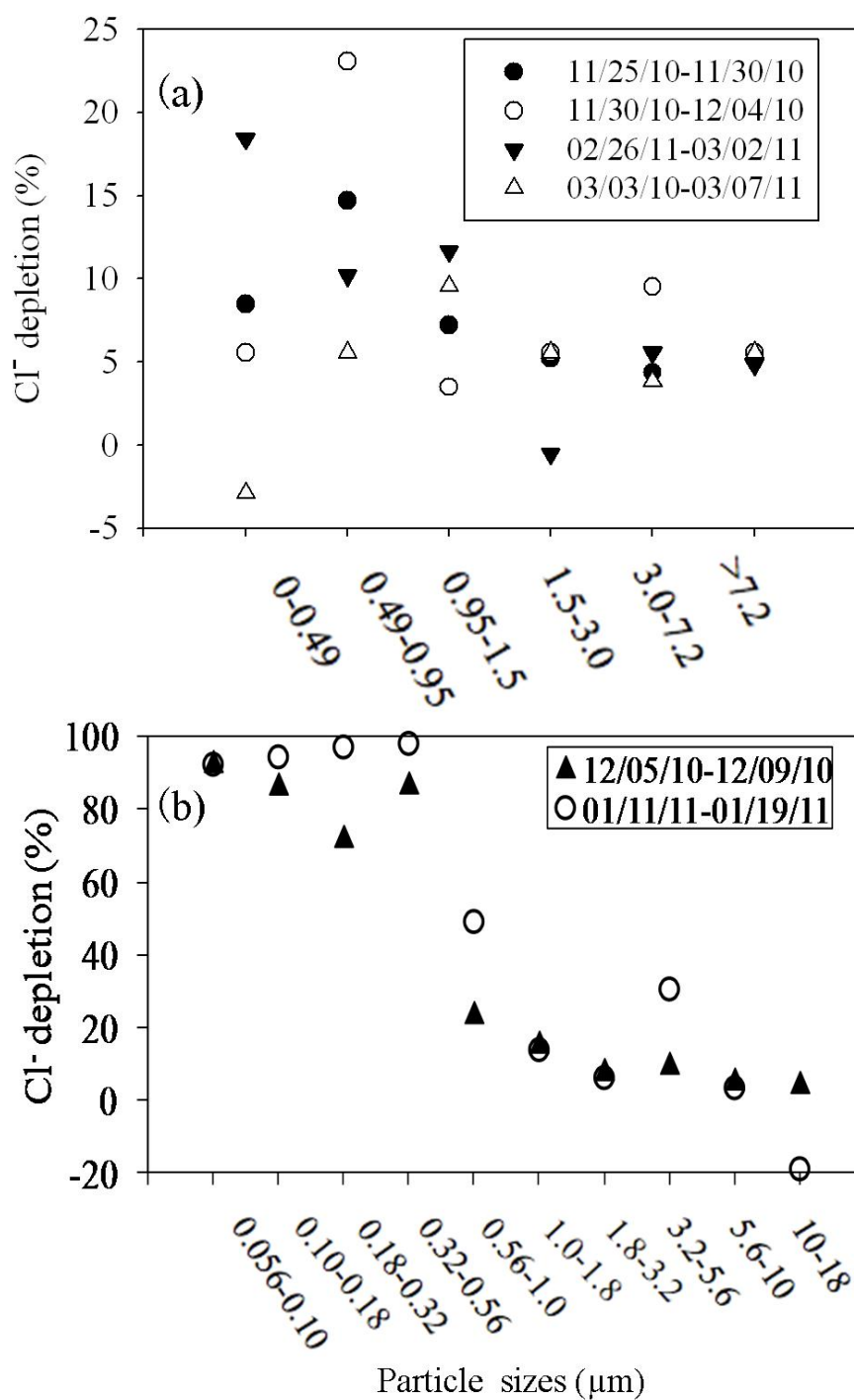
Figure 2.10 Chloride depletion as a function of aerosol particle sizes (a) over the Southern Ocean, and (b) over coastal East Antarctica.
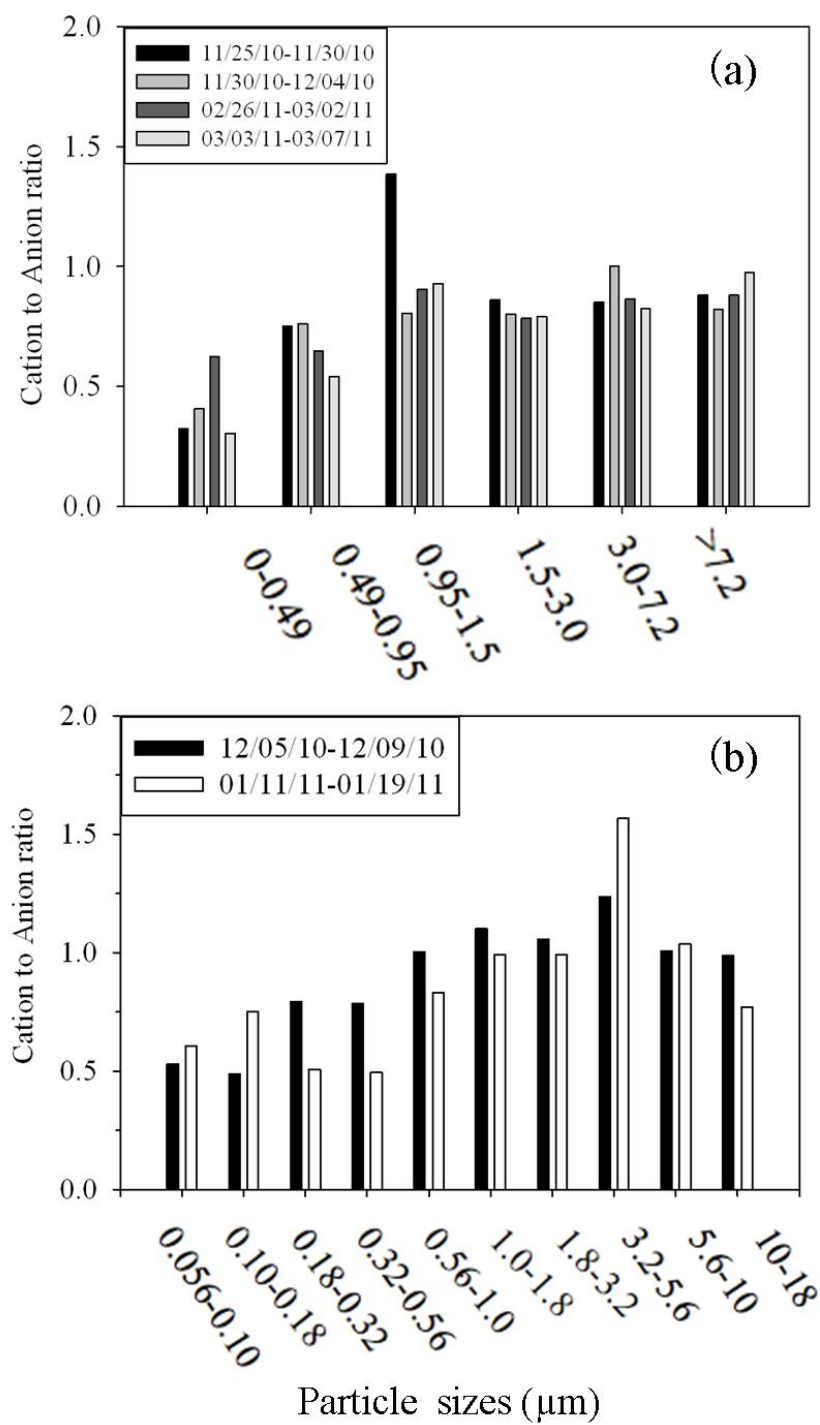
Figure 2.11 Cation-to-anion ratios associated with water-soluble ionic species in aerosols.

(a) is for the Southern Ocean, and (b) is for coastal East Antarctica (Note: The values of

the ratios are calculated from each size range of different samples).

Chapter 3: Atmospheric Trace Elements in Aerosols Observed over the Southern Ocean and Coastal East Antarctica[2]

Abstract

Atmospheric aerosol samples were collected over the Southern Ocean (SO) and coastal East Antarctica (CEA) during the austral summer of 2010-2011. Samples were analysed for trace elements including Na, Mg, K, Al, Fe, Mn, Ni, Cd and Se by inductively coupled plasma mass spectrometry (ICP-MS). The mean atmospheric concentrations over the SO were 1100 ng m^{-3} for Na, 190 ng m^{-3} for Mg, 150 ng m^{-3} for Al, 14 ng m^{-3} for Fe, 0.46 ng m^{-3} for Mn and 0.25 ng m^{-3} for Se. Over CEA, the mean concentrations were 990 ng m^{-3} for Na, 180 ng m^{-3} for Mg, 190 ng m^{-3} for Al, 26 ng m^{-3} for Fe, 0.70 ng m^{-3} for Mn and 0.29 ng m^{-3} for Se. Particle size distributions, enrichment factors and correlation analysis indicate that Na, Mg and K mainly came from the marine source, while Al, Fe and Mn were mainly from the crustal source, which also contributed to Mg and K over CEA. High enrichment factors were associated with Ni, Cd and Se, suggesting likely contributions from mixed sources from the Antarctic continent, long-range transport, marine biogenic emissions and anthropogenic emissions. Sea salt elements (Na, Mg, K) were mainly accumulated in the coarse mode, and crustal elements (Al, Fe, Mn) presented a bimodal size distribution pattern. Bioactive elements (Fe, Ni, Cd) were enriched in the fine mode, especially with samples collected over the SO, possibly affecting biogeochemical cycles in this oceanic region.

Keywords: Southern Ocean; Coastal East Antarctica; Trace elements; Size distribution; Sources.

3.1 Introduction

The Southern Ocean plays a critical role in regulating the global carbon cycle (Reid et al. 2009), and atmospheric aerosols over this region may contribute to regional biogeochemical cycles and atmospheric chemistry [*Jickells et al*., 2005; *Heimburger et al*., 2012; *Gao et al*., 2013]. Atmospheric sea salt and biogenic sulphur are among the major aerosol components over the SO [*Murphy et al*., 1998; *Berg et al*., 1998]. Sea salt aerosol particles contain elements such as Na, Mg, K, Ca [*Murphy et al*., 1998; *D O'Dowd and De Leeuw,* 2007] and sea salt fractionation due to fresh sea ice formation can alter atmospheric chemistry over polar regions [*Hara et al*., 2012]. The seawater bubble bursting processes can also be a source for atmospheric Se, in addition to volcanic and biogenic sources [*Schneider*, 1985; *Weller et al*., 2008]. On the other hand, the trace elements of continental sources (Fe, Mn, Ni) provided by atmospheric long-range transport are required for organisms during photosynthesis, respiration and nitrogen fixation processes [*Price and Morel*, 1990; *Twining and Baines*, 2013; *Moore et al.*, 2013]. Although some of these bioactive elements (Cd, Ni) may act as toxicants at high concentrations to certain marine organisms [*Whitfield*, 2001; *Echeveste et al*., 2014], Fe is a limiting and essential micronutrient for all organisms [*Jickells et al*., 2005]. Recent field measurements have shown that upwelling, dust deposition, entrainment from shelf sediment, and advection of subtropical waters are among the sources of bioavailable iron

to SO waters [*Boyd et al.*, 2004; *Blain et al.*, 2007; *Sedwick et al.*, 2008]. Enhancements in nitrogen fixation and biological blooms correspond to the episodic supply of iron [*Boyd et al.*, 2004; *Frew et al.*, 2001]. In the SO, the atmospheric Fe input contributes to the pool of dissolved Fe [*Blain et al.*, 2007; *Gao et al.*, 2013; *Heimburger et al.*, 2013]. Observations of atmospheric trace elements over the SO have been reported for the Atlantic sector [*Rädlein and Heumann,* 1995; *Witt et al.*, 2006; *Boye et al.*, 2012]. Direct measurements of atmospheric deposition of trace elements has been reported by *Heimburger et al.* [2012] over the Kerguelen Islands (49°18'S, 70°07'E) in the Indian Ocean sector of the SO, and *Witt et al.* [2006] measured the atmospheric concentrations of trace elements during an Indian Ocean Transect at 32°S from Durban, South Africa, to Perth, Australia. However, few observations of atmospheric trace elements have been made south of 50°S in the Indian Ocean sector of the SO.

Antarctica is the most pristine region on the planet, isolated by the SO and circumpolar cyclonic vortex from neighboring continents. This provides ideal opportunities for studying the background of aerosols far from continental sources [*Artaxo et al.*, 1992; *Mouri et al.*, 1997; *Zoller et al.*, 1974; *Dick*, 1991; *Arimoto et al.*, 2008]. Previous observations of trace elements in aerosols were made at the South Pole [*Duce et al.*, 1975; *Maenhaut et al.*, 1979; *Arimoto et al.*, 2008] and over coastal West Antarctica [*Saxena and Ruggiero*, 2013; *Mishra et al.*, 2004]. Even though seasonal patterns of heavy metal concentrations deposited in snow have been conducted in Lambert Glacier basin, East Antarctica [*Hur et al.*, 2007], atmospheric trace elements over coastal East Antarctica (CEA) and the Indian Ocean sector of the SO during the austral summer have

hitherto not been investigated simultaneously.

To quantify the concentrations and size distributions of trace elements in aerosols, atmospheric particulate samples were collected during an Antarctic cruise in the SO and CEA. In this paper, we present the distributions of selected atmospheric trace elements and explored possible sources for them. Results from this study can provide valuable information on aerosol properties over both SO and CEA, contributing to a better understanding of biogeochemical cycles in these regions.

3.2 Sampling and Methods

3.2.1 Shipboard Aerosol Sampling

Aerosol sampling was conducted between the SO and China's Zhongshan Station (69°22'S, 76°22'E), and between Zhongshan Station and Australia's Casey Station (66°17'S, 110°32'E) during the Austral summer from November, 2010 to March, 2011, onboard the Chinese icebreaker, *Xue Long* (Figure 3.1). In this study, the SO was defined as the region between 40°S and 65°S, and coastal Antarctica was defined as the region between 65°S-69°S. The divisions of SO and CEA were made based on three considerations. Firstly, the sea ice extent, which may impact the marine primary productivity [*Nicol et al.*, 2000; *Smith and Comiso,* 2008], is different between these two regions. In austral summer, the region south of 40°S is ice-free, while CEA is covered with pack ice. Sea ice extent and biological productivity could determine the source strength of marine biogenic aerosols, resulting in changes in aerosol chemical composition and size characteristics [*Andreae*, 1986; *Mosher et al.*, 1987; *Trevena and*

Jones, 2012]. Secondly, the air mass origins and wind patterns in the SO and CEA were different. The origins of air masses affecting samples collected over the SO were mainly in the SO (Figure 3.2-1), while samples collected in CEA were mainly impacted by air masses from the Antarctic continent (Figure 3.2-2). This is also confirmed by wind patterns: the SO is under westerly winds, but CEA is affected by katabatic winds from the Antarctic continent [*Hogan*, 1975; *Jourdain and Legrand*, 2001]. Thirdly, the polar front is a distinct boundary between warm and cold air masses, where cyclonic storm systems develop [*Bjerknes and Solberg*, 1922]. *Turner and Thomas* [1994] found that high frequencies of vortex activities occurred within coastal Antarctic regions, which is different from the situation in SO.

Air samplers were assembled on a 3×6 m^2 platform on the ship's eighth floor front deck about 25 meters above the sea surface. To collect size-segregated atmospheric particle samples over the SO, a high-volume cascade impactor (CI) with a flow rate of ~ 1m^3 min^{-1} (Tisch Environmental, Inc., Cleves, Ohio) was used, and acid-washed Whatman 41 cellulose filters were used as the sampling media. The aerodynamic cut-off diameters of this sampler were 0.49, 0.95, 1.5, 3.0, and 7.2 μm, respectively. To separate the fine and coarse mode particles, 1.5 μm was used as a cut-off size. Over CEA, a 10-stage Micro-Orifice Uniform Deposit Impactor (MOUDI, MSP Corp., Shoreview, MN) with flow rate of 30 L min^{-1} was used, and Teflon filters (Pall Corp., 47 mm diameter, 1 μm pore size) were used as sampling substrates to collect the size-segregated aerosol samples. The 50% cut-off mass median aerodynamic diameters of the MOUDI were 0.056, 0.10, 0.18, 0.32, 0.56, 1.0, 1.8, 3.2, 5.6, 10 and 18 μm. A cut-off size 1.8 μm was used to separate the fine

and coarse aerosol fractions. Total suspended particles were also collected during this cruise, using Model 3500 Chemcomb Cartridge devices (Thermo Scientific, MA) with a flow rate of ~ 15 L min^{-1} and polytetrafluoroethylene filters (47 mm diameter, 1.0 μm pore size) as sampling substrates. To avoid contamination from the ship, a wind speed and direction system installed on the same sampling platform was utilized to control all sampling instruments, which operated sampling only when the wind was from a sector 90° left and right on the centre line of the ship's path and at wind speeds > 2 m s^{-1}. During sampling, loading and unloading of the filters were conducted in a 100-class high-efficiency particulate air -filtered laminar flow clean-room hood in the ship's chemical laboratory, following clean-room operation procedures. After sampling, sample filters with field blanks were kept in the refrigerator at 4°C in the ship. Detailed sampling information is in Table 3.1.

3.2.2 Chemical Analyses

Aerosol samples were analysed for elements, including Na, Mg, K, Al, Fe, Mn, Ni, Cd, and Se through ICP-MS (7500ce, Agilent) at the Third Institute of Oceanography, China, following the same methods described by *Gao et al.* [2013]. Briefly, one quarter from each aerosol sample filter was digested with concentrated HNO_3 in a Microwave Accelerated Reaction System (MARs, CEM Corporation). Three steps in the digestion process were used: (1) heating to 170±5 °C in 5.5 min, (2) keeping at 170±5 °C for 30 min for finishing digestion, and (3) cooling down for 20 min. Digested solutions were diluted with Milli-Q water to achieve an acidity of 4% and then injected into the ICP-MS system. The detection limits were ~0.001 ng m^{-3} for Na, Mg and K; ~0.003 ng m^{-3} for Fe,

Ni and Se and ~0.005 ng m^{-3} for Cd in this study. The average precision for replicate

samples was ~2%, and the overall average field blank levels were ~2% relative to

samples. The recoveries of trace elements by this digestion method were determined by

utilizing the environmental calibration standard 5183-4688 from Agilent Technologies,

based on the same digestion and analysis as our samples. The results showed that the

recoveries of Na, Mg, K, Al, Fe, Mn, Ni, Cd, Se ranged from 93% to 101%. External

standards curves were constructed (R^2>0.9999) for the determinations of trace elements

in samples. The final concentrations of selected trace elements in samples were obtained

after subtraction of their appropriate field blanks.

3.2.3 Data Analyses

(1) Meteorological Data Analyses

During sampling periods, the meteorological data including air temperature, air pressure,

relative humidity, wind speed and wind direction were obtained from the ship's weather

stations (Table 3.1). To explore possible sources of the observed trace elements in

aerosols, air mass back trajectories were performed at 50 and 500 m height above the

ground over the sampling locations every six hours, going backward seven days. The

trajectories were calculated from the National Oceanic and Atmospheric Administration

Global Data Assimilation System meteorology database [*Draxler and Rolph*, 2014],

using the HYbrid Single-Particle Lagrangian Integrated Trajectory (HYSPLIT) program.

(2) Enrichment factor (EF)

The use of an enrichment factor (EF) is a first-step of source identification to differentiate

the possible sources of atmospheric trace elements observed in this study. EF is defined as follows:

$$EF_i=(X_i/X_r)_{air} /(X_i/X_r)_{sou}$$

where EFi is the EF of element i, r is the reference element, $(X_i/X_r)_{air}$ is the concentration ratio of element i over the reference element r in aerosols, and $(X_i/X_r)_{sou}$ is the abundance ratio of element i over r in source materials. In this paper, EFs_i is the EF for the source of sea water by utilizing Na as the reference element abundant in the ocean waters [*Millero*, 2013]. EFc_i is the enrichment factor for crustal source, with Fe being chosen as the representative element of crustal materials [*Taylor*, 1964], as good correlations among typical crustal elements (Fe, Mn and Al) were found in this study over the SO and CEA ($R^2>0.5$, n=17). If an EF value for an element is less than 10, the source represented by element r is likely the source for element i; if EF>10, it can be considered that element i has another source, as the element i is greatly enriched relative to element r [*Chester et al.,* 1991; *Weller et al.*, 2008].

3.3. Results and Discussions

3.3.1 Mass Concentration Distributions

3.3.1.1 Elements Na, Mg, K

Results showed that the average concentrations of Na were 1100 ng m^{-3} over the SO and 990 ng m^{-3} over CEA, while the highest observed Na concentrations were 2700 ng m^{-3} over the SO and 1800 ng m^{-3} over CEA (Table 3.2). The mean concentration of Na observed over CEA was comparable with that reported by *Artaxo et al.* [1992] over the Antarctic Peninsula, which was 1046.2 ng m^{-3}. *Xu et al.* [2013] showed that sea-salt

aerosols in bulk samples contributed to ~72% of the mass over the SO and ~56% in CEA. Significant latitudinal gradient of sea salt aerosol indicated by Na was observed over the SO (Table 3.2) affected by the variation of wind speeds. The strong westerly wind with speed >13 m s^{-1} over the SO could explain the observed high concentrations of sea salt elements. The average concentrations of both Mg and K were < 200 ng m^{-3} over the SO and CEA. Sea spray or bubble-bursting processes in the SO was the dominant source for the observed sea salt elements over these regions [*Minikin et al.*, 1998; *Wagenbach et al.*, 1998]. The concentrations of sea-salt elements (Na, Mg and K) observed in CEA during this study in austral summer were more than four times higher than those at Neumayer Station, located at 70°39'S, 8°15'W [*Weller et al.*, 2008]. This difference in sea salt concentrations could be explained by the distance to open water as aerosol sampling conducted by *Weller et al*. [2008] was made on land, about 1.5 km south of Neumayer Station which is more than 10 km from open water. The presence of sea ice in CEA may contribute to Na depletion in sea salt aerosol from sea ice through the formation of mirabilite ($Na_2SO_4 \cdot 10H_2O$) [*Kalnajs et al.*, 2013; *Yang et al.*, 2008; *Fattori et al.*, 2005]. *Rankin and Wolff* [2003] found that over the coast of the Weddell Sea, 60% of the total sea salt came from brine and frost flowers on the sea ice rather than open water. *Hara et al*. [2012] conducted aerosol sampling at Syowa Station and found that fractionated sea-salt particles were accumulated in the ultrafine-coarse modes, with higher Mg^{2+}/Na^+ and K^+/Na^+ ratios compared with those of bulk seawater. In this study, higher Mg^{2+}/Na^+ and K^+/Na^+ ratios than those of bulk seawater were also found in aerosol samples collected in CEA, implying that Na depletion may affect the EF calculation using Na as the representative element for sea water. However, *Weller et al*. [2008] concluded that sea

salt fractionation could cause ~11.8% of Na depletion by mass, leading to an increase of the EF to ~1.12 in winter, when sea salt fractionation was most active. Therefore, the Na depletion process may not affect the general EF results in this study. Further investigation is needed to solve this problem.

3.3.1.2 Elements Al, Fe, Mn

The concentrations of total Al ranged from 77 to 240 ng m^{-3} over the SO (average 150 ng m^{-3}) and from 130 to 310 ng m^{-3} over CEA (average 190 ng m^{-3}) (Table 3.2). Over the SO, the concentrations of total Fe ranged from 6.1 to 38 ng m^{-3} (average: 14 ng m^{-3}) and 14 to 56 ng m^{-3} (average: 27 ng m^{-3}) over CEA. One explanation for the high Fe concentration (56 ng m^{-3}) observed in the areas of 64-66°S, 103°E could be due to possible contributions by local dry lands as suggested by *Gao et al*. [2013]. Compared with the results (average Fe: 130 ng m^{-3}) from McMurdo Station (77°51'S, 166°40'E) [*Mazzera et al*., 2001], relatively low Fe concentrations in aerosols were observed over both the SO and CEA during this study. The high Fe concentrations around McMurdo Station could be affected by local sources and an active volcano existed [*Kyle et al*., 1990]. The concentrations of total Mn ranged from 0.2 to 0.9 ng m^{-3} over the SO (average: 0.46 ng m^{-3}) and from 0.45 to 1.2 ng m^{-3} over CEA (average: 0.70 ng m^{-3}) (Table 3.2). Low Mn concentrations were observed over the South Pole during the austral summer with arithmetic mean of 0.013 ng m^{-3} [*Maenhaut et al*., 1979], while high Mn concentrations (average: 2.5 ng m^{-3}) in ambient PM_{10} samples were observed at McMurdo Station [*Mazzera et al*., 2001]. *Wagenbach et al*. [1988] utilized Mn as the reference element for crustal aerosol and founded the maximum Mn over coastal west

Antarctica (70°S, 8°W) in the austral summer, during which crustal aerosol concentration was more than two times higher than the mean concentration. Similar seasonal maxima for crustal elements in aerosols were also observed at Neumayer Station by *Weller et al.* [2008], who concluded that the crustal elements (Al, La, Ce and Nd) in aerosols showed the maximum during the austral summer, with the summer mean 1.7 times the annual mean. The concentrations of crustal elements (Fe, Mn) observed during this study were comparable with studies in the SO and coastal Antarctic sites by other investigators [*Bowie et al.*, 2009; *Chester et al.*, 1991; *Mishra et al.*, 2004; *Rädlein and Heumann*, 1992]. In addition, significant spatial variations in the concentrations of both Fe and Mn were found over the SO. Aerosol samples collected over the SO, especially aerosol collected from $< 40^{o}S$ near west Australia, could be influenced by dust from Australia deserts [*Tanaka and Chiba*, 2006], although dust may also be carried by long-range transport from the continents, such as Patagonia [*Johnson et al.*, 2011] and South Africa [*Gassó and Stein,* 2007]. However, aerosols over CEA could be affected by coastal Antarctic local sources, which can be indicated by the air mass back trajectories (Figure 3.2). The McMurdo Dry Valleys is one potential source contributing to the observed high crustal elements concentrations in this study, as discussed in more detail in *Gao et al.* [2013].

3.3.1.3 Elements Ni, Cd, Se

The observed Ni concentrations ranged from 0 to 0.07 ng m^{-3} over the SO (average: 0.01 ng m^{-3}) and from 0 to 2.2 ng m^{-3} over CEA (average: 0.75 ng m^{-3}), while the observed Cd concentrations ranged from 0 to 0.02 ng m^{-3} over the SO (average: 0.004 ng m^{-3}) and

from 0 to 0.05 ng m^{-3} over CEA (average: 0.017 ng m^{-3}) during the austral summer. These results were comparable to previous observations over the SO and CEA. *Ezat et al.* [1994] investigated the long-range atmospheric transport of aerosols to the Southern Indian Ocean, and they found that the average ambient concentration of Ni was 0.25 ng m^{-3}. *Artaxo et al.* [1992] conducted aerosols observations over the Antarctic Peninsula, and they concluded that in the fine mode particles, the Ni concentration was 0.076 ng m^{-3} during the summer, while PM$_{10}$ observation at McMurdo Station revealed that the average Ni concentration was 0.14 ng m^{-3} [*Mazzera et al.*, 2001]. However, *Maenhaut et al.* [1979] measured the concentrations and size distributions of trace elements in aerosols in the South Pole atmosphere, and reported that the arithmetic means atmospheric concentration of Cd was <0.018 ng m^{-3}. *Annibaldi et al.* [2007] conducted research on water-soluble and insoluble fractions of Cd in Antarctic aerosols at Terra Nova Bay and found that total extractable (soluble portion and in-soluble portion) fractions of Cd in PM$_{10}$ aerosol samples ranged from 0.0006 ng m^{-3} to ~ 0.006 ng m^{-3} (average concentration 0.003 ng m^{-3}). Higher average concentrations of Ni and Cd over CEA than these over the SO may suggest possible sources for these elements around coastal Antarctica, although other factors may also affect their concentrations in this region, such as the impacts of different meteorological conditions and long-range transport from other continents [*Mishra et al.*, 2004].

The observed Se concentrations ranged from 0.09 to 0.4 ng m^{-3} over the SO (average: 0.25 ng m^{-3}) and from 0.09 to 0.64 ng m^{-3} over CEA (average: 0.29 ng m^{-3}) during the austral summer. Observations over the South Pole showed that the average ambient

concentration of Se was ~ 0.006 ng m^{-3} during the summer time [*Zoller et al.*, 1974; *Cunningham and Zoller*, 1981], while observations by *Artaxo et al.* [1992] showed that average atmospheric concentration of Se was 0.064 ng m^{-3} over the Antarctic Peninsula. At Neumayer Station, *Weller et al.* [2008] reported that average ambient concentration of Se was 0.025 ng m^{-3} during the austral summer. Different source processes could explain the geographical variability of Se concentrations. *Weller et al.* [2008] further investigated the potential source of Se and concluded that a distinct ambient Se concentration maximum existed in austral summer and there was a significant correlation between Se and sulphur-containing species (methane sulfonate (MSA) and non-sea salt sulphate (nss-SO$_4^{2-}$)) (r(MSA)=0.66; r(nss-SO$_4^{2-}$) =0.67), indicating a potential marine biogenic source for this element. However, no good correlation between MSA or nss-SO$_4^{2-}$ and Se (r(MSA)=0.09; r(nss-SO$_4^{2-}$)=0.22) was found in this study, which implies that the existence of Se in aerosols in these regions is not solely explained by marine biogenic emissions. Other potential sources of Se could be volcanic emissions, as pointed out by *Cunningham and Zoller* [1981] who stated that the atmospheric load of volatile elements including Se could be influenced by volcanic emissions. Sea spray, volcanoes and the biogenic emissions could explain ~60% of the atmospheric Se budget [*Weller et al.*, 2008]. In general, the concentrations of Ni, Cd and Se observed during this study were low and comparable with previous observations [*Rädlein and Heumann*, 1992 and 1995; *Annibaldi et al.*, 2007; *Weller et al.*, 2008].

3.3.2 Particle Size Distributions

3.3.2.1 Over the Southern Ocean

Figure 3.3 shows the size distributions of selected trace elements (Na, Mg, K, Al, Fe, Mn, Ni, Cd and Se) in aerosols over the SO derived from four sets of CI samples. The element Na, Mg and K were mainly accumulated in the coarse mode with particle size >3μm. Sea-salt aerosol over the SO was strongly influenced by westerly winds, which was consistent with the concentration variation and size distribution of sea salt under the high wind speed condition reviewed by *D O'Dowd et al.* [1997]. *Chester et al.* [1990] also concluded that sea-salt-generated elements mainly existed in particle size range from approximately 3 μm to more than 7 μm. The elements Al, Fe and Mn showed a bimodal size distribution, with size peaks both in the fine mode (<0.95 μm) and coarse modes (>3 μm), but the mass concentrations were mainly accumulated in the fine mode. However, the elements Ni and Cd were mainly accumulated in the fine mode (size <0.49 μm) over the SO, while Se presented a size distribution pattern with peaks at size <0.49 μm, 0.95-1.5 μm and 3-7.2 μm. The coarse mode fractions of Al, Fe, Mn, Ni, Cd and Se in aerosols could be explained by the crustal source, having mass median diameters ranging from about 1 to about 3 μm [*Chester*, 1990]. The fine mode fractions, in contrast, could be attributed to long-range transported dust, volcanic processes, and anthropogenic processes [*Chester*, 1990].

3.3.2.2 Over Coastal East Antarctica

Figure 3.4 shows the size distributions of selected trace elements (Na, Mg, K, Al, Fe, Mn, Ni, Cd and Se) in aerosols over CEA derived from two sets of MOUDI samples (Figure 3.4). The results showed that Na, Mg and K mainly existed in the coarse mode (particle size >1.8 μm), which could be explained by the contributions from sea spray over the

Antarctic coastal seas [*Minikin et al.,* 1998; *Wagenbach et al*., 1998]. The element Al, Fe, Mn, Ni, Cd and Se displayed bimodal size distribution patterns, peaking at both fine mode (size <1.8 μm) and coarse mode (size >1.8 μm), but their mass concentrations were mainly accumulated in the coarse mode, except for Cd and Se. *Gao et al*. [2013] indicated that the size peak of atmospheric Fe in the coarse mode could be derived from crustal substances from regional sources in Antarctica. They investigated the dust source region with air mass back trajectories and suggested that McMurdo Dry Valleys could bring in crustal materials to coastal Antarctic sites. Therefore, the presence of Al, Fe, Mn, Ni, Cd and Se in coarse mode particles could be attributed to local aeolian inputs; however, further research is required to justify this interpretation. Different chemical and physical processes (such as the chemical weathering of rocks and wind speeds) may be involved and reflected by different size distributions of these elements in the regions, and the size distributions of different metals should depend on the balance of different sources: marine, crustal, biogenic and anthropogenic [*Grgić*, 2009].

3.3.3 Sources Identification of Trace Elements in Aerosols

3.3.3.1 Enrichment Factor

Results from both CI and MOUDI samples were separated into fine and coarse modes to explore the possible particle-size distribution/sources relationships. The calculated EF (EFs and EFc) of trace elements in both fine and coarse particles over the SO is shown in Figure 3.5. Mg and K in both fine and coarse modes had EFs<10 and EFc>10, suggesting they originated from marine sources. In contrast, Mn and Al in both modes had EFs>10 and EFc<10, suggesting they were derived from crustal sources (Figure 3.5). However,

EFs and EFc of Ni, Cd and Se were much higher than the threshold (10) both for marine

and crustal sources, suggesting additional sources for these elements. The calculated EFs

and EFc of trace elements in both fine and coarse particles over CEA are shown in Figure

3.6. Both EFs and EFc of Cd and Se were higher than the marine and crustal threshold

(10). Therefore, additional sources, such as biogenic emissions, volcano eruptions and

anthropogenic emissions, need to be considered to explore the additional sources for

these two elements [*Rädlein and Heumann,* 1995; *Pacyna and Pacyna,* 2001]. Mn and Al

in both particle size modes were from the crustal source as EFc<10 and EFs>10, while

Mg and K in both modes had EFs<10. However, K in both modes had EFc<10, and Mg

in fine mode had EFc<10 over CEA. Crustal sources may therefore contribute to Mg and

K in CEA. Ni in fine mode had EFc<10, but EFs>1000, indicating that contributions

from crustal source may explain this fraction of Ni in aerosols [*Cempel and Nikel*, 2006].

3.3.3.2 Correlations between Selected Trace Elements

To further explore sources of selected trace elements (Na, Mg, K, Al, Fe, Mn, Ni, Cd and

Se) in aerosols over the SO and CEA, correlations between each element were calculated

in both fine and coarse modes (n=6), which are shown in Table 3.3. In the fine mode

particles, significant correlations were found between Na and Mg (Pearson coefficient

>0.9, p<0.001), and between K and Mg (Pearson coefficient >0.8, p<0.05), suggesting

that Na and Mg were mainly derived from seawater, even though Mg and K had certain

contributions from crustal sources in CEA, as inferred by the EF. Good correlations

(Pearson coefficient >0.9, p<0.001) between Fe, Al and Mn revealed that these three

elements in the fine mode shared common sources. Notable correlations were also found

between Cd, Se and Fe (Pearson coefficient >0.8, p<0.05), suggesting that atmospheric Fe, Al, Mn, Cd and Se in the fine fraction could be derived from dust carried by long-range transport, during which particle fractionation occurred and their lifetime as smaller particles in the atmosphere was extended [*Seinfeld and Pandis,* 2006]. In the coarse mode, significant correlations appeared between Fe, Al, Mn and K (Pearson coefficient >0.9, p<0.001, except for that between Fe and K (Pearson coefficient >0.8, p<0.05). Together with the EF results (EFs and EFc), this indicates that Fe, Al and Mn mainly came from crustal sources, which also contributed to K in coarse mode particles. Significant correlation between Mn, Cd and Se (Pearson coefficient >0.9, p<0.001) imply crustal inputs of these elements in coarse mode particles, while significant correlations between Mg, Cd and Se (Pearson coefficient >0.8, p<0.05) also indicated that sea salt could be the source of these elements in the coarse mode.

3.4 Implication for Aerosol Impacts on Climate and Biogeochemical Cycling

Aerosols play an important role in climate and biogeochemistry cycling [*Charlson et al*., 1987; *Jickells et al*., 2005; *Mahowald*, 2011]. These particles modify the radiation budget of the atmosphere, both directly and indirectly [*D O'Dowd and De Leeuw*, 2007]. Aerosols affect the radiation budget indirectly through affecting microphysical, optical and radiative properties of clouds by serving as cloud condensation nuclei (CCN) or ice nuclei (IN) [*Albrecht*, 1989; *DeMott et al*., 2003], depending on their chemical composition and size [*Dusek et al*., 2006]. In this study, the particle size distributions of Fe and Mn in aerosols observed over the SO were mainly accumulated at the fine mode (<0.49 μm), largely in the size mode of CCN. This result implies that these fine mineral

aerosol particles could act as CCN, affecting cloud albedo over the SO. Mineral aerosols can also interact with sulphate and nitrogen containing species during their transport in the atmosphere, and form internally mixed particles, further modifying the ability of mineral particles acting as CCN [*Dentener et al*., 1996; *Levin et al*., 2005]. Moreover, mineral aerosols have been known to be effective IN, playing a vital role in ice crystal formation in high clouds [*DeMott et al*., 2003; *Cziczo et al*., 2009]. These ice crystals could affect the radiation budget, the hydrological cycle, and water vapor distribution in the atmosphere [*Demott et al.* 2010; *Avramov and Harrington* 2010]. Sea salt particles can also act as efficient CCN [*Murphy at al*., 1998; *Pierce and Adams*, 2006].

Additionally, over the global ocean, the mean concentrations of atmospheric Fe, Ni and Cd were 550 ng m^{-3}, 2.1 ng m^{-3}, and 0.1 ng m^{-3}, respectively [*Heintzenberg et al*., 2000]. Once deposited, these bioactive elements can affect the growth of phytoplankton in the euphotic zone of the ocean [*Bruland et al.,* 1991; *Morel and Price,* 2003]. Profiles for dissolved Fe, Ni and Cd in the ocean generally show the patterns of surface depletion and deep-water enrichment, resulting from the uptake by biota in surface waters and regeneration of sinking particles in deep waters [*Norisuye et al.*, 2007; *Millero*, 2013]. These elements are required by phytoplankton during various metabolic processes [*Price and Morel,* 1991; *Cullen et al*., 1999]. *Lane and Morel* [2000] reported that Cd could act as a Cd-specific carbonic anhydrase in certain diatoms. In general, Fe, Ni and Cd in seawater play a critical role in regulating oceanic phytoplankton growth and, hence, may influence the global carbon cycle.

However, measurements of in-situ speciation and bio-reactivity of bioactive elements are few, both in the surface waters of the SO and its marine atmosphere. *Sarthou et al.* [2011] showed that higher values of labile Fe(II) were found in the surface mixed layer than in deep waters toward high latitudes, which could be contributed to atmospheric Fe(II) deposition [*Gao et al.*, 2013]. *Gao et al.* [2013] reported that total dissolvable Fe air-sea deposition fluxes were 0.007-0.52 mg m^{-2} yr^{-1} over the SO. The atmospheric dissolvable Fe input contributes to the dissolved Fe pool in SO surface waters, supporting marine primary production [*Chever et al.*, 2010]. In any case, once these elements get into the seawater, they are present in different chemical forms such as free ionic, labile bound, and strongly bound to organic ligands [*Baeyens et al.*, 2011]. However, not all of these forms are accessible to phytoplankton, and they need to be in free ionic or labile bound forms [*Baeyens et al.*, 2011; *Davlson and Zhang*, 1994*; Morel and Price*, 2003] in order to cross the phytoplankton cell membrane. In this study, the observed atmospheric Ni and Cd concentrations were low compared with Fe, but these three elements (Fe, Ni and Cd) were mainly accumulated in the fine mode. Once deposited into the ocean, these elements in fine particles may be more easily dissolved than coarse mode particles and get involved in bio-interaction through colloidal aggregation and organic complexation by phytoplankton [*Wells*, 2002]. However, precisely defining these elements' bioavailability precisely is challenging, as it involves complicated interactions among biogeochemical processes, biological organisms, trace elements chemistry, and ambient environmental conditions.

Table 3.1 Sampling information.

Sample type	No.	Sampling date	Lat(°S), Long (°E)	WS* (m s⁻¹)	AT* (°C)	RH* (%)	AP* (hPa)
TSP (T)	T1	25/11/10 - 27/11/10	34°S, 109°E-41°S, 100°E	14.1	8.8	68.4	1026
	T2	27/11/10 - 30/11/10	42°S, 100°E-56°S, 94°E	6.9	13.1	78.2	1014
	T3	30/11/10 - 02/12/10	56°S, 94°E-62°S, 81°E	14.5	0.7	94.5	995
	T4	03/12/10 - 04/12/10	65°S, 78°E-69°S, 94°E	13.4	-3.4	79.5	985
	T5	05/12/10 - 07/12/10	69°S, 76°E-69°S, 76°E	4.2	-2	55.9	996
	T6	11/01/11 - 19/01/11	69°S, 75°E-64°S, 102°E	5.8	0.5	83.3	997
	T7	19/01/11	64°S, 103°E-66°S, 110°E	5.9	0.7	76.2	999
	T8	26/01/11 - 28/01/11	66°S, 110°E-65°S, 87°E	8.1	0.1	73.5	988
	T9	28/01/11-30/01/11	64°S, 84°E-69°S, 76°E	6.3	-0.6	78.3	996
	T10	10/02/11-11/02/11	69°S, 78°E	6	-4.3	45.3	986
	T11	12/02/11-15/02/11	69°S, 77°E	7.8	-4.4	48	992
	T12	15/02/11-18/02/11	69°S, 77°E-69°S, 78°E	11.7	-3.6	47.8	995
	T13	22/02/11-23/02/11	69°S, 77°E - 69°S, 75°E	9.2	-7.1	62	982
	T14	26/02/11-01/03/11	69°S, 76°E-57°S, 76°E	10.6	-1.9	82.3	983
	T15	02/03/11-04/03/11	58°S, 81°E-44°S, 96°E	9.4	8.6	70.1	1018
	T16	04/03/11-06/03/11	44°S, 96°E-36°S, 102°E	7.7	13.7	67.5	1023
	T17	06/03/11-08/03/11	35°S, 102°E-32°S, 115°E	13.8	20	59.9	1019
Cascade Impactor (CI)	CI1	25/11/10-30/11/11	34°S,109°E-56°S, 94°E	11.3	9.9	74.1	1019
	CI2	30/11/10-04/12/10	56°S, 94°E-69°S, 76°E	16.1	-1.2	89.2	988
	CI3	26/02/11-02/03/11	69°S, 76°E-52°S, 84°E	11.3	-0.3	85.4	987
	CI4	03/03/11-07/03/11	48°S, 89°E-33°S, 110°E	9.3	14.3	63.6	1023
MOUDI (M)	M1	11/01/11-19/01/11	69°S, 75°E-66°S, 110°E	5.8	0.5	82.7	997
	M2	26/01/11-30/01/11	66°S, 110°E-69°S, 76°S	7.4	-0.2	76	991

*WS stands for wind speed; AT stands for air temperature; RH stands for relative humidity; AP stands for air pressure.

Table 3.2 Elements concentration over the Southern Ocean (SO) and coastal East Antarctica (CEA).

Region	Sample ID	Trace Elements (ng m^{-3})								
		Na	Mg	K	Al	Fe	Mn	Ni	Cd	Se
SO	T1	2700	360	150	110	8.1	0.29	0	0	0.19
	T2	180	49	58	77	6.1	0.2	0	0	0.09
	T3	1700	230	120	140	10	0.25	0	0	0.17
	T14	230	88	100	140	11	0.46	0	0	0.4
	T15	1200	220	210	240	38	0.73	0.07	0.02	0.11
	T16	880	220	140	180	15	0.9	0	0.01	0.36
	T17	790	130	140	160	12	0.39	0	0	0.4
	Range	180-2700	49-360	58-210	77-240	6.1-38	0.2-0.9	0-0.07	0-0.02	0.09-0.4
	Average	1100	190	130	150	14	0.46	0.01	0.004	0.25
CEA	T4	620	150	220	270	29	0.75	0.59	0	0.2
	T5	160	62	76	160	14	0.61	0	0	0.11
	T6	1800	260	170	150	20	0.54	1.7	0.02	0.09
	T7	1800	310	340	310	56	1.2	2.2	0.04	0.48
	T8	1000	150	150	130	31	0.50	1.6	0.03	0.11
	T9	1500	220	160	160	14	0.45	0	0	0.46
	T10	360	90	120	160	20	0.77	0	0.02	0.49
	T11	440	89	120	150	30	0.53	0.27	0.05	0.11
	T12	610	140	120	160	22	0.67	0.06	0.01	0.16
	T13	1600	330	270	220	29	0.95	1.1	0	0.64
	Range	160-1800	62-330	76-340	130-310	14-56	0.45-1.2	0-2.2	0-0.05	0.09-0.64
	Average	990	180	170	190	27	0.70	0.75	0.017	0.29

Table 3.3 Correlations between trace elements concentrations (N=6) of aerosol particles.

Trace elements of fine mode	Na	Mg	K	Al	Fe	Mn	Ni	Cd	Se
Na	1	0.98**	0.71	-0.61	-0.79	-0.82*	-0.79	-0.98**	-0.63
Mg		1	0.82*	-0.46	-0.67	-0.71	-0.88*	-0.94**	-0.49
K			1	0.12	-0.13	-0.18	-0.98**	-0.59	0.068
Al				1	0.97**	0.95**	0.0044	0.72	0.98**
Fe					1	0.99**	0.25	0.87*	0.96**
Mn						1	0.31	0.90**	0.95**
Ni							1	0.69	0.045
Cd								1	0.75
Se									1
Trace elements of coarse mode	Na	Mg	K	Al	Fe	Mn	Ni	Cd	Se
Na	1	0.86*	0.72	0.55	0.32	0.48	-0.027	0.51	0.56
Mg		1	0.97**	0.90*	0.75	0.86*	-0.29	0.87*	0.89*
K			1	0.97**	0.85*	0.95**	-0.36	0.95**	0.96**
Al				1	0.97**	0.95**	0.0044	0.72	0.98**
Fe					1	0.97**	-0.47	0.89*	0.90*
Mn						1	-0.44	0.96**	0.97**
Ni							1	-0.34	-0.32
Cd								1	0.99*
Se									1

* Correlation is significant at the 0.05 level (2-tailed); ** Correlation is significant at the 0.01 level (2-tailed).
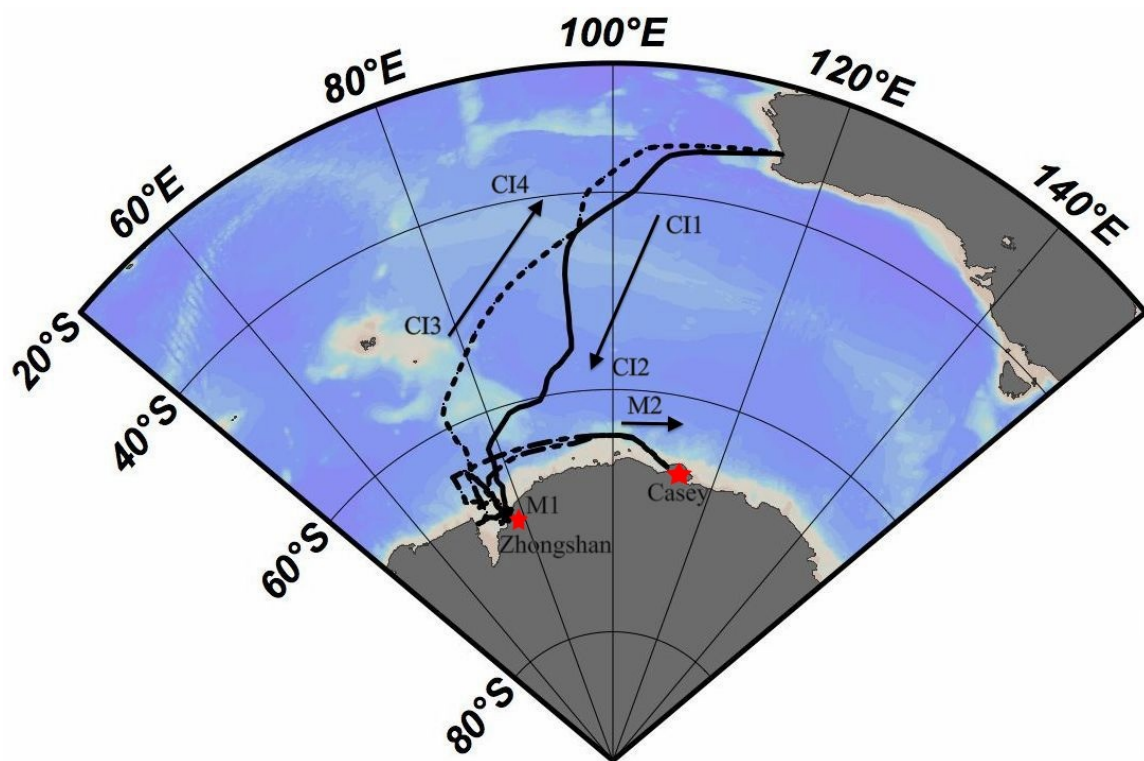
Figure 3.1 Cruise tracks and sampling locations. The solid line represents the leg from Fremantle, Australia to Chinese Antarctic Zhongshan Station (CI1, CI2); the dashed line represents the legs between Zhongshan Station and Australia Antarctic Casey Station (M1, M2); the dash-dot line represents the leg from Zhongshan Station to Fremantle (CI3, CI4).

Figure 3.2-1 Air-mass back trajectories (AMBTs) for samples collected over the Southern Ocean. These samples were (a) Sample T1; (b) Sample T2; (c) Sample T3; (d) Sample T15; (e) Sample T16; (f) Sample T17. The calculations were based on the National Oceanic and Atmospheric Administration (NOAA) GDAS meteorology data base, using the HYbrid Single-Particle Lagrangian Integrated Trajectory (HYSPLIT) program. AMBTs were performed at 50 and 500 m height above ground level over the sampling locations every six hours with backward 7 days, and units of the altitude axis was meter.

Figure 3.2-2 Air-mass back trajectories (AMBTs) for samples collected over the coastal East Antarctica. These samples were (a) Sample T4; (b) Sample T6; (c) Sample T7; (d) Sample T10; (e) Sample T12; (f) Sample T14. The calculations were similar as above. AMBTs were performed at 50 and 500 m height above the ground level over the sampling locations every six hours with backward 7 days, and units of the altitude axis was meter.
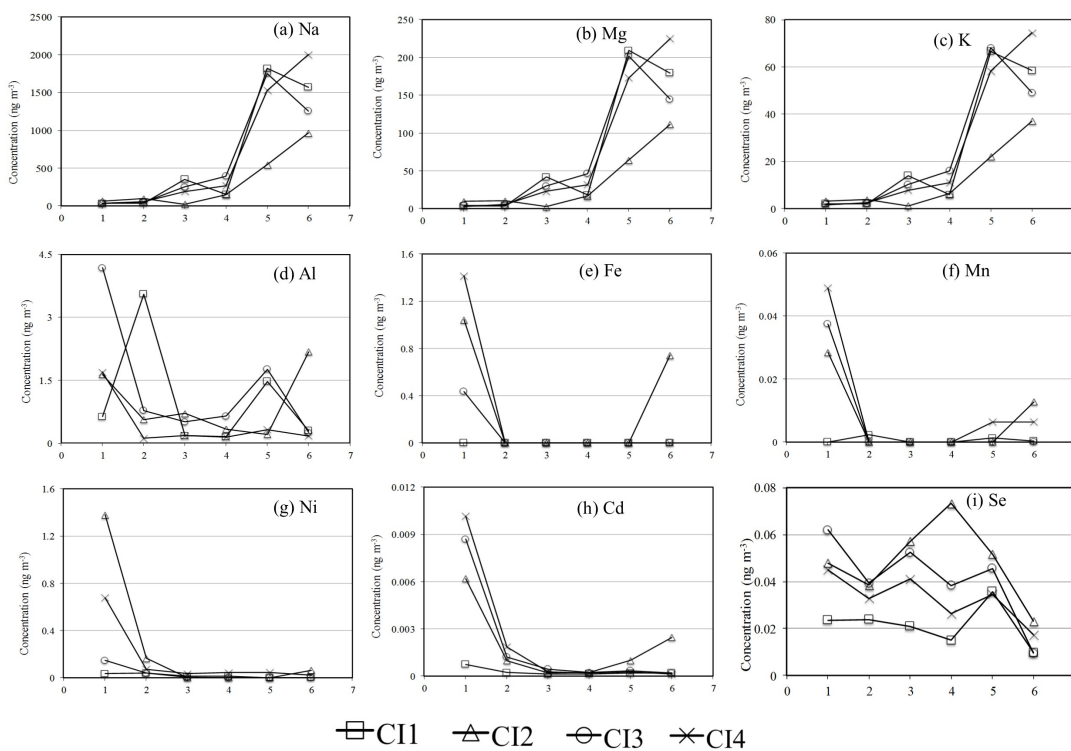
Figure 3.3 Particle size distributions of selected elements over the Southern Ocean (Note: In x-axis, 1 represents size range <0.49 μm; 2 represents size range 0.49-0.95 μm; 3 represents size range 0.95-1.5 μm; 4 represents size range 1.5-3 μm; 5 represents size range 3-7.2 μm; 6 represents size range >7.2 μm).
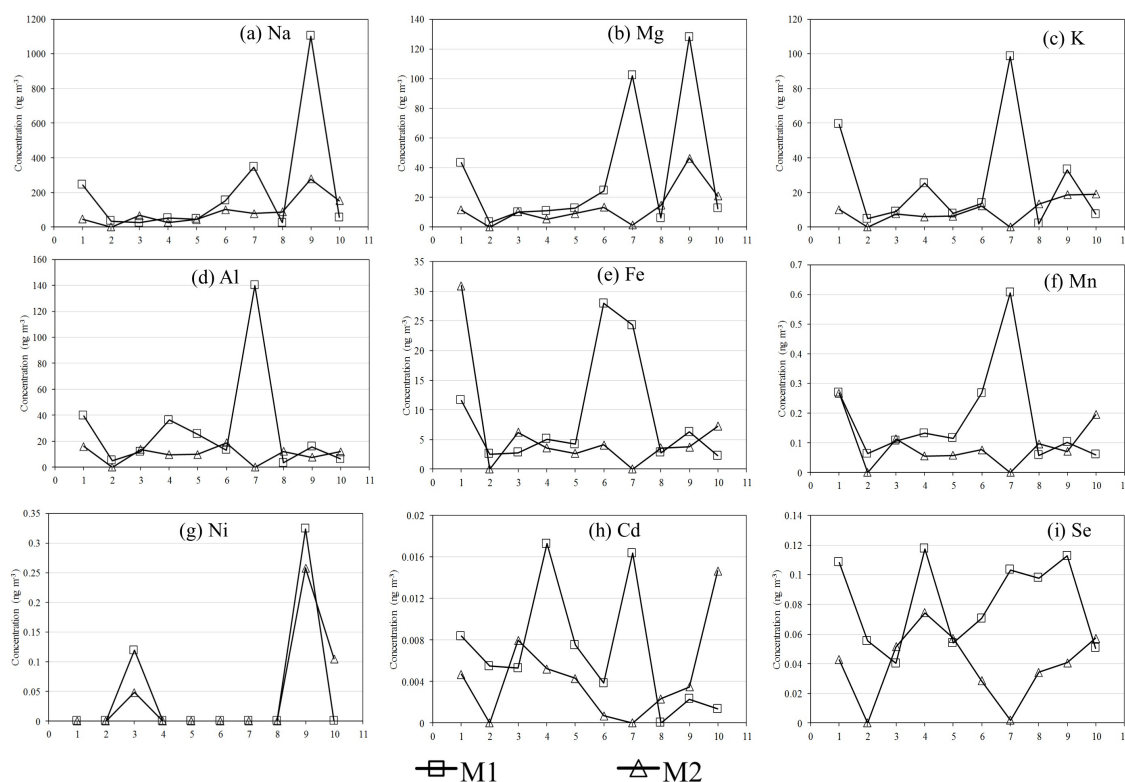
Figure 3.4 Particle size distributions of selected elements over coastal East Antarctica

(Note: In x-axis, 1 represents size range 0.056-0.10 μm; 2 represents size range 0.10-0.18 μm; 3 represents size range 0.18-0.32 μm; 4 represents size range 0.32-0.56 μm; 5 represents size range 0.56-1.0 μm; 6 represents size range 1.0-1.8 μm; 7 represents size range 1.8-3.2 μm; 8 represents size range 3.2-5.6 μm; 9 represents size range 5.6-10 μm; 10 represents size range 10-18 μm).
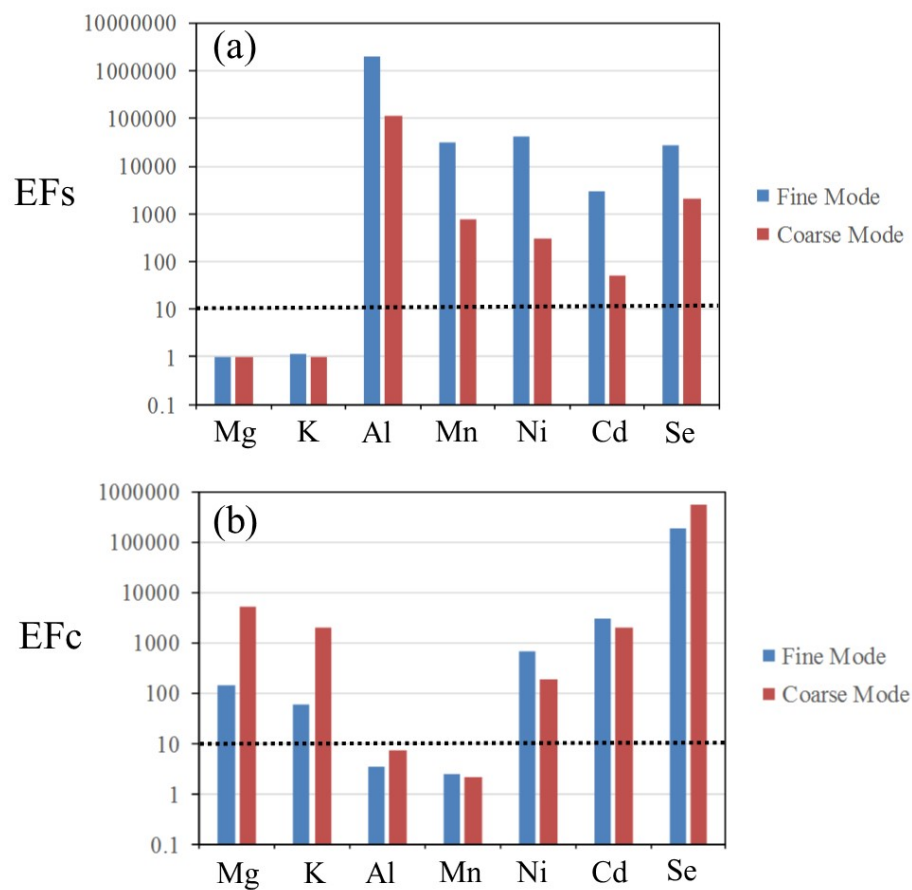
Figure 3.5 Enrichment factors of elements in aerosols over the Southern Ocean (SO) against reference material composition: (a) with Na as the reference element for marine source; (b) with Fe as the reference element for crustal material. The dashed line indicates the value of 10 that operationally separates from the reference source.
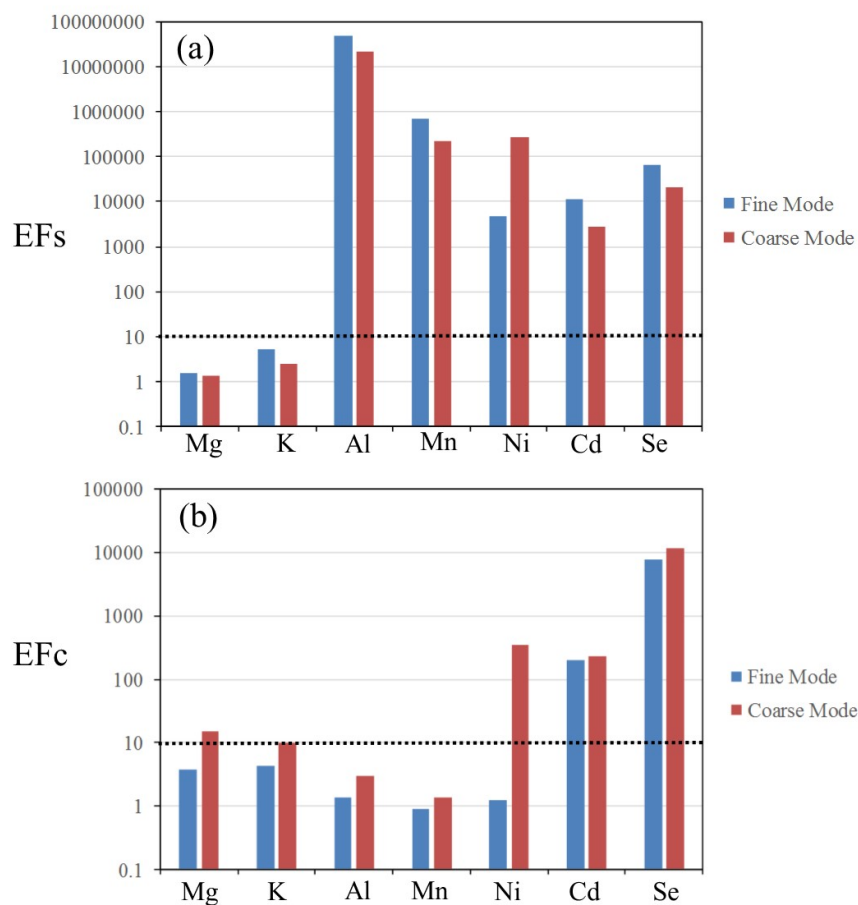
Figure 3.6 Enrichment factors of elements in aerosols over the coastal East Antarctica (CEA) against reference material composition: (a) with Na as the reference element for marine source; (b) with Fe as the reference element for crustal material. The dashed line indicates the value of 10 that operationally separates from the reference source.

Chapter 4 Characterization of Marine Aerosols and Precipitation through Shipboard Observations on the Transect between 31°N-32°S in the West Pacific[3]

Abstract

To characterize the chemical composition, size distributions, and fractional Fe solubility of atmospheric particles over Asian marginal seas, South Indian Ocean and Australian coast, selected water-soluble inorganic and organic species in aerosols and precipitation, trace metals and soluble Fe in aerosols were analyzed by multi-instruments. Results showed that sea salt and non-sea-salt sulfate (nss-SO_4^{2-}) were the main components in aerosols. Over Asian marginal seas, Cl^- and Na^+ were the dominant ions in precipitation, accounting for ~72% of the total ions. Both SO_4^{2-} and NO_3^- accounted for ~26% of the total anions, controlling the acidity of the precipitation. Non-sea-salt Ca^{2+} (nss-Ca^{2+}) accounted for 6.9% of the total cations, dominating the neutralizing component in rainwater. Observed methane sulfonate (MSA) concentrations and MSA/nss-SO_4^{2-} increased southward. The concentrations of sea salt were affected by wind speeds, which was mainly accumulated in particle size>10 μm. Particle size distributions of nss-SO_4^{2-} and NH_4^+ mainly peaked in the fine mode, while NO_3^- was mainly accumulated in the coarse modes. Oxalate presented a bimodal size distribution pattern in both fine and coarse mode. Based on the air mass back trajectories, enrichment factors and Fe/Al, V/Al ratios, aerosol samples collected over Asian marginal seas could be affected by both long-range transported dust and anthropogenic emissions. Good relationship was found

between total dissolved iron and nss-SO_4^{2-}, indicating that acid processing during long-range transport could play an important role in fractional iron solubility in aerosols. The inverse relationship between atmospheric total Fe and fractional Fe solubility fitted in the global-scale trend. This study implicates that dust and acidic air pollutants from continental sources can interact and affect iron solubility in aerosols in the marine atmosphere. However, due to the small size of samples in this study, more investigations need to be conducted in future.

Keywords: Water-soluble Species; Trace elements; Size distribution; Iron solubility.

4.1 Introduction

Marine aerosols are made up of a variety of individual species. Among them, sea salt and sulfate aerosols are the two dominant inorganic aerosol components in the marine atmosphere [*Bates et al*., 2001; *Read et al*., 2008; *Yang et al*., 2011; *Xu et al*., 2013]. Sea salt particles, produced by bursting of seawater bubbles on the surface of the ocean by winds, largely control the mass of the supermicron aerosol fraction [*Murphy et al*., 1998; *Quinn et al*., 1998; *D O'Dowd and De Leeuw*, 2007]. During the bubbles bursting processes, the sea-salt sulfate (ss-SO_4^{2-}) is injected into the atmosphere. Sulfate aerosol can also come from the gas-to-particle conversion of SO_2 derived from dimethysulfide (DMS) by marine phytoplankton [*Charlson et al*., 1987] and anthropogenic emissions, which is named as nss-SO_4^{2-}. Besides inorganic aerosol species, marine aerosols also consist of a large amount of organic compounds. Among the water- soluble compounds, MSA is a species mainly produced by the oxidation of DMS from marine phytoplankton. Oxalic acid ($H_2C_2O_4$) is the most abundant dicarboxylic acid in aerosols [*Kerminen et al*.,

2000], which may affect the aerosols' hygroscopic and cloud-nucleating properties [*Abbatt et al.*, 2005].

On the other side, marine aerosols also contain a variety of trace elements, including iron (Fe), Manganese (Mn), Cobalt (Co), Znic (Zn), Copper (Cu), and Nickel (Ni), which are essential nutrients to marine biota [*Butler*, 1998; *Whitfield*, 2001]. These elements could come either from crustal sources or from anthropogenic emissions [*Buck et al.*, 2010; *Hsu et al.*, 2010]. In the remote oceans, particularly in the high-nutrient low-chlorophyll (HNLC) regions, the atmospheric deposition could be an important source of bioavailable Fe to stimulate biological production in surface seawaters [*Bishop et al.*, 2002; *Jickells et al.*, 2005]. However, the information on the properties of marine aerosols over Asian marginal seas, South Indian Ocean and Australian coast remains limited.

To characterize marine aerosols and precipitation in the marine atmospheric boundary layer between 31°N-32°S in the west Pacific, bulk aerosol samples (known as total suspended particles (TSP)), size-segregated aerosol samples and precipitation samples were collected through shipboard measurements. Results from this work provide information on chemical composition, size distributions and iron solubility in marine aerosols and precipitation over this region, and potential sources of these aerosol components, particularly anthropogenic emissions, are explored.

4.2 Methods

4.2.1 Shipboard Sampling

Aerosol sampling was conducted on the 31°N-32°S transect between Asian marginal

seas, South Indian Ocean and Australian coast between November 2010 and March 2011,

onboard the Chinese icebreaker, *Xue Long* (Figure 4.1). In this study, Asian marginal

seas is defined as the region between 31°N and 4°S, and South Indian Ocean and

Australian coast is defined as the region between 7°S and 31°S. The discussions of data

were based on two sets of results from these two distinct regions. Air samplers were

installed on a 3×6 m^2 platform on the ship's eighth floor front deck about 25 meters

above the sea surface. Size-segregated, bulk aerosol samples (as TSP) and precipitation

samples were collected during this cruise. To collect size-segregated aerosol samples, a

10-stage Micro-Orifice Uniform Deposit Impactor (MOUDI, MSP Corp., Shoreview,

MN) with the flow rate of 30 L min^{-1} was used, with Teflon filters (Pall Corp., 47 mm

diameter, 1 μm pore size) as sampling substrates. The 50% cut-off mass median

aerodynamic diameters (MMAD) of the MOUDI were 0.056, 0.10, 0.18, 0.32, 0.56, 1.0,

1.8, 3.2, 5.6, 10 and 18 μm, and the size of 1.8 μm was used as a cutoff size to separate

the fine and coarse aerosol fractions. Bulk aerosol samples (as TSP) were collected

during this cruise, using a High-Volume bulk aerosol sampler (Aquaero Tech, Miami,

FL) with a flow rate of ~ 1 m^3 min^{-1} and Whatman-41 filters as sampling substrates. To

avoid contamination from the ship emissions, a wind speed and direction system installed

on the same sampling platform was utilized to control all sampling instruments, which

operated sampling only when the wind was from a sector 90° left and right on the centre

line of the ship's path and at wind speeds > 2 m s^{-1}. During sampling, loading and

unloading of the filters were conducted in a 100-class high-efficiency particulate air

(HEPA)-filtered laminar flow clean-room hood in the ship's chemical laboratory, following clean-room operation procedures. After sampling, sample filters with field blanks were kept in the refrigerator at 4°C in the ship. For collection of precipitation, several sets of polypropylene funnels and Teflon bottles were pre-cleaned in the lab following the procedures for precipitation collection by *Kim et al.* [2000]. They were triple bagged during the shipment and storage before collection. After sampling, each sample was handled within a HEPA-filtered laminar flow 100-class clean-room hood in the ship's chemical laboratory and was analyzed for ionic species in the lab after the cruise.

In summary, 5 TSP samples, 1 set of size-segregated aerosol sample and 6 rain samples were collected over Asian marginal seas, and 5 TSP samples, 1 set of size-segregated aerosol sample were collected over South Indian Ocean and Australian coast. Detailed sampling information and associated meteorological data are in Table 4.S1.

4.2.2 Chemical Analysis

Aerosol and precipitation samples were analyzed for water-soluble inorganic and organic species, including Na^+, NH_4^+, sulfate (SO_4^{2-}), nitrate (NO_3^-), MSA, and oxalate through the use of a Dionex ICS-2500 ion chromatograph (IC). The method detection limits for Na^+, NH_4^+, SO_4^{2-}, NO_3^-, MSA and oxalate were 20, 9, 7, 3, 0.4 and 2.4 $\mu g\ L^{-1}$, respectively. The precision of the analytical procedures based on seven spiked samples was <5%. Results showed that strong positive linear correlations existed between total

anions and cations with a slope of 1.2 (R^2=0.99, n=10), suggesting that good electric

charge balance existed between anions and cations in aerosols collected in this study.

Aerosol samples were also analyzed for Na, Mg, K, Al, Fe, Mn, Ni, Cd, and Se through

the use of ICP-MS (7500ce, Agilent). The method detection limits were ~1 ppt for all

trace elements analyzed in this study, and the precision of the method was ~2%. The final

concentrations of selected trace elements in samples were obtained after subtraction of

field blanks.

To explore the iron solubility in aerosols, the atmospheric concentrations of Fe(II) and

Fe(III) in samples were determined by UV/Visible spectroscopy. The concentrations of

Fe(II) in the sample solutions were determined at 562 nm using a TIDAS-1 spectrometer

module with a 200 cm liquid waveguide capillary flow cell (World Precision Instruments

Inc., FL, USA) using the procedures in *Gao et al.* (2013). The solution used for the batch

leaching experiments was 0.5 mM ammonia acetate that has been used in previous

studies in other regions [*Baker et al.,* 2006; *Trapp et al.,* 2010]. A brief method

description for leaching aerosol filter sample is as follows: one quarter of each filter was

placed in 20 mL of 0.5 mM ammonia acetate for 1h. Fe(TD) in this study is defined as the

sum of Fe(II) and Fe(III) in the leaching solutions. The ferrozine solution (0.01 M) was

added to the Fe(II) filtrate portion, and the sample solution remained for 30 min before

filtration. 0.01 M hydroxylamine hydrochloride was added to the Fe(TD) filtrate portion

to reduce Fe(III) to Fe (II), and the sample solution was set aside for 1 h to ensure

complete reduction of Fe(III) to Fe(II) before adding the same ferrozine solution as for

the Fe(II) filtrate portion. The Fe(III) can be determined as the difference between the Fe(TD) and Fe(II). The method detection limit for Fe(II) was 0.26 nM. All field blanks were treated in the same way as for samples.

4.3 Results and Discussion

4.3.1 Water-Soluble Inorganic and Organic Species

Concentration distributions in aerosols: High sea salt concentrations (9.8, 14, 29 μg m^{-3} in sample T4, T9, T10, respectively) were associated with high wind speeds (11, 21, 16 m s^{-1}) during the cruise, which were supported by the conclusion by *Lewis and Schwartz* [2004] that increase in sea-salt mass concentrations was associated with increasing wind speeds. nss-SO$_4^{2-}$ and nitrate concentrations observed in this study were at the lower end by comparing with other cruise results over the China marginal seas [*Zhang et al.*, 2013; *Uematsu et al.*, 2010; *Hsu et al.*, 2010]. The NO$_3^-$/nss-SO$_4^{2-}$ mass ratio in this study was 0.37, while *Uematsu et al.* [2010] found that this ratio was 0.19 over East China Sea. The ratio was found to be 0.34 over the South Yellow Sea and East China Sea by *Zhang et al.* [2013]; *Hsu et al.* [2010] collected aerosol samples from the East China Sea and results showed that the ratio was 0.52. Differences in the NO$_3^-$/nss-SO$_4^{2-}$ mass ratios among all cruise observations revealed the spatial and temporal variations of NO$_3^-$ and nss-SO$_4^{2-}$ in aerosols over the Asian marginal seas affected by different pollution emission intensity [*Arimoto et al.*, 1996]. The MSA/nss-SO$_4^{2-}$ ratios ranged from non-detectable (ND) to 0.0068 (average 0.0032) over Asian marginal seas and from 0.0044 to 0.07 (average 0.028) over the South Indian Ocean, which were constant with observations conducted by *Chen et al.* [2012]. They also found that the MSA/nss-SO$_4^{2-}$ ratios were increased from

ND-0.0031 over Asian marginal seas to approximately 0.0024-0.06 in the tropical

regions. The increased concentrations of MSA and MSA/nss-SO_4^{2-} as sampling sites

towards the high southern latitudes may reflect the increased marine biogenic production.

The concentrations of oxalate in aerosols in this study were comparable with

investigation over the western Pacific Ocean (35°N-50°S). *Wang et al.* [2006] found that

atmospheric concentrations of oxalic acids ranged from 0.98 to 98 ng m^{-3} (average 38 ng

m^{-3}). *Kawamura and Sakaguchi* [1999] collected aerosol samples over the western North

Pacific to equatorial Pacific (34°N–14°S, 140°E-150°W), and reported that oxalic acid

concentrations ranged from 6.5 to 161 ng m^{-3} (average 40 ng m^{-3}). In this study, the

highest oxalate concentration (77 ng m^{-3}) was observed in the sample collected over the

South Indian Ocean, while low oxalate concentrations (ND) were observed over the coast

of China Sea and Australia coast. The long-range transport of primary and secondary

aerosols of continental origin and photochemical oxidation may explain the observed

high oxalate concentrations in aerosols. *Fu et al.* [2013] investigated spatial distributions

of water-soluble dicarboxylic acids by collecting marine aerosols at low- to mid-latitudes

in the Northern Hemisphere and they found that oxalic acid was the predominant

dicarboxylic acids. They utilized a tracer for terrestrial biogenic emission, and found

higher values over the open oceans than those over the coastal regions, suggesting the

continuous production of oxalic acid during long-range transport that could explain the

observed high oxalic acid concentrations in the remote atmosphere. As a major

component of dicarboxylic acids, oxalic acid was mainly produced by in-cloud process in

the atmosphere by the evidence of high correlation between ambient oxalate and sulphate

[*Yu et al.*, 2005]. The oxalate concentrations were low compared with nss-SO_4^{2-} in this

study, and when nss-SO_4^{2-} concentrations went up, oxalate didn't go up. There was poor correlation between these two species during this study, which inferred that they were possibly produced through different pathways. *Kawamura and Sakaguchi* [1999] concluded that these diacids in the Pacific atmosphere were likely in situ produced through photochemical oxidation of gaseous and particulate precursors pathways.

Concentration distributions in precipitation: The major water-soluble inorganic and organic compounds in precipitation over Asian marginal seas were shown in Table 4.1. In general, the average concentrations of ionic species showed an order of $Cl^->Na^+>SO_4^{2-}>Mg^{2+}>Ca^{2+}>NO_3^->K^+>NH_4^+>$Formate>Acetate>Oxalate, on an equivalent basis. It was found that Cl^- and Na^+ were the major ions in precipitation, accounting for ~72% of the total ions, with Cl^-/Na^+ equivalent ratio of 1.09, similar to the results observed by *Zhang et al.* [2007] over the Yellow Sea and East China Sea and close to the ratio of seawater (1.16), indicating that the composition of precipitation over Asian marginal seas was highly affected by marine aerosols, as Na^+ and Cl^- were mainly from marine sources. Results showed that the concentrations of Cl^-, NO_3^-, sulphate, NH_4^+, Mg^{2+} and Ca^{2+} in rainwater (Table 4.1) were enclosed into the concentration range observed by *Zhang et al.* [2007] over China coastal seas. SO_4^{2-} accounted for 19% of the total anions, NO_3^- accounted for 6.6% of the total anions, both of which were the major anions responsible for the acidic nature of the precipitation. On the other side, NH_4^+ accounted for 0.94% of the total cations, non-sea- salt Ca^{2+} (nss-Ca^{2+}) accounted for 6.9% of the total cations, inferring that the main neutralizing component in rainwater was Ca^{2+}, not NH_4^+. The major ion data from this study showed that total cations (Na^+, NH_4^+, K^+, Mg^{2+} and Ca^{2+})

presented good positive correlation with total anions (Cl^-, SO_4^{2-}, NO_3^-, Formate, Acetate and Oxalate), with the slope of the regression line is 1.0 and Pearson value =0.99 (p-value<0.01, n=6), suggesting good electric charge equilibrium existed between cations and anions. The concentration variety of ions in precipitation provided information on the current state of atmospheric composition over Asian marginal seas.

Size distributions of ionic species in aerosols: Figure 4.2 showed the size distributions of size-segregated aerosols based on two sets of MOUDI samples collected at two different areas (Table 4.S1). Bimodal size distribution of Na^+, which could represent sea salt aerosol, mainly existed in coarse mode in particle sizes 1.8-5.6 and 10-18 μm shown in Figure 4.2(a); nss-SO_4^{2-} in both aerosol samples was mainly accumulated in the fine mode with particle size 0.32-0.56 μm as illustrated in Figure 4.2(b). It was reported that in-cloud heterogeneous oxidation was the main formation pathways of fine mode sulfate [*Whitby*, 1978]. However, there existed a small peak in the coarse mode with particle size peaking at 5.6-10 μm in sample M1. The existence of nss-SO_4^{2-} in the coarse mode may indicate its reactions with sea salt [*Zhuang et al.*, 1999]. On the other side, there was no particle size peak shown in the coarse mode in sample M2, one possible reason was that sample M2 was influenced by air masses both from marine and continental sources, whereas sample M1 was mainly influenced by air masses from continental sources. Figure 4.2(c) showed that NO_3^- was mainly accumulated in the coarse mode, peaking at 1.8-10 μm. The peak of NO_3^- was consistent with Na^+ in the size range 1.8-3.2 μm, which indicated that NO_3^- was likely produced in the surface of sea-salt aerosol through the reaction between NaCl and nitric acid gas [*Seinfeld and Pandis*, 2006]. Size distributions

of ammonium mainly peaked at fine mode with particle size 0.32-1.0 μm, as shown in

Figure 4.2(d). The enhancement of NH_4^+ in the fine-mode particles was consistent with

that of nss-SO_4^{2-}, suggesting that sulfuric acid can be neutralized by ammonia. The nss-

SO_4^{2-} abundance and gas phase and aqueous phase reactions between gaseous precursor

NH_3 and acidic species could affect the formation of NH_4^+ in the fine mode [*Zhang et al.*,

2008]. However, the highest nss-SO_4^{2-} was correspondent to a very low ammonium

concentration in sample M1, which indicated that the ammonium was formed through

aerosol nucleation pathways. Figure 4.2(e) showed the bimodal size distribution patterns

of MSA over Asian marginal seas, South Indian Ocean and Australian coast, which

peaked at 0.32-1.0 μm in the fine mode, and at 1.8-5.6 μm in the coarse mode. Fine mode

MSA could be explained either by gas-to- particle conversion or in-cloud oxidation

processes in the marine boundary layer [*Read et al.*, 2008]; Particle size distributions of

oxalate presented a bimodal size distribution pattern, peaking at size range 0.32-0.56 μm

in the fine mode, and at >1.8 μm in the coarse mode, while the mass concentration of

oxalate was mainly accumulated in the coarse mode as illustrated in Figure 4.2(f). *Rinaldi*

et al. [2011] collected "clean-sector" aerosol samples at two coastal stations at Mace

Head and Amsterdam Island. They found that oxalate was presented a seasonal trend and

the size distribution of oxalate was presented in a bimodal distribution pattern, which was

different from the predominant fine mode (0.32-0.56 μm) distribution pattern occurred in

polluted regions [*Zhao and Gao*, 2008a]. Thus, it can be inferred that the observed

oxalate in this study was formed through a mixture of different production processes

[*Rinaldi et al.*, 2011], which is either produced from the atmospheric photo-oxidation of

volatile organic compounds [*Sullivan and Prather*, 2007], or in-cloud processing [*Blando and Turpin*, 2000].

4.3.2 Trace Elements in Aerosols

The highest concentration of Al was 320 ng m^{-3} associated with sample T10 collected in the areas of 22-31°N, 122-127°E during March, 2011. The air mass back-trajectories of the sample T10 showed that air mass at 1000 m height level came from western China, and at 50 and 500 m height came from northern China. Two main Asian dust sources, that is, the Taklamakan Desert in western China and the Gobi deserts in northern China and Mongolia [*Zhang et al.*, 2003] could provide a large amount of dust to the mid-latitudes over the North Pacific [*Gao et al.*, 1992], which could explain the high Al concentration observed during this study. The concentrations of total Fe were shown in Table 4.2, which were comparable with previous investigation over the Pacific Ocean, but higher than those over the Southern Ocean and coastal East Antarctica by *Gao et al.* [2013]. More discussion on Fe solubility was shown in later sections. The highest concentrations of Fe (420 ng m^{-3}), Mn (15 ng m^{-3}) and Al (320 ng m^{-3}) appeared in the same sample T10, and good correlation was also found between Al and Fe (R^2=0.83, n=10), Al and Mn (R^2=0.84, n=10), Fe and Mn (R^2=0.91, n=10), thus the dominant source of Mn and Fe in these samples likely was of crustal origin. To further explore the possible sources, enrichment factors (EFs) of trace elements in aerosol particles was calculated, as shown in Figure 4.3. Results of EFs showed that Fe and Mn were mainly derived from crustal sources, while most of the EFs values of V, Zn and Cu were > 5, indicating potential non-crustal sources. Fe/Al ratios were also calculated to assess the

potential sources. Over Asian marginal seas, the average ratio of Fe/Al was 1.41, while it was 1.47 over the South Indian Ocean. However, sample T6, which was associated with air mass from Australia had the lowest Fe/Al ratio (0.51) during this study, which was also smaller than the ratio of Australian continental aerosols (0.77-0.85) reported by *Radhi et al*. [2010]. *Witt et al*. [2006] collected aerosol samples over the South Indian Ocean and measured trace metals, and they found that the Fe/Al ratios decreased eastwards as influenced by air masses changing from southern African to Australia, which may suggest the differences in elemental composition in dust from different sources. On the other hand, the Fe/Al ratios were higher than those measured during the super Asian Dust Storm (0.61±0.05) by *Hsu et al*. [2013], as well as those of the Chinese desert and loess dust [*Zhang et al*., 2003]. This result indicated that the involvement of anthropogenic sources could contribute to the extra Fe concentrations. Therefore, possible sources of atmospheric trace elements over the Asian marginal seas, could be from both long-range transported dust and anthropogenic emissions of gases and aerosols [*Hsu et al*., 2010]. The concentrations of Zn and Cu were shown in Table 4.2. These results were similar to other studies. EF of Zn and Cu in several samples was much higher than five, suggesting that additional sources, such as vehicle emissions, fossil fuel and coal combustion, and other anthropogenic emissions, need to be considered to explore the potential sources for Zn and Cu. *Gao and Anderson* [2001] conducted individual-particle analysis of east Asian aerosol samples and inferred that atmospheric long-range transport of pollutants derived from anthropogenic emissions, such as coal burning, could contribute to the enrichment of Zn in aerosol particles over remote oceanic

environment, as Zn tended to concentrate on the fine mode with a long residence time in the atmosphere.

4.3.3 Fe Solubility

Soluble Fe concentration distributions: The concentrations of soluble Fe (Fe(II) and total dissolved iron (Fe(TD))) were shown in Table 4.2. In average, the concentrations of Fe(II) accounted for ~90% of the total dissolved Fe over Asian marginal seas and ~68% over the South Indian Ocean and Australian coast. The high Fe(II)/Fe(TD) ratio could be attributed to the high Fe(II) concentrations. Over Asian marginal seas, there existed two highest Fe(II) concentrations, 28 ng m^{-3} in 22-31°N, 122-127°E in Sample T10 and 4.5 ng m^{-3} in 10-21°N, 127°E in Sample T9, as illustrated in Figure 4.4(a). Sample T10 with Fe(II) concentration being ~4 times of the average Fe(II) concentration over Asian marginal seas was also associated with the highest concentrations of Fe(TD) (30 ng m^{-3}) and total iron (Fe(T)) (420 ng m^{-3}), shown in Figure 4.4(a). The results of air mass back trajectory analysis of sample T10 showed that the observed high Fe(II), Fe(TD), Fe(T) concentrations were likely associated with dust from long-range transport, during which the aerosol particles aging resulted in the high Fe fractional solubility [*Jickells and Spokes*, 2001]. The sample T1 was also associated with air mass coming from west and north China, but it was collected in November, during which periods there was no dust events. Asian dust storms annually occurred in later winter and spring over west and north China [*Zhang et al.*, 2003], and Sample T10 was collected within the dust storm time periods over East China Sea. *Tan et al.* [2012] found that one of main receptacles of Asian Dust was west Pacific other than the East Chinese marginal seas, which included

the Bohai, Yellow, and East China Seas, as well as the Sea of Japan. *Hsu et al.* [2013] conducted super Asian dust storm research and further highlighted that long-range transported Asian dust during episodes could have more significantly impact over the Northwestern Pacific in spatial and temporal extents.

A good correlation between nss-SO_4^{2-} and Fe(TD) (R^2=0.86, n=9, p<0.001, the highest Fe(T) sample T10 was excluded as a outlier by running a Grubbs' test) was found in this study (Figure 4.4(b)). The interactions of aerosol Fe with acidic S-containing species have been suggested to affect Fe solubility, in particular in the marine atmosphere affected by anthropogenic emissions [*Moffet et al.*, 2012]. *Hsu et al.* [2010] conducted the aerosol iron solubility research over the East China Sea, and their results also showed that atmospheric soluble iron had good positive correlation with nss-SO_4^{2-}, which may infer that anthropogenic acids could enhance the iron solubility. *Luo et al.* [2008] concluded that ~30% of iron deposited into the ocean near East Asia comes from coal combustion. The nss-SO_4^{2-} in this study over Asian marginal seas, transported from continental plumes, was also likely mainly from coal combustion. Therefore, aged aerosol particles were internally mixed with nss-SO_4^{2-} during long-range transport, which may solubilize Fe and enhance the redox reaction of Fe(III) to Fe(II) [*Cwiertny et al.*, 2008].

Fractional Fe Solubility: The fractional Fe(TD) solubility ($S_{Fe(TD)}$) in aerosols from this study ranged from 4.5% to 10.6% over Asian marginal seas and from 1.1% to 3.7% over the South Indian Ocean and Australian coast (Figure 4.4(c)). In this study, sample T1 was

associated with the highest fractional Fe solubility (10.6%), even though the total Fe

concentration of sample T1 (35 ng m^{-3}) was low compared with the highest concentration

in sample T10. Among likely sources for sample T1 could be combustion, and this is

consistent with recent studies. *Luo et al*. [2008] modeled the iron produced during

combustion and highlighted the importance of the iron from combustion sources, which

included fossil fuel combustion, industrial processes, biofuels, agricultural wastes and

natural biomass burning. Numerous studies have utilized high V/Al, Ni/Al mass ratios as

the tracer of fuel oil combustion [*Sholkovitz et al*., 2009]. *Sedwick et al*. [2007] and

Sholkovitz et al. [2009] collected aerosols over the Sargasso Sea, and they found that high

fractional Fe solubility values were associated with increased V/Al and Ni/Al mass ratios.

Higher mass ratios of V/Al (0.03) and Ni/Al (0.02) were also found in sample T1, while

the V/Al mass ratio was 0.01, Ni/Al mass ratio was 0.006 in sample T10, substantially

lower compared with those in T1. These results implied that the fractional Fe solubility in

aerosol in this study was influenced by the presence of V and Ni enriched aerosols

[*Sholkovitz et al*., 2009]. Sample T10 with the highest Fe(TD) collected over the East

China Sea presented the second highest fraction iron solubility, which was 7.1%. In

general, $S_{Fe(TD)}$ observed over Asian marginal seas was more than two times higher than

those observed over the South Indian Ocean and Australia coast. Previous research has

found higher Fe solubility from combustion than that from mineral dust [*Sedwick et al*.,

2007; *Sholkovitz et al*., 2009; *Moffet et al*., 2012]. Thus, aerosol particles transported

from coal combustion sources to Asian marginal seas had higher $S_{Fe(TD)}$ than aerosol

samples collected over the South Indian Ocean and Australian coast associated with air

mass from Australian continent. It was found that $S_{Fe(TD)}$ obtained from this study could

be expressed as a function of the total Fe concentrations in aerosols in the marine boundary layer over Asian marginal seas, South Indian Ocean and Australian coast by the equation,

$$S_{Fe(TD)} = 10.8 \times C_{Fe(T)}^{-0.22}$$

Based on the nonlinear regression analysis, this relationship has $R^2=0.12$ (p-value=0.01, n=9, the highest Fe(T) sample T10 was excluded as a outlier), shown in Figure 4.4(d). *Sholkovitz et al.* [2012] synthesized a global-scale data set of fractional Fe solubility (%Fe_s) and found a robust inverse relationship between the total Fe loadings and fractional Fe solubility. The relationship between $S_{Fe(TD)}$ and Fe(T) in aerosols from this study followed the trend of data compiled from the global set. Observation results along this cruise, specifically over tropical Pacific, South Indian Ocean and Australian coast, could fill in the data gap of the $S_{Fe(TD)}$ and Fe(T) relationship in the west Pacific region.

4.4 Conclusions

This work on chemical composition of aerosols and ionic species in precipitation over the west Pacific leads to the following conclusions:

Sea salt and nss-SO_4^{2-} were the main components of marine aerosols over this region, of which high sea salt concentrations were associated with high wind speeds, while high nss-SO_4^{2-} could mainly come from anthropogenic emissions, especially over Asian marginal seas. The particle size distributions of sea salt and NO_3^- in aerosols were mainly accumulated in the coarse mode, while nss-SO_4^{2-} and NH_4^+ mainly peaked in the fine mode. Cl^- and Na^+ were the major ions in precipitation. In anions, SO_4^{2-} accounted for

19% of the total anions, NO_3^- accounted for 6.6% of the total anions, both of which

controlled the acidic nature of the precipitation. In cations, NH_4^+ accounted for 0.94%

and nss-Ca^{2+} accounted for 6.9% of the total cations, indicating that the main neutralizing

component was Ca^{2+} in precipitation.

Based on the air mass back-trajectories, enrichment factors and Fe/Al, V/Al ratios,

aerosol samples collected over Asian marginal seas could be affected by both long-range

transport dust and anthropogenic emissions. A good relationship was found between total

dissolved iron and nss-SO_4^{2-}, indicating that fractional iron solubility was affected by

acid processing. The inverse relationship between total Fe and fractional Fe solubility

could fit into the global-scale trend.

These results indicate that continental dust could significantly interact with acidic

atmospheric pollutants from anthropogenic emissions, changing the iron solubility by

aging during long-range transport. However, more investigation should be conducted in

future for better understanding the acid processing in iron solubility over polluted oceanic

regions.

Supporting Material Available

5-day air-mass back trajectories (AMBTs) (Figure 4.S1), Spatial distributions of MSA,

MSA/nss-SO$_4^{2-}$ (Figure 4.S2), Sampling information (Table 4.S1), Sea salt

concentrations and wind speeds (Table 4.S2). This information is also available free of

charge via the Internet at http://www.atmospolres.com.

Table 4.1 Ionic species concentration in rainwater samples over Asian marginal seas
(unit: μeq L^{-1}).

Ions	R1	R2	R3	R4	R5	R6	Average
Cl^-	460	450	390	53	33	440	300
NO_3^-	6.2	88	66	0.57	0.39	1.9	27
Sulfate	140	140	110	9.8	17	49	77
MSA	0.0	0.02	0.02	0.0	0.01	0.02	0.01
Acetate	6.2	0.0	3.0	0.14	1.1	0.62	1.8
Formate	8.9	0.27	7.5	1.3	1.3	2.1	3.6
Oxalate	0.54	0.49	0.81	0.06	0.07	0.12	0.35
Na^+	390	420	370	48	18	430	280
NH_4^+	8.4	4.6	6.8	0.27	1.4	0.44	3.7
K^+	8.2	9.9	8.7	1.4	0.93	5.6	5.8
Mg^{2+}	89	110	100	7.0	1.1	86	66
Ca^{2+}	16	110	78	5.1	2.5	9.5	37

Table 4.2 Statistical summary of concentrations of aerosol chemical species (unit: ng m^{-3}).

	Asian marginal seas (n=5)			South Indian Ocean and Australian coast (n=5)		
	Range	Median	Geometric Mean	Range	Median	Geometric Mean
Al	4.3-320	31	39	34-130	82	86
Fe(II)	0.52-28	3.5	2.8	0.6-4.2	1	1.7
Fe(TD)	0.6-30	3.7	3.1	0.9-5.5	2.3	2.5
Fe	13-420	35	47	42-150	83	90
Mn	0.2-15	1.6	1.3	0.6-1.4	1.2	1.2
V	0.2-3.4	0.7	0.72	0.3-1	0.8	0.7
Zn	0.6-47	4.4	4.1	0.4-5.5	1.2	2
Cu	0.2-2.3	0.4	0.6	0.2-0.8	0.4	0.4
Cl$^-$	1720-16500	2240	3900	780-5520	3200	3390
NO$_3^-$	130-860	340	400	360-1210	800	750
nss-SO$_4^{2-}$	200-3220	1250	1090	350-2330	1050	1190
MSA	ND-5	4.3	3.0	10-30	24	21
Oxalate	ND-71	18	33	0.9-77	27	30
Na$^+$	920-8280	1430	2110	830-2900	2000	1920
NH$_4^+$	17-115	57	44	27-240	130	116

Table 4.S1 Sampling information*.

Sample type	No.	Sampling date	Lat (^{o}S), Long (^{o}E)	Volume (m^3)	WS (m/s)	AT (^{o}C)	RH (%)	AP (hPa)
	T1	11/11/10 10:00 to 11/14/10 00:57	21°N, 115°E to 7°N, 120°E	7033	9.5	26	67	1014
	T2	11/14/10 04:50 to 11/16/10 09:45	7°N, 120°E to 6°S, 117°E	5667	3.6	29	71	1009
	T3	11/16/10 14:26 to 11/19/10 08:44	7°S, 116°E to 24°S, 113°E	7571	7.2	28	67	1009
	T4	11/19/10 11:23 to 11/20/10 23:00	24°S, 113°E to 32°S, 115°E	3484	11	25	61	1007
TSP (T)	T5	11/22/10 01:40 to 11/23/10 00:11	32°S, 116°E	2605	6.7	21	71	1013
	T6	03/17/11 09:54 to 3/19/11 10:16	31°S, 114°E to 19°S, 114°E	6231	7.4	30	65	1009
	T7	03/19/11 11:35 to 3/21/11 23:30	18°S, 114°E to 4°S, 118°E	7698	4.6	29	73	1008
	T8	03/22/11 08:51 to 3/25/11 01:40	1°S, 119°E to 10°N, 127°E	5757	8.5	27	81	1008
	T9	03/25/11 02:30 to 3/27/11 07:39	10°N, 127°E to 21°N, 127°E	6712	21	21	75	1016

					WS	AT	RH	AP
	T10	03/27/11 10:09 to 3/29/11 03:57	22°N, 127°E to 31°N, 122°E	4744	16	16	65	1023
MOUDI (M)	M1	03/17/11 09:54 to 3/21/11 23:30	31°S, 114°E to 4°S, 118°E	197	5.9	30	69	1009
	M2	3/22/11 08:51 to 3/27/11 07:39	1°S, 119°E to 21°N, 127°E	174	14	24	78	1007
	R1	11/06/10 04:35 to 11/06/10 09:39	27°N, 121°E-26°N, 121°E	N/A	14	20	100	1017
	R2	11/12/10 03:18 to 11/12/10 05:00	18°N, 117°E-17°N, 117°E	N/A	5.8	24	100	1009
Rain (R)	R3	11/12/10 09:28 to 11/12/10 10:30	16°N, 118°E-16°N, 118°E	N/A	9.7	25	98	1009
	R4	03/22/11 08:40 to 3/23/11 03:35	2°S, 119°E-3°N, 122°E	N/A	3.1	27	79	1009
	R5	03/23/11 04:10 to 3/23/11 08:00	3°N, 122°E	N/A	4.4	26	89	1008
	R6	03/25/11 02:20 to 3/25/11 10:20	10°N, 127°E-11°N, 127°E	N/A	12	11	74	1026

*WS stands for average wind speed; AT stands for average air temperature; RH stands for average relative humidity; AP stands for average air pressure; N/A means not available.

Table 4.S2 Sea salt concentrations and wind speeds.

Sample No.	Sea salt (μg m^{-3})	Wind speed (m s^{-1})
T1	4.3	9.5
T2	3.1	3.6
T3	6.1	7.2
T4	9.8	11
T5	5.1	6.7
T6	8.1	7.4
T7	2	4.6
T8	3.2	8.5
T9	14	21
T10	29	16
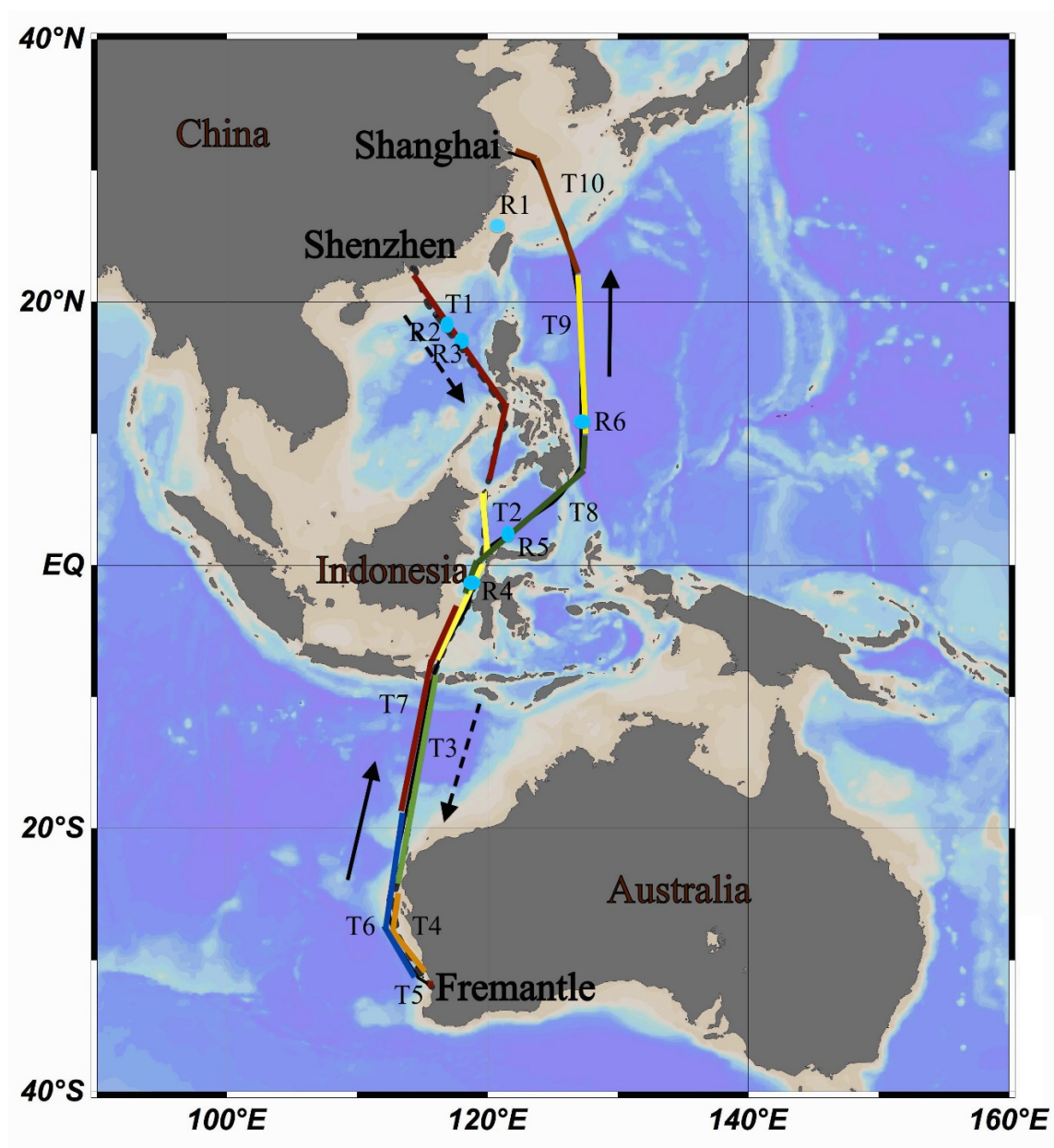
Figure 4.1 Cruise track and aerosol and precipitation samples collection locations.
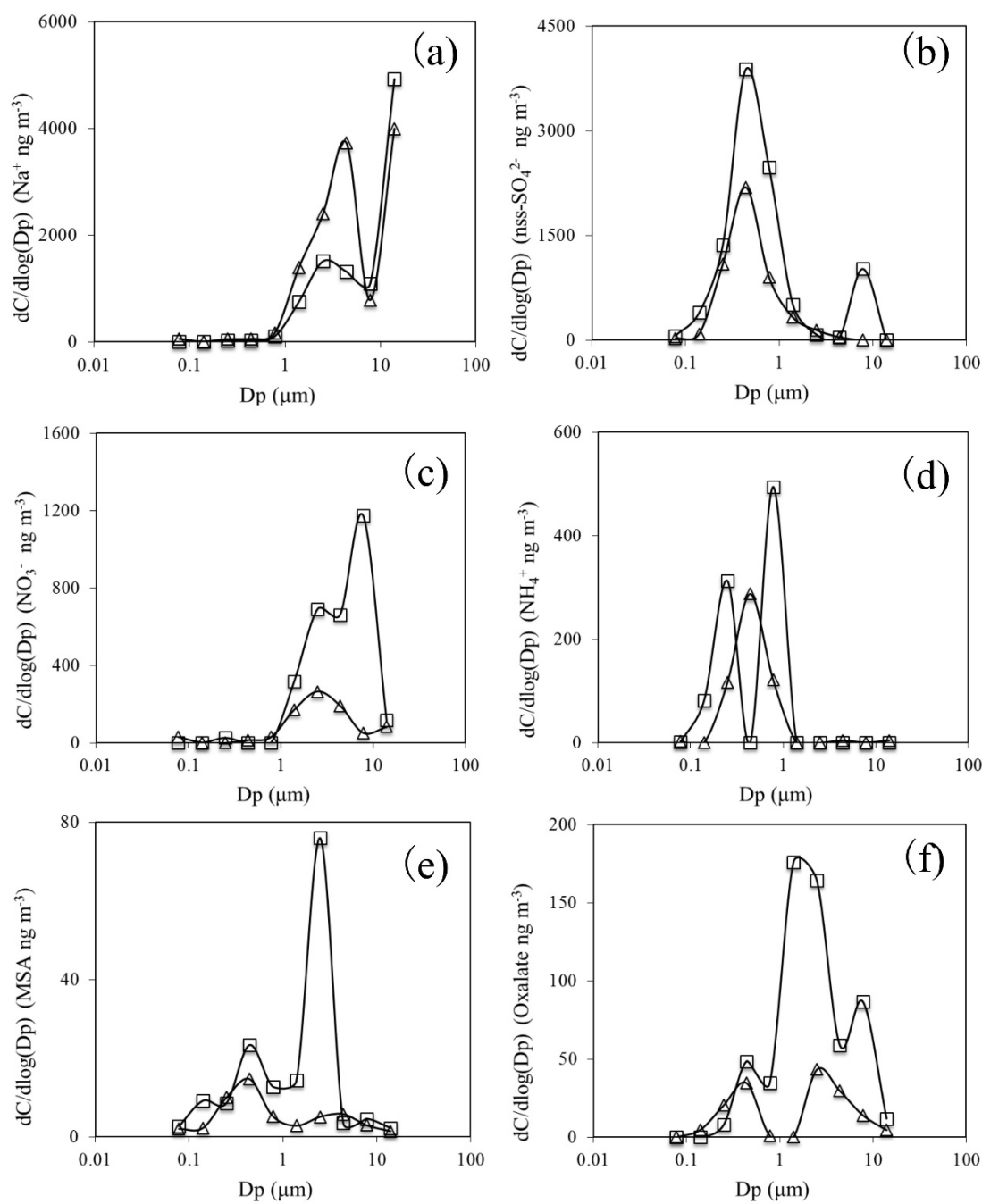
Figure 4.2 Size distributions of water-soluble inorganic and organic compounds in aerosols observed over South Indian Ocean and Australian coast (square symbol represented sample M1), Asian marginal seas (triangle symbol represented sample M2).
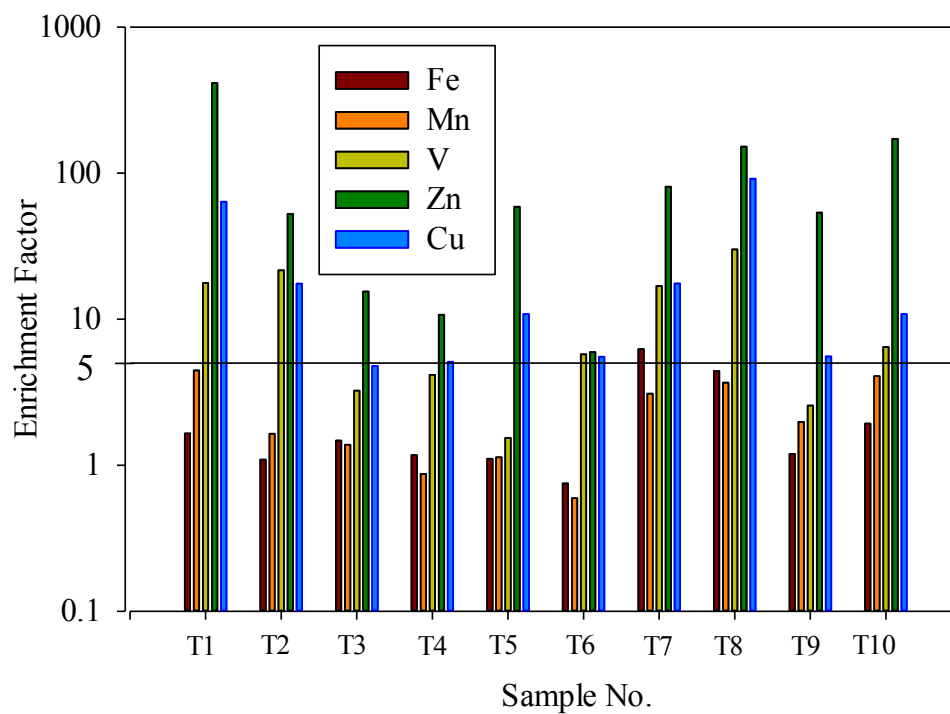
Figure 4.3 Enrichment factors of elements in aerosols over Asian marginal seas, South Indian Ocean and Australian coast against Al as the reference element for crustal material. The solid line indicates the value of 5 that operationally separates from the reference source.
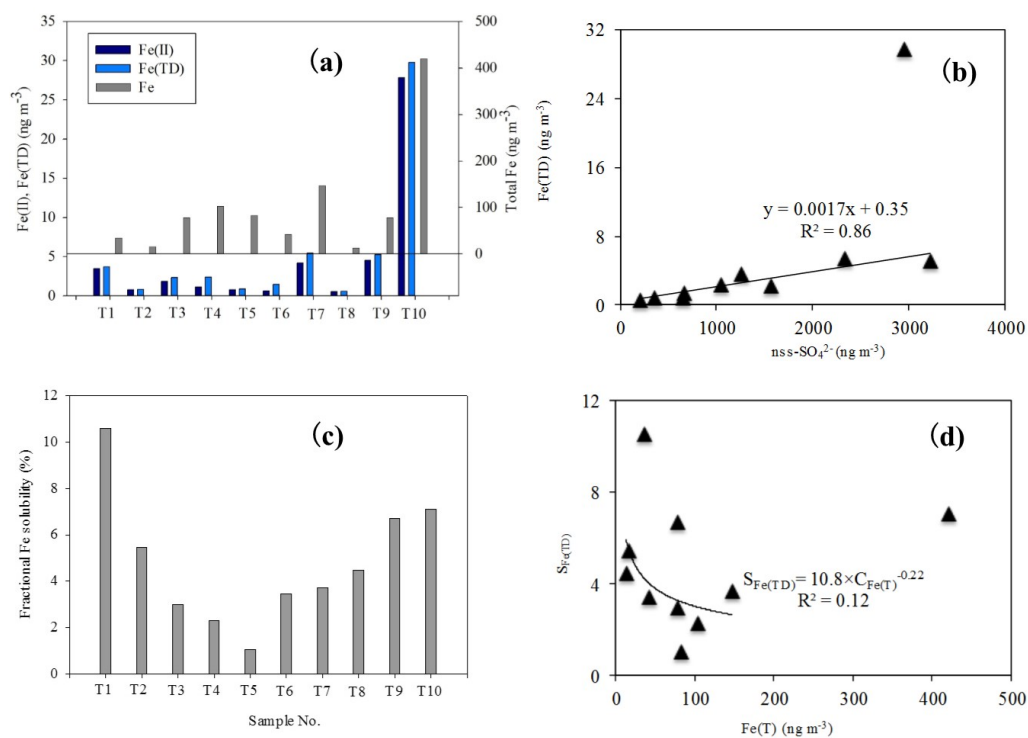
Figure 4.4 (a) Concentrations of atmospheric Fe(II), total dissolved iron (Fe(TD)), total Fe (Fe(T)); (b) Correlations of total dissolved iron and nss-SO_4^{2-} over Asian marginal seas, South Indian Ocean and Australian coast; (c) fractional Fe solubility over Asian marginal seas and South Indian Ocean; (d) Variation of fractional Fe solubility as a function of the total Fe in aerosols over Asian Marginal seas, South Indian Ocean and Australian coast.
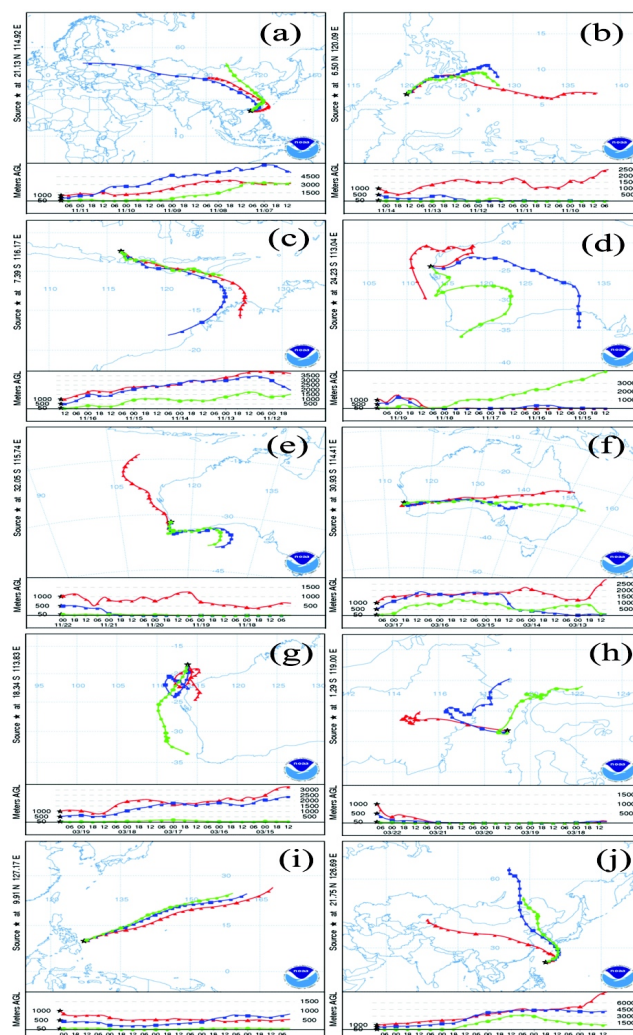
Figure 4.S1 5-day air-mass back trajectories (AMBTs) for samples collected over Asian Marginal seas, South Indian Ocean and Australian coast. These samples were (a) Sample T1; (b) Sample T2; (c) Sample T3; (d) Sample T4; (e) Sample T5; (f) Sample T6; (g) Sample T7; (h) Sample T8; (i) Sample T9; (j) Sample T10. The calculations were based on the National Oceanic and Atmospheric Administration (NOAA) GDAS meteorology data base, using the Hybrid Single-Particle Lagrangian Integrated Trajectories (HYSPLIT) program. AMBTs were performed at 50m, 500m and 1000 m height levels over the sampling locations every six hours with backward 5 days.
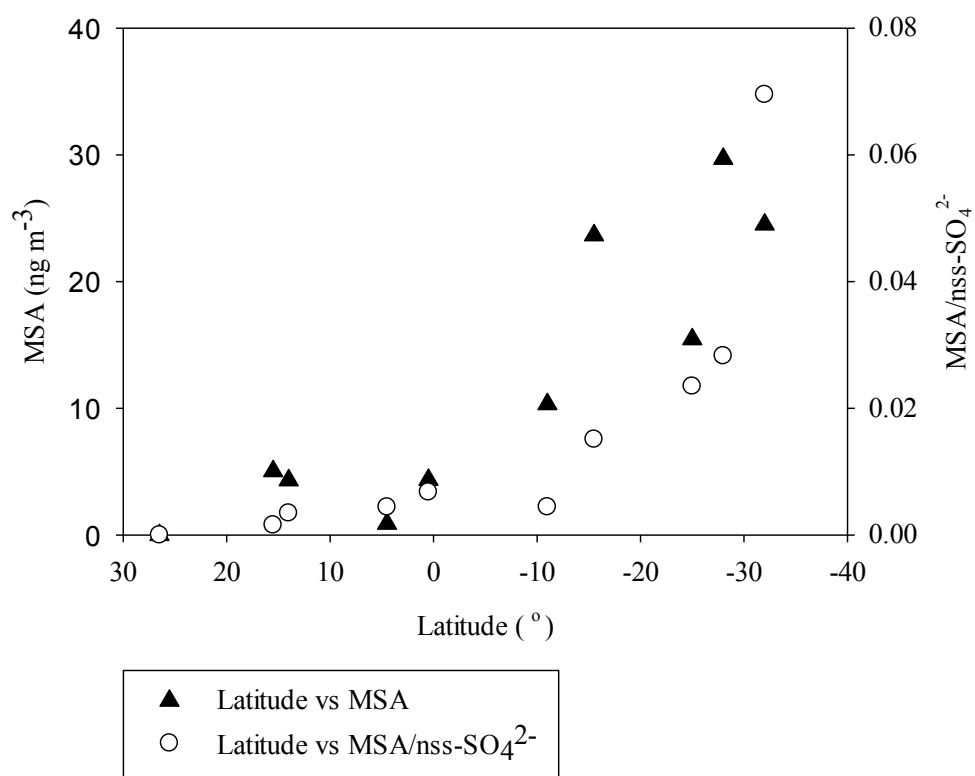
Figure 4.S2 Spatial distributions of MSA, MSA/nss-SO$_4^{2-}$.

Chapter 5: Conclusions, Limitations and Future Work

5.1 Conclusions

Bulk and size-segregated aerosol samples were collected during a cruise from November 2010 to March 2011 over the Southern Ocean, coastal East Antarctica, Asian marginal seas, South Indian Ocean and Australian coast. Water-soluble organic and inorganic species, selected trace elements and soluble iron species in aerosols were measured to characterize the chemical and physical properties of marine aerosols. Major findings from this work are as follows.

(1). Sea salt was the major component of the total aerosol mass, accounting for 72% over the Southern Ocean and 56% over coastal East Antarctica. The average concentrations of nss-SO_4^{2-} in aerosols varied from 420 ng m^{-3} over the Southern Ocean to 480 ng m^{-3} over coastal East Antarctica, while oxalate varied from 3.8 ng m^{-3} over the Southern Ocean to 2.2 ng m^{-3} over coastal East Antarctica. MSA ranged from 63 to 87 ng m^{-3} over the Southern Ocean and from 46 to 170 ng m^{-3} in coastal East Antarctica. Aerosol mass displayed a bimodal size distribution, peaked at 0.32-0.56 μm and 3.2-5.6 μm, respectively, over coastal East Antarctica. The aerosol nss-SO_4^{2-}, MSA and oxalate were mainly enriched in the fine mode. Higher neutralization capacity of the marine atmosphere over coastal East Antarctica was suggested by higher cation-to-anion and NH_4^+/nss-SO_4^{2-} ratios in aerosols compared to that over the Southern Ocean.

(2). Selected trace elements, including Na, Mg, K, Al, Fe, Mn, Ni, Cd and Se in aerosols, were measured by ICP-MS. The average concentrations of Na varied from 1100 ng m^{-3} over the Southern Ocean to 990 ng m^{-3} over the coastal East Antarctica. The concentrations of Fe varied from 14 ng m^{-3} over the Southern Ocean to 26 ng m^{-3} over the coastal East Antarctica, and Se varied from 0.25 ng m^{-3} over the Southern Ocean to 0.29 ng m^{-3} over the coastal East Antarctica. The aerosol Na, Mg and K were mainly accumulated in the coarse mode and Al, Fe and Mn presented a bimodal size distribution pattern. The combined particle-size distributions, enrichment factors and correlation analysis indicated that Na, Mg and K were dominated by the marine source, while Al, Fe and Mn were mainly from the crustal source. Ni, Cd and Se featured with high enrichment factors may contribute from mixed sources possibly from the long-range transport, marine biogenic emissions and anthropogenic emissions.

(3). During the same cruise, chemical composition, size distributions, and fractional Fe solubility in aerosol particles were also characterized over Asian marginal seas, South Indian Ocean and Australian coast. Sea salt and nss-SO_4^{2-} were the main components in aerosols, while Cl^- and Na^+ were the dominant ions in precipitation over Asian marginal seas. The concentrations of MSA and MSA/nss-SO_4^{2-} ratios increased southward. The mass of sea salt mainly accumulated in particles of >10 μm in diameter, while nss-SO_4^{2-} and NH_4^+ peaked in the fine mode and NO_3^- was enriched in the coarse mode. Oxalate presented a bimodal size distribution in both fine and coarse modes. Total dissolved iron and nss-SO_4^{2-} displayed a good relationship, indicating that acid processing during long-

range transport could affect fractional iron solubility in aerosols. Aerosols over Asian marginal seas could be affected by both Asian dust and anthropogenic emissions.

5.2 Limitations

Although this study generated new data and insights for the Southern Ocean, coastal East Antarctica, South Indian Ocean and Asian marginal seas, there are still substantial limitations associated with this study that need to be addressed in future studies. Major limitations include:

(1). Statistical analysis should have been strengthened for data processing. For example, the plot of size-distributions of Se generated from four sets of cascade impactor samples (Figure 3.3, page 73 in the thesis) should have been interpreted with more statistical analyses. Using the DistFit software package (Chimera technologies, Inc.) that is widely used in aerosol sciences, I re-plotted the concentrations of Se versus particle sizes, first shown in Figure 5.1 and then in Figure 5.2. The new results suggest a bimodal (fine mode and coarse mode) fit of particle size distributions of Se over the Southern Ocean (χ^2_{target}=0.02). This kind of analysis should be applied more to future data analyses.

(2). Particle-size distributions of aerosols as a function of relative humidity (RH) should have been investigated in more details. The presentation of aerosol size-distributions in this study was made with the consideration of ambient RH only when samples were collected, such as the mass-size distribution generated by samples collected by MOUDI (Figure 2.4, page 40 in the thesis). However, the particle size distributions for certain aerosol

components could be influenced by ambient conditions, especially RH, and this is particularly true for sea salt aerosol. *Zeng et al*. [2013] conducted lab simulations by using x-ray phase contrast imaging and found that sea salt particle deliquesced on a large RH scale between 34% and 97%. *Tang and Munkelwiz* [1984] reported that the deliquescence RH value was 75% for NaCl particle with size > 100 nm. In this study, sea salt particle size distributions could have been affected by deliquesce processes. With the average RH of 89% that we observed over coastal East Antarctica, I re-plotted the size-distributions of sea salt aerosol with additional two levels of RH, 40% and 98%, calculated with particle-growth formulas [*Peter*, 1988] (Figure 5.3). The results show that the peak of sea salt shifted to the left (smaller size) as the RH decreases to 40% and shifts to the right (larger size) as the RH increases to 98%. However, more investigations should be conducted in the future to confirm the calculated results.

(3). The Fe solubility determination in this study was operationally defined and was limited to a fixed pH level. The acidity of a leaching solution is an important factor affecting the determination of fractional iron solubility in aerosols; however, in this study, the aerosol-leaching experiments was made using a buffer at pH 5.1 [*Gao et al*., 2013], and this pH value was used as it was the pH level in precipitation that we collected in the Southern Ocean on the same cruise for the purpose of simulating cloud processes, but it was different from the pH of seawater (~pH=8.2). It is in question what Fe solubility could be if our aerosol samples were leached with seawater, as when aerosol particles deposit into the surface ocean, the physicochemical conditions of seawater, such as pH, seawater temperature, dissolved oxygen concentration will impact iron solubility. Figure 5.4 shows

the speciation of Fe in 0.7 mol kg^{-1} NaCl at 25°C as a function of pH. It's crucial to characterize iron solubility in seawater for better understanding Fe biogeochemical cycles.

5.3 Recommendations for Future Work

This dissertation was motivated by the lack of in situ observations on atmospheric aerosols over the vast Southern Ocean and coastal Antarctica. Further extensive cruise investigations should be made onboard, and long-term observations should be specifically conducted over costal Antarctic regions. Comprehensive atmospheric composition observations, including greenhouse gases (CO_2, N_2O, CH_4), O_3, DMS, carbonaceous aerosols and direct measurement of CCN and IN need to be simultaneously investigated during the cruise and land-based observations. Based on the research conducted in this dissertation, two major compelling questions or hypothesis have been raised and the following research is recommended in near future.

(1) I plan to identify the sources of atmospheric Fe over the Southern Ocean and coastal Antarctica. To achieve this goal, I will develop the hypothesis that sources within the Antarctic mainly contribute to the atmospheric Fe fertilization in the Southern Ocean and Antarctic coastal waters. To test this hypothesis, dissolved stable iron isotope ratios (δ^{56}Fe) and atmospheric iron concentrations will be measured. The unique δ^{56}Fe signatures can differentiate iron sources and estimate contributions from each source.

(2) I want to conduct field studies of aerosol Fe solubility in seawater. The area of research is based on the hypothesis that aerosol Fe dissolution in seawater is more impacted by physicochemical conditions of seawater than the source and

composition of aerosols. To address this scientific question, aerosol and surface seawater samples will be collected to quantify fractional iron solubility of aerosols and correlations between fractional iron solubility and seawater temperature, pH and dissolved oxygen concentration, versus aerosol source and composition will be generated.
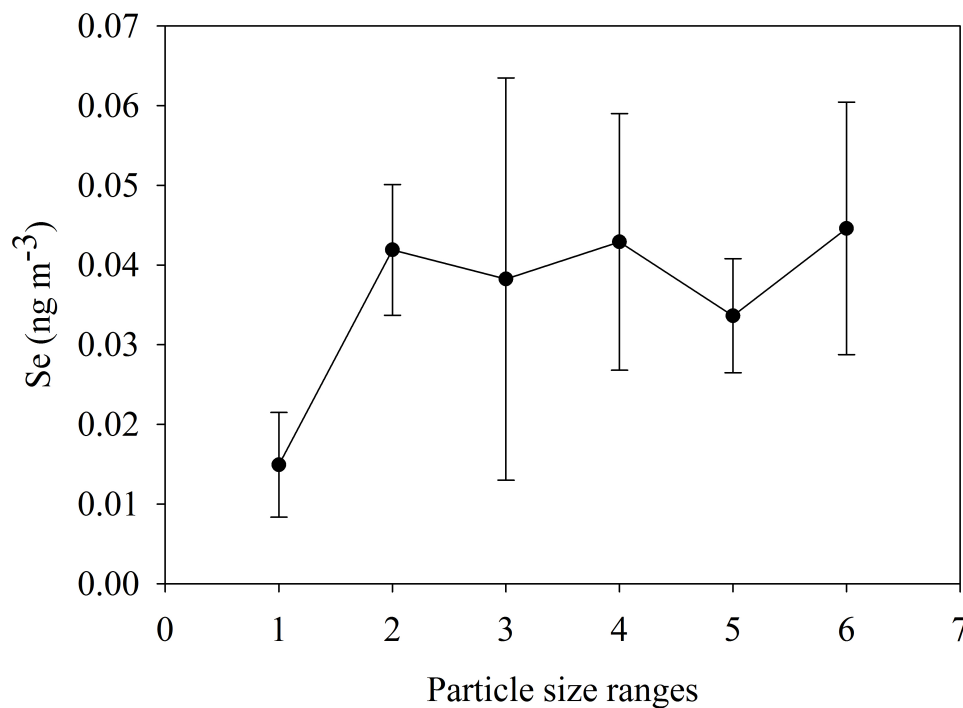
Figure 5.1 Particle size distributions of Se over the Southern Ocean (Note: In x-axis, 1 represents size range <0.49 µm; 2 represents size range 0.49-0.95 µm; 3 represents size range 0.95-1.5 µm; 4 represents size range 1.5-3 µm; 5 represents size range 3-7.2 µm; 6 represents size range >7.2 µm).
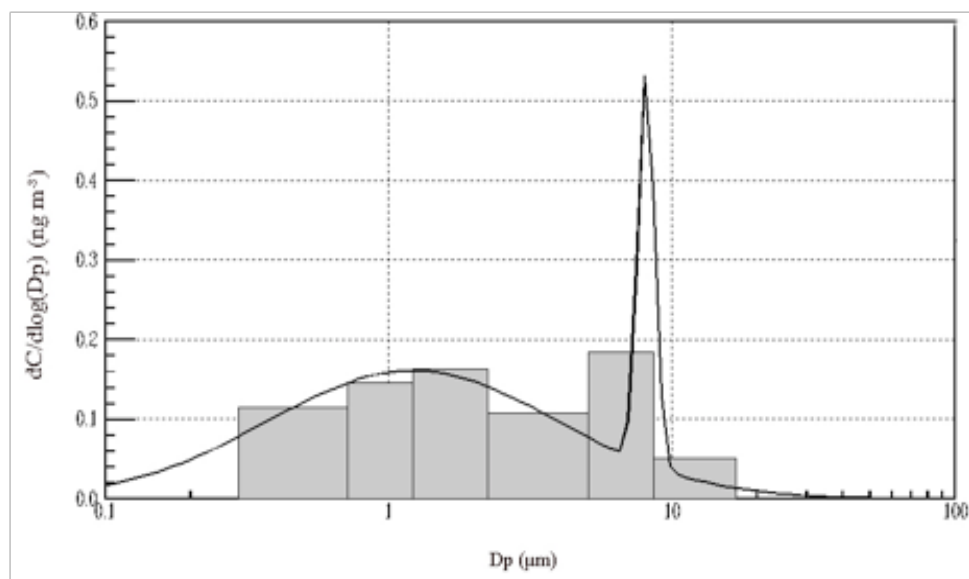
Figure 5.2 Bimodal particle size distributions of Se over the Southern Ocean (χ^2_{target}=0.02).
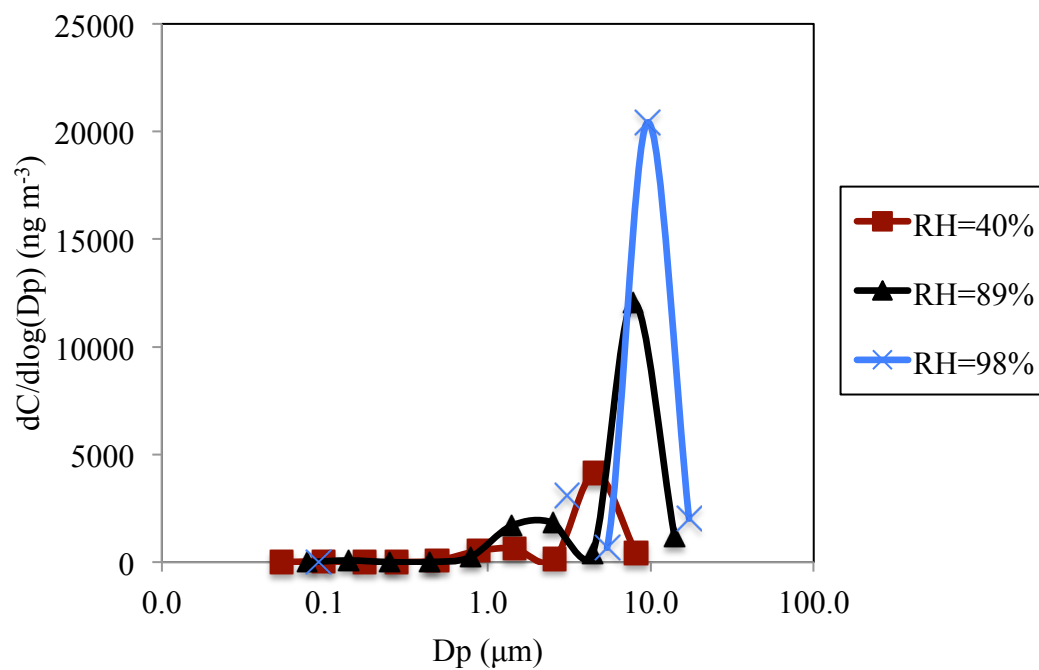
Figure 5.3 Aerosol sea salt size distributions as a function of RH.
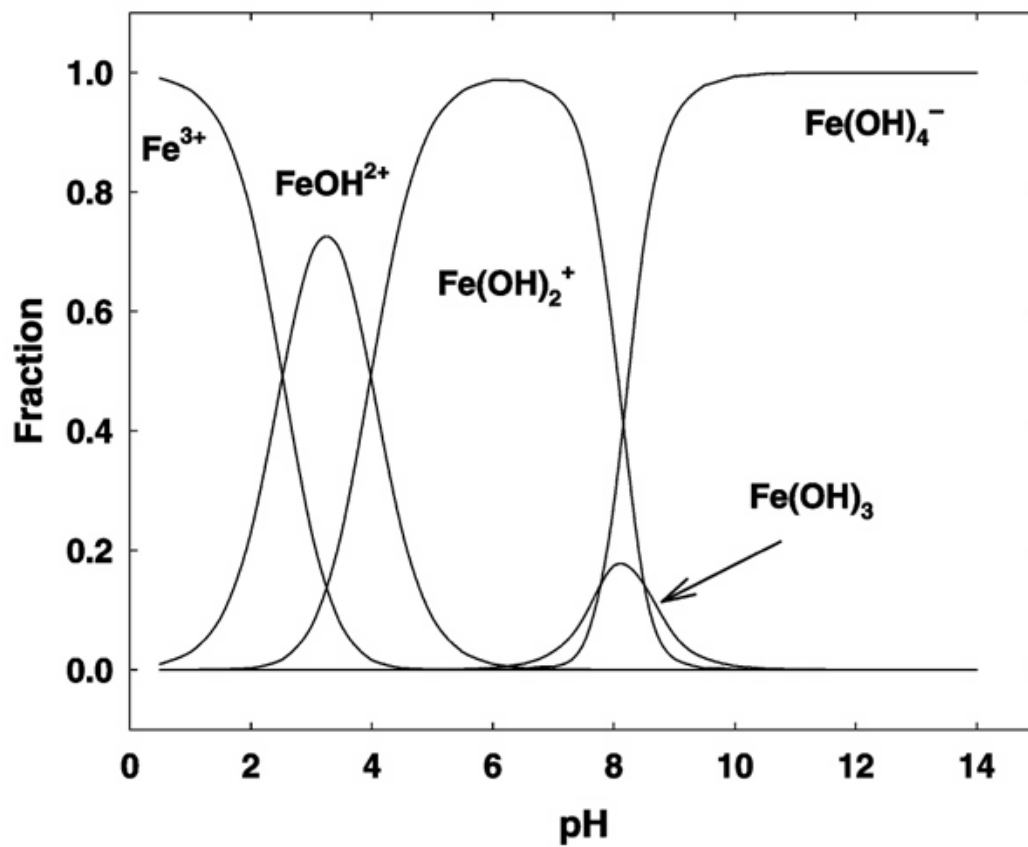
Figure 5.4 The speciation of Fe in 0.7 mol kg^{-1} NaCl at 25°C (Reproduced from *Millero* (2001)).

Reference:

Abbatt, J., K. Broekhuizen, and P. Pradeep Kumar (2005), Cloud condensation nucleus activity of internally mixed ammonium sulfate/organic acid aerosol particles, *Atmospheric Environment*, *39*(26), 4767-4778.

Albrecht, B. A. (1989), Aerosols, cloud microphysics, and fractional cloudiness, *Science*, *245*(4923), 1227-1230.

Annibaldi, A., C. Truzzi, S. Illuminati, E. Bassotti, and G. Scarponi (2007), Determination of water-soluble and insoluble (dilute-HCl-extractable) fractions of Cd, Pb and Cu in Antarctic aerosol by square wave anodic stripping voltammetry: distribution and summer seasonal evolution at Terra Nova Bay (Victoria Land), *Analytical and bioanalytical chemistry*, *387*(3), 977-998, doi:10.1007/s00216-006-0994-0.

Anttila, T., and V. M. Kerminen (2002), Influence of organic compounds on the cloud droplet activation: A model investigation considering the volatility, water solubility, and surface activity of organic matter, *J. Geophys. Res*, *1074*662.

Andreae, M. O. (1986), The ocean as a source of atmospheric sulfur compounds, in *The role of air-sea exchange in geochemical cycling*, edited, pp. 331-362, Springer.

Andreae, M. O., W. Elbert, Y. Cai, T. W. Andreae, and J. Gras (1999), Non-sea-salt sulfate, methanesulfonate, and nitrate aerosol concentrations and size distributions at Cape Grim, Tasmania, *Journal of geophysical research*, *104*(21), 695-621.

Arimoto, R., R. A. Duce, D. L. Savoie, J. M. Prospero, R. Talbot, J. D. Cullen, U. Tomza, N. F. Lewis, and B. J. Ray (1996), Relationships among aerosol constituents from Asia and the North Pacific during PEM-West A, *J. Geophys. Res.*, *101*(D1), 2011–2023, doi:10.1029/95JD01071.

Arimoto, R., T. Zeng, D. Davis, Y. Wang, H. Khaing, C. Nesbit, and G. Huey (2008), Concentrations and sources of aerosol ions and trace elements during ANTCI-2003, *Atmos. Environ.*, *42*(12), 2864-2876, doi:10.1016/J.Atmosenv.2007.05.054.

Arimoto, R., A. S. Nottingham, J. Webb, C. A. Schloesslin, and D. D. Davis (2001), Non-sea salt sulfate and other aerosol constituents at the South Pole during ISCAT, *Geophys. Res. Lett.*, *28*(19), 3645-3648, doi:10.1029/2000GL012714.

Arsene, C., I. Barnes, and K. H. Becker (1999), FT-IR product study of the photo-oxidation of dimethyl sulfide: Temperature and O2 partial pressure dependence, *Phys. Chem. Chem. Phys.*, *1*(24), 5463-5470, doi:10.1039/A907211J.

Artaxo, P., M. L. C. Rabello, W. Maenhaut, and R. V. A. N. Grieken (1992), Trace elements and individual particle analysis of atmospheric aerosols from the Antarctic peninsula, *Tellus B*, *44*(4), 318-334, doi:10.1034/j.1600-0889.1992.00010.x.

Ayers, G. P., and J. L. Gras (1991), Seasonal relationship between cloud condensation nuclei and aerosol methanesulphonate in marine air, *Nature*, *353*(6347), 834–835, doi:10.1038/353834a0.

Avramov, A., and J. Y. Harrington (2010), Influence of parameterized ice habit on simulated mixed phase Arctic clouds, *Journal of Geophysical Research: Atmospheres*, *115*(D3), D03205, doi:10.1029/2009JD012108.

Baeyens, W., A. R. Bowie, K. Buesseler, M. Elskens, Y. Gao, C. Lamborg, M. Leermakers, T. Remenyi, and H. Zhang (2011), Size-fractionated labile trace elements in the Northwest Pacific and Southern Oceans, *Marine Chemistry*, *126*(1-4), 108-113, doi:10.1016/j.marchem.2011.04.004.

Baker, A. R., S. D. Kelly, K. F. Biswas, M. Witt, and T. D. Jickells (2003), Atmospheric deposition of nutrients to the Atlantic Ocean, *Geophysical Research Letters*, *30*(24), 2296.

Baker, A. R., T. D. Jickells, M. Witt, and K. L. Linge (2006), Trends in the solubility of iron, aluminium, manganese and phosphorus in aerosol collected over the Atlantic Ocean, *Marine Chemistry*, *98*(1), 43-58, doi:10.1016/j.marchem.2005.06.004.

Baker, A., and P. Croot (2010), Atmospheric and marine controls on aerosol iron solubility in seawater, *Marine Chemistry*, *120*(1), 4-13, doi: 10.1016/j.marchem.2008.09.003

Bardouki, H., H. Liakakou, C. Economou, J. Sciare, J. Smolík, V. Ždímal, K. Eleftheriadis, M. Lazaridis, C. Dye, and N. Mihalopoulos (2003), Chemical composition of size-resolved atmospheric aerosols in the eastern Mediterranean during summer and winter, *Atmos. Environ.*, *37*(2), 195-208, doi:10.1016/S1352-2310(02)00859-2.

Barnes, I., J. Hjorth, and N. Mihalopoulos (2006), Dimethyl sulfide and dimethyl sulfoxide and their oxidation in the atmosphere, *Chem. Rev.*, *106*(3), 940-975, doi:10.1021/Cr020529+.

Bates, T. S., J. A. Calhoun, and P. K. Quinn (1992), Variations in the Methanesulfonate to Sulfate Molar Ratio in Submicrometer Marine Aerosol-Particles over the South-Pacific Ocean, *J. Geophys. Res.*, *97*(D9), 9859-9865, doi:10.1029/92jd00411.

Bates, T. S., P. K. Quinn, D. J. Coffman, J. E. Johnson, T. L. Miller, D. S. Covert, A. Wiedensohler, S. Leinert, A. Nowak, and C. Neusüss (2001), Regional physical and chemical properties of the marine boundary layer aerosol across the Atlantic during Aerosols99: An overview, *J. Geophys. Res.,*106(D18), 20767–20782, doi:10.1029/2000JD900578.

Bates, T. S., P. K. Quinn, D. Coffman, K. Schulz, D. S. Covert, J. E. Johnson, E. J. Williams, B. M. Lerner, W. M. Angevine, and S. C. Tucker (2008), Boundary layer

aerosol chemistry during TexAQS/GoMACCS 2006: Insights into aerosol sources and transformation processes, *J. Geophys. Res*, *113*D00F01.

Berresheim, H., and F. L. Eisele (1998), Sulfur Chemistry in the Antarctic Troposphere Experiment: An overview of project SCATE, *J. Geophys. Res.,* 103(D1), 1619–1627, doi:10.1029/97JD00103.

Berg, O. H., E. Swietlicki, and R. Krejci (1998), Hygroscopic growth of aerosol particles in the marine boundary layer over the Pacific and Southern Oceans during the First Aerosol Characterization Experiment (ACE 1), *Journal of Geophysical Research: Atmospheres*, *103*(D13), 16535-16545, doi:10.1029/97JD02851.

Berresheim, H., J. W. Huey, R. P. Thorn, F. L. Eisele, D. J. Tanner, and A. Jefferson (1998), Measurements of dimethyl sulfide, dimethyl sulfoxide, dimethyl sulfone, and aerosol ions at Palmer Station, Antarctica, *J. Geophys. Res.*, 103(D1), 1629–1637, doi:10.1029/97JD00695.

Bishop, J. K., R. E. Davis, and J. T. Sherman (2002), Robotic observations of dust storm enhancement of carbon biomass in the North Pacific, *Science*, *298*(5594), 817-821.

Bjerknes, J., and H. Solberg (1922), *Life cycle of cyclones and the polar front theory of atmospheric circulation*, Grondahl.

Blackall, T. D., L. J. Wilson, M. R. Theobald, C. Milford, E. Nemitz, J. Bull, P. J. Bacon, K. C. Hamer, S. Wanless, and M. A. Sutton (2007), Ammonia emissions from seabird colonies, *Geophys. Res. Lett.*, 34, L10801, doi:10.1029/2006GL028928.

Blain, S., et al. (2007), Effect of natural iron fertilization on carbon sequestration in the Southern Ocean, *Nature*, *446*(7139), 1070-1074, doi:10.1038/nature05700.

Blando, J. D., and B. J. Turpin (2000), Secondary organic aerosol formation in cloud and fog droplets: a literature evaluation of plausibility, *Atmos. Environ.*, *34*(10), 1623-1632, doi:10.1016/S1352-2310(99)00392-1.

Bowie, A. R., D. Lannuzel, T. A. Remenyi, T. Wagener, P. J. Lam, P. W. Boyd, C. Guieu, A. T. Townsend, and T. W. Trull (2009), Biogeochemical iron budgets of the Southern Ocean south of Australia: Decoupling of iron and nutrient cycles in the subantarctic zone by the summertime supply, *Global Biogeochemical Cycles*, *23*(4), GB4034, doi:10.1029/2009GB003500.

Boyd, P., G. McTainsh, V. Sherlock, K. Richardson, S. Nichol, M. Ellwood, and R. Frew (2004), Episodic enhancement of phytoplankton stocks in New Zealand subantarctic waters: Contribution of atmospheric and oceanic iron supply, *Global Biogeochemical Cycles*, *18*(1).

Boye, M., B. D. Wake, P. Lopez Garcia, J. Bown, A. R. Baker, and E. P. Achterberg (2012), Distributions of dissolved trace metals (Cd, Cu, Mn, Pb, Ag) in the southeastern Atlantic and the Southern Ocean, *Biogeosciences*, *9*(8), 3231-3246, doi:10.5194/bg-9-3231-2012.

Bruland, K. W., J. R. Donat, and D. A. Hutchins (1991), Interactive Influences of Bioactive Trace-Metals on Biological Production in Oceanic Waters, *Limnology and Oceanography*, *36*(8), 1555-1577.

Buck, C. S., W. M. Landing, and J. A. Resing (2010), Particle size and aerosol iron solubility: A high-resolution analysis of Atlantic aerosols, *Marine Chemistry*, *120*(1), 14-24.

Buck, C. S., W. M. Landing, and J. Resing (2013), Pacific Ocean aerosols: Deposition and solubility of iron, aluminum, and other trace elements, *Marine Chemistry*, *157*, 117-130, doi: 10.1016/j.marchem.2013.09.005.

Butler, A. (1998), Acquisition and utilization of transition metal ions by marine organisms, *Science*, *281*(5374), 207-209.

Cempel, M., and G. Nikel (2006), Nickel: a review of its sources and environmental toxicology, *Polish Journal of Environmental Studies*, *15*(3), 375-382.

Charlson, R. J., J. E. Lovelock, M. O. Andreae, and S. G. Warren (1987), Oceanic phytoplankton, atmospheric sulphur, cloud albedo and climate, *Nature*, *326*(6114), 655-661.

Chen, L., J. Wang, Y. Gao, G. Xu, X. Yang, Q. Lin, and Y. Zhang (2012), Latitudinal distributions of atmospheric MSA and MSA/nss-SO42− ratios in summer over the high latitude regions of the Southern and Northern Hemispheres, *Journal of Geophysical Research: Atmospheres*, *117*(D10), D10306, doi:10.1029/2011JD016559.

Chester, R. 1990. Marine Geochemistry. Unwin Hyman, London, 698 pp.

Chester, R., A. Berry, and K. Murphy (1991), The distributions of particulate atmospheric trace metals and mineral aerosols over the Indian Ocean, *Marine Chemistry*, *34*(3), 261-290.

Chever, F., G. Sarthou, E. Bucciarelli, S. Blain, and A. Bowie (2010), An iron budget during the natural iron fertilisation experiment KEOPS (Kerguelen Islands, Southern Ocean), *Biogeosciences*, *7*, 455-468.

Cruz, C. N., and S. N. Pandis (1997), A study of the ability of pure secondary organic aerosol to act as cloud condensation nuclei, *Atmospheric Environment*, *31*(15), 2205-2214.

Cullen, J. T., T. W. Lane, F. M. M. Morel, and R. M. Sherrell (1999), Modulation of cadmium uptake in phytoplankton by seawater CO2 concentration, *Nature*, *402*(6758), 165-167.

Cunningham, W. C., and W. H. Zoller (1981), The chemical composition of remote area aerosols, *Journal of Aerosol Science*, *12*(4), 367-384, doi: 10.1016/0021-8502(81)90026-4.

Cwiertny, D. M., J. Baltrusaitis, G. J. Hunter, A. Laskin, M. M. Scherer, and V. H. Grassian (2008), Characterization and acid mobilization study of iron containing mineral dust source materials, *Journal of Geophysical Research: Atmospheres (1984–2012)*, *113*(D5).

Cziczo, D. J., O. Stetzer, A. Worringen, M. Ebert, S. Weinbruch, M. Kamphus, S. J. Gallavardin, J. Curtius, S. Borrmann, and K. D. Froyd (2009), Inadvertent climate modification due to anthropogenic lead, *Nature geoscience*, *2*(5), 333-336.

Dachs, J., M. L. Calleja, C. M. Duarte, S. del Vento, B. Turpin, A. Polidori, G. J. Herndl, and S. Agustí (2005), High atmosphere-ocean exchange of organic carbon in the NE subtropical Atlantic, *Geophys. Res. Lett.,* 32, L21807, doi:10.1029/2005GL023799.

Davlson, W., and H. Zhang (1994), In situ speciation measurements of trace components in natural waters using thin-film gels, *Nature*, *367*(6463), 546-548.

Davis, D. D., et al. (2004), An overview of ISCAT 2000, *Atmos. Environ.*, *38*(32), 5363-5373, doi:10.1016/J.Atmosenv.2004.05.037.

Davis, D., G. Chen, A. Bandy, D. Thornton, F. Eisele, L. Mauldin, D. Tanner, D. Lenschow, H. Fuelberg, and B. Huebert (1999), Dimethyl sulfide oxidation in the equatorial Pacific: Comparison of model simulations with field observations for DMS, SO2, H2SO4 (g), MSA (g), MS and NSS, *Journal of geophysical research*, *104*(D5), 5765-5784.

de Baar, H. J. W., J. T. M. de Jong, D. C. E. Bakker, B. M. Loscher, C. Veth, U. Bathmann, and V. Smetacek (1995), Importance of iron for plankton blooms and carbon dioxide drawdown in the Southern Ocean, *Nature*, *373*(6513), 412-415.

DeMott, P. J*.,* K. Sassen*,* M. R. Poellot*,* D. Baumgardner*,* D. C. Rogers*,* S. D. Brooks*,* A. J. Prenni*, and* S. M. Kreidenweis *(*2003*),* African dust aerosols as atmospheric ice nuclei*, Geophys. Res. Lett*.*,* 30*, 1732,* doi*:*10.1029/2003GL017410*,* 14.

DeMott, P. J., A. J. Prenni, X. Liu, S. M. Kreidenweis, M. D. Petters, C. H. Twohy, M. S. Richardson, T. Eidhammer, and D. C. Rogers (2010), Predicting global atmospheric ice nuclei distributions and their impacts on climate, *Proceedings of the National Academy of Sciences*, doi:10.1073/pnas.0910818107.

Dentener, F. J., G. R. Carmichael, Y. Zhang, J. Lelieveld, and P. J. Crutzen (1996), Role of mineral aerosol as a reactive surface in the global troposphere, *Journal of Geophysical Research: Atmospheres*, *101*(D17), 22869-22889, doi:10.1029/96JD01818.

Dick, A. L. (1991), Concentrations and sources of metals in the Antarctic Peninsula aerosol, *Geochimica et cosmochimica acta*, *55*(7), 1827-1836.

Draxler, R.R. and G.D. Rolph (2014), HYSPLIT (HYbrid Single-Particle Lagrangian Integrated Trajectory) Model access via NOAA ARL READY Website (http://ready.arl.noaa.gov/HYSPLIT.php), NOAA Air Resources Laboratory, Silver Spring, MD.

Duce, R. A., G. L. Hoffman, and W. H. Zoller (1975), Atmospheric Trace Metals at Remote Northern and Southern Hemisphere Sites: Pollution or Natural?, *Science*, *187*(4171), 59-61, doi:10.1126/science.187.4171.59.

Dusek, U., et al. (2006), Size Matters More Than Chemistry for Cloud-Nucleating Ability of Aerosol Particles, *Science*, *312*(5778), 1375-1378, doi:10.1126/science.1125261.

Echeveste, P., A. Tovar-Sánchez, and S. Agustí (2014), Tolerance of polar phytoplankton communities to metals, *Environmental pollution*, *185*(0), 188-195, doi: 10.1016/j.envpol.2013.10.029.

Eisele, F., et al. (2008), Antarctic Tropospheric Chemistry Investigation (ANTCI) 2003 overview, *Atmos. Environ.*, *42*(12), 2749-2761, doi:10.1016/J.Atmosenv.2007.04.013.

Ervens, B., G. Feingold, G. J. Frost, and S. M. Kreidenweis (2004), A modeling study of aqueous production of dicarboxylic acids: 1. Chemical pathways and speciated organic mass production, *J. Geophys. Res.,* 109, D15205, doi:10.1029/2003JD004387.

Ervens, B., B. J., Turpin, and R. J., Weber (2011), Secondary organic aerosol formation in cloud droplets and aqueous particles (aqSOA): a review of laboratory, field and model studies, *Atmos. Chem. Phys.,* 11, 11069-11102, doi:10.5194/acp-11-11069-2011.

Ezat, U., H. Cachier, G. Polian, and B. Ardouin (1994), 14. P. 12 Long-range atmospheric transport of aerosols to the Southern Indian Ocean (Amsterdam Island: 37° 48′ S 77° 34′ E), *Journal of Aerosol Science*, *25*, 133-134.

Fattori, I., S. Becagli, S. Bellandi, E. Castellano, M. Innocenti, A. Mannini, M. Severi, V. Vitale, and R. Udisti (2005), Chemical composition and physical features of summer aerosol at Terra Nova Bay and Dome C, Antarctica, *J Environ Monitor*, *7*(12), 1265-

1274, doi:10.1039/B507327H.

Finlayson-Pitts, B., J.N., Pitts (2000), Chemistry of the Upper and Lower Atmosphere: theory, experiment, and application-chapter 9, Academic Press, 381–391 pp.

Fitzgerald, J. W. (1991), Marine aerosols: A review, *Atmospheric Environment. Part A. General Topics*, *25*(3-4), 533-545.

Frew, R., A. Bowie, P. Croot, and S. Pickmere (2001), Macronutrient and trace-metal geochemistry of an in situ iron-induced Southern Ocean bloom, *Deep Sea Research Part II: Topical Studies in Oceanography*, *48*(11–12), 2467-2481, doi: 10.1016/S0967-0645(01)00004-2.

Fu, P., K. Kawamura, and K. Miura (2011), Molecular characterization of marine organic aerosols collected during a round-the-world cruise, *J. Geophys. Res.*, *116*(D13), D13302, doi:10.1029/2011jd015604.

Fu, P., K. Kawamura, K. Usukura, and K. Miura (2013), Dicarboxylic acids, ketocarboxylic acids and glyoxal in the marine aerosols collected during a round-the-world cruise, *Marine Chemistry*, *148*, 22-32.

Fuentes, E., H. Coe, D. Green, G. De Leeuw, and G. McFiggans (2010), Laboratory-generated primary marine aerosol via bubble-bursting and atomization, *Atmos. Meas. Tech., 3*(1), 141-162, doi:10.5194/amt-3-141-2010.

Gao, Y., R. Arimoto, M. Zhou, J. Merrill, and R. Duce (1992), Relationships between the dust concentrations over eastern Asia and the remote North Pacific, *Journal of Geophysical Research: Atmospheres (1984–2012)*, *97*(D9), 9867-9872.

Gao, Y., R. Arimoto, R. A. Duce, L. Q. Chen, M. Y. Zhou, and D. Y. Gu (1996), Atmospheric non-sea-salt sulfate, nitrate and methanesulfonate over the China Sea, *J. Geophys. Res.*, 101(D7),12601-12611, doi:10.1029/96JD00866.

Gao, Y., and J. R. Anderson (2001), Characteristics of Chinese aerosols determined by individual-particle analysis, *Journal of Geophysical Research: Atmospheres*, *106*(D16), 18037-18045, doi:10.1029/2000JD900725.

Gao, Y. (2002), Atmospheric nitrogen deposition to Barnegat Bay, *Atmos. Environ.*, *36*(38), 5783-5794, doi:10.1016/S1352-2310(02)00656-8.

Gao, Y., G. Xu, J. Zhan, J. Zhang, W. Li, Q. Lin, L. Chen, and H. Lin (2013), Spatial and particle size distributions of atmospheric dissolvable iron in aerosols and its input to the Southern Ocean and coastal East Antarctica, *J. Geophys. Res. Atmos.*, 118, 12,634–12,648, doi:10.1002/2013JD020367.

Gassó, S., and A. F. Stein (2007), Does dust from Patagonia reach the sub-Antarctic Atlantic Ocean?, *Geophysical Research Letters*, *34*(1), L01801, doi:10.1029/2006GL027693.

Gras, J. L. (1983), Ammonia and ammonium concentrations in the antarctic atmosphere, *Atmos. Environ.*, *(1967)*, *17*(4), 815-818, doi:10.1016/0004-6981(83)90431-6.

Grgić, I. (2009), Metals in Aerosols, in *Environmental Chemistry of Aerosols*, edited, pp. 117-139, Blackwell Publishing Ltd., doi:10.1002/9781444305388.ch5.

Hara, K., K. Osada, K. Matsunaga, T. Sakai, Y. Iwasaka, and K. Furuya (2002), Concentration trends and mixing states of particulate oxalate in Arctic boundary layer in winter/spring, *J. Geophys. Res.*, *107*(D19), 4399, doi:10.1029/2001jd001584.

Hara, K., K. Osada, M. Yabuki, and T. Yamanouchi (2012), Seasonal variation of fractionated sea   salt particles on the Antarctic coast, *Geophysical Research Letters*, *39*(18).

Harris, E., et al. (2013), Enhanced Role of Transition Metal Ion Catalysis During In-Cloud Oxidation of SO2, *Science*, 340(6133), 727-730, doi:10.1126/science.1230911.

Heimburger, A., R. Losno, S. Triquet, F. Dulac, and N. Mahowald (2012), Direct measurements of atmospheric iron, cobalt, and aluminum-derived dust deposition at Kerguelen Islands, *Global Biogeochem. Cycles*, 26, GB4016, doi:10.1029/2012GB004301.

Heimburger, A., R. Losno, and S. Triquet (2013), Solubility of iron and other trace elements in rainwater collected on the Kerguelen Islands (South Indian Ocean), *Biogeosciences*, *10*(10), 6617-6628, doi:10.5194/bg-10-6617-2013.

Heintzenberg, J., D. Covert, and R. Van Dingenen (2000), Size distribution and chemical composition of marine aerosols: a compilation and review, *Tellus B*, *52*(4), 1104-1122.

Herner, J. D., Q. Ying, J. Aw, O. Gao, D. P. Y. Chang, and M. J. Kleeman (2006), Dominant Mechanisms that Shape the Airborne Particle Size and Composition Distribution in Central California, *Aerosol Sci. Tech.*, *40*(10), 827-844, doi:10.1080/02786820600728668.

Hesse, P. P. (1994), The record of continental dust from Australia in Tasman Sea sediments, *Quaternary Science Reviews*, *13*(3), 257-272.

Hogan, A. W. (1975), Antarctic aerosols, *J Appl Meteorol*, *14*(4), 550-559.

Honrath, R. E., M. C. Peterson, S. Guo, J. E. Dibb, P. B. Shepson, and B. Campbell (1999), Evidence of NOx production within or upon ice particles in the Greenland snowpack,

Geophys. Res. Lett., *26*(6), 695-698, doi:10.1029/1999GL900077.

Hsu, S.-C., G. T. Wong, G.-C. Gong, F.-K. Shiah, Y.-T. Huang, S.-J. Kao, F. Tsai, S.-C. Candice Lung, F.-J. Lin, and I. Lin (2010), Sources, solubility, and dry deposition of aerosol trace elements over the East China Sea, *Marine Chemistry*, *120*(1), 116-127.

Hsu, S. C., F. Tsai, F. J. Lin, W. N. Chen, F. K. Shiah, C. Huang Jr, C. Y. Chan, C. C. Chen, T. H. Liu, and H. Y. Chen (2013), A super Asian dust storm over the East and South China Seas: Disproportionate dust deposition, *Journal of Geophysical Research: Atmospheres*, *118*(13), 7169-7181.

Hur, S. D., X. Cunde, S. Hong, C. Barbante, P. Gabrielli, K. Lee, C. F. Boutron, and Y. Ming (2007), Seasonal patterns of heavy metal deposition to the snow on Lambert Glacier basin, East Antarctica, *Atmospheric Environment*, *41*(38), 8567-8578, doi:10.1016/j.atmosenv.2007.07.012.

Jickells, T. D., and L. J. Spokes (2001), Atmospheric iron inputs to the oceans, *IUPAC series on analytical and physical chemistry of environmental systems*, *7*, 85-122.

Jickells, T. D., S. D. Kelly, A. R. Baker, K. Biswas, P. F. Dennis, L. J. Spokes, M. Witt, and S. G. Yeatman (2003), Isotopic evidence for a marine ammonia source, *Geophys. Res. Lett.*, 30, 1374, doi:10.1029/2002GL016728, 7.

Jickells, T., Z. An, K. K. Andersen, A. Baker, G. Bergametti, N. Brooks, J. Cao, P. Boyd, R. Duce, and K. Hunter (2005), Global iron connections between desert dust, ocean biogeochemistry, and climate, *Science*, *308*(5718), 67-71, doi:10.1126/science.1105959.

Johnson, M. T., and T. G. Bell (2008), Coupling between dimethylsulfide emissions and the ocean–atmosphere exchange of ammonia, *Environ. Chem.*, *5*(4), 259-267.

Johnson, M. S., N. Meskhidze, V. P. Kiliyanpilakkil, and S. Gassó (2011), Understanding the transport of Patagonian dust and its influence on marine biological activity in the South Atlantic Ocean, *Atmospheric Chemistry and Physics*, *11*(6), 2487-2502, doi:10.5194/acp-11-2487-2011.

Jones, A. E., R. Weller, P. S. Anderson, H. W. Jacobi, E. W. Wolff, O. Schrems, and H. Miller (2001), Measurements of NO_x emissions from the Antarctic snowpack, *Geophys. Res. Lett.*, *28*(8), 1499-1502, doi:10.1029/2000GL011956.

Jourdain, B., and M. Legrand (2001), Seasonal variations of atmospheric dimethylsulfide, dimethylsulfoxide, sulfur dioxide, methanesulfonate, and non sea salt sulfate aerosols at Dumont d'Urville (coastal Antarctica)(December 1998 to July 1999), *Journal of Geophysical Research: Atmospheres (1984–2012)*, *106*(D13), 14391-14408.

Jourdain, B., and M. Legrand (2002), Year-round records of bulk and size-segregated aerosol composition and HCl and HNO$_3$ levels in the Dumont d'Urville (coastal Antarctica) atmosphere: Implications for sea-salt aerosol fractionation in the winter and summer, *J. Geophys. Res.*, 107, 4645, doi:10.1029/2002JD002471.

Kalnajs, L. E., L. M. Avallone, and D. W. Toohey (2013), Correlated measurements of ozone and particulates in the Ross Island region, Antarctica, *Geophysical Research Letters*, *40*(23), 2013GL058422, doi:10.1002/2013GL058422.

Kawamura, K., and K. Ikushima (1993), Seasonal changes in the distribution of dicarboxylic acids in the urban atmosphere, *Environ. Sci. Technol., 27*(10), 2227-2235, doi:10.1021/es00047a033.

Kawamura, K., H. Kasukabe, and L. A. Barrie (1996a), Source and reaction pathways of dicarboxylic acids, ketoacids and dicarbonyls in arctic aerosols: One year of observations, *Atmos. Environ.*, *30*(10–11), 1709-1722, doi:10.1016/1352-2310(95)00395-9.

Kawamura, K., R. Seméré, Y. Imai, Y. Fujii, and M. Hayashi (1996b), Water soluble dicarboxylic acids and related compounds in Antarctic aerosols, *J. Geophys. Res.*, 101(D13), 18,721–18,728, doi:10.1029/96JD01541.

Kawamura, K., and F. Sakaguchi (1999), Molecular distributions of water soluble dicarboxylic acids in marine aerosols over the Pacific Ocean including tropics, *Journal of Geophysical Research: Atmospheres*, *104*(D3), 3501-3509, doi:10.1029/1998JD100041.

Keene, W. C., and J. N. Galloway (1988), The biogeochemical cycling of formic and acetic acids through the troposphere: an overview of current understanding, *Tellus B, 40B*(5), 322-334, doi: 10.1111/j.1600-0889.1988.tb00106.x.

Kerminen, V.-M., T. A. Pakkanen, and R. E. Hillamo (1997), Interactions between inorganic trace gases and supermicrometer particles at a coastal site, *Atmos. Environ.*, *31*(17), 2753-2765, doi:10.1016/S1352-2310(97)00092-7.

Kerminen, V. M., K. Teinilä, R. Hillamo, and T. Mäkelä (1999), Size-segregated chemistry of particulate dicarboxylic acids in the Arctic atmosphere, *Atmospheric Environment*, *33*(13), 2089-2100.

Kerminen, V.-M., C. Ojanen, T. Pakkanen, R. Hillamo, M. Aurela, and J. Meriläinen (2000), Low-molecular-weight dicarboxylic acids in an urban and rural atmosphere, *Journal of Aerosol Science*, *31*(3), 349-362.

Kerminen, V.-M., R. Hillamo, K. Teinilä, T. Pakkanen, I. Allegrini, and R. Sparapani

(2001), Ion balances of size-resolved tropospheric aerosol samples: implications for the acidity and atmospheric processing of aerosols, *Atmos. Environ.*, *35*(31), 5255-5265, doi:10.1016/S1352-2310(01)00345-4.

Kim, G., J. R. Scudlark, and T. M. Church (2000), Atmospheric wet deposition of trace elements to Chesapeake and Delaware Bays, *Atmospheric Environment*, *34*(20), 3437-3444, doi:10.1016/S1352-2310(99)00371-4.

Kim, E., P. K. Hopke, T. V. Larson, and D. S. Covert (2003), Analysis of Ambient Particle Size Distributions Using Unmix and Positive Matrix Factorization, *Environ. Sci. Technol.*, *38*(1), 202-209, doi:10.1021/es030310s.

Koçak, M., N. Mihalopoulos, and N. Kubilay (2007), Chemical composition of the fine and coarse fraction of aerosols in the northeastern Mediterranean, *Atmospheric Environment*, *41*(34), 7351-7368.

Kyle, P. R., K. Meeker, and D. Finnegan (1990), Emission rates of sulfur dioxide, trace gases and metals from Mount Erebus, Antarctica, *Geophysical Research Letters*, *17*(12), 2125-2128.

Lane, T. W., and F. M. M. Morel (2000), A biological function for cadmium in marine diatoms, *Proceedings of the National Academy of Sciences*, *97*(9), 4627-4631, doi:10.1073/pnas.090091397.

Lapina, K., C. L. Heald, D. V. Spracklen, S. R. Arnold, J. D. Allan, H. Coe, G. McFiggans, S. R. Zorn, F. Drewnick, and T. S. Bates (2011), Investigating organic aerosol loading in the remote marine environment, *Atmospheric Chemistry and Physics*, *11*(17), 8847-8860.

Legrand, M., C. Feniet-Saigne, E. S. Sattzman, C. Germain, N. I. Barkov, and V. N. Petrov (1991), Ice-core record of oceanic emissions of dimethylsulphide during the last climate cycle, *Nature*, *350*(6314), 144-146.

Legrand, M., F. Ducroz, D. Wagenbach, R. Mulvaney, and J. Hall (1998), Ammonium in coastal Antarctic aerosol and snow: Role of polar ocean and penguin emissions, *J. Geophys. Res*., 103(D9), 11043–11056, doi:10.1029/97JD01976.

Legrand, M., S. Preunkert, B. Jourdain, and B. Aumont (2004), Year-round records of gas and particulate formic and acetic acids in the boundary layer at Dumont d'Urville, coastal Antarctica, *J. Geophys. Res.*, 109, D06313, doi:10.1029/2003JD003786.

Legrand, M*., V. Gros*, S. Preunkert*, R. Sarda-Estève*, A.-M. Thierry*, G. Pépy*, and* B. Jourdain *(*2012*),* A reassessment of the budget of formic and acetic acids in the boundary layer at Dumont d'Urville (coastal Antarctica): The role of penguin emissions on the budget of several oxygenated volatile organic compounds*, J. Geophys. Res.,* 117*, D06308, doi:*10.1029/2011JD017102*.

Levin, Z., A. Teller, E. Ganor, and Y. Yin (2005), On the interactions of mineral dust, sea-salt particles, and clouds: A measurement and modeling study from the Mediterranean Israeli Dust Experiment campaign, *Journal of Geophysical Research: Atmospheres (1984–2012)*, *110*(D20).

Lewis, R., and E. Schwartz (2004), *Sea salt aerosol production: mechanisms, methods, measurements and models—a critical review*, American Geophysical Union.

Limbeck, A., M. Kulmala, and H. Puxbaum (2003), Secondary organic aerosol formation in the atmosphere via heterogeneous reaction of gaseous isoprene on acidic particles, *Geophys. Res. Lett.,*30, 1996, doi:10.1029/2003GL017738, 19.

Liss, P. S., and J. N. Galloway (1993), Air-Sea exchange of sulphur and nitrogen and their interaction in the marine atmosphere, in: *Interactions of C,N,P and S Biogeochemical Cycles and Global Change*, edited by R. Wollast, F. T. Mackenzie, and L. Chou, Springer Verlag, Berlin.

Liss, P. S., and J. E. Lovelock (2007), Climate change: the effect of DMS emissions, *Environ. Chem.*, *4*(6), 377-378, doi:10.1071/EN07072.

Luo, C., N. Mahowald, T. Bond, P. Chuang, P. Artaxo, R. Siefert, Y. Chen, and J. Schauer (2008), Combustion iron distribution and deposition, *Global Biogeochemical Cycles*, *22*(1).

Maenhaut, W., W. H. Zoller, R. A. Duce, and G. L. Hoffman (1979), Concentration and size distribution of particulate trace elements in the south polar atmosphere, *Journal of Geophysical Research*, *84*(C5), 2421, doi:10.1029/JC084iC05p02421.

Mahowald, N. (2011), Aerosol indirect effect on biogeochemical cycles and climate, *Science*, *334*(6057), 794-796, doi:10.1126/science.1207374.

Martinelango, P. K., P. K. Dasgupta, and R. S. Al-Horr (2007), Atmospheric production of oxalic acid/oxalate and nitric acid/nitrate in the Tampa Bay airshed: Parallel pathways, *Atmos. Environ.*, *41*(20), 4258-4269, doi:10.1016/j.atmosenv.2006.05.085.

Mazzera, D. M. et al. (2001a), Sources of PM_{10} and sulfate aerosol at McMurdo station, Antarctica, *Chemosphere*, 45(3), 347-356, doi:10.1016/S0045-6535(00)00591-9.

Mazzera, D. M., D. H. Lowenthal, J. C. Chow, J. G. Watson, and V. Grubĭsíc (2001b), PM10 measurements at McMurdo Station, Antarctica, *Atmos. Environ.*, *35*(10), 1891-1902, doi:10.1016/S1352-2310(00)00409-X.

McInnes, L. M., D. S. Covert, P. K. Quinn, and M. S. Germani (1994), Measurements of chloride depletion and sulfur enrichment in individual sea-salt particles collected

from the remote marine boundary layer, *J. Geophys. Res.*, 99(D4), 8257–8268, doi:10.1029/93JD03453.

Millero, F. j., and M. L. Sohn (1992), *Chemical Oceanography*, 531 pp., CRC Press, Boca Raton, Fla.

Millero, F. (2001), Speciation of metals in natural waters, *Geochemical Transactions*, *2*(1), 57.

Millero, Frank J. (2013), Minor elements in seawater. In *Chemical oceanography*: CRC Press. Pp. 91-102.

Minikin, A., M. Legrand, J. Hall, D. Wagenbach, C. Kleefeld, E. Wolff, E. C. Pasteur, and F. Ducroz (1998), Sulfur-containing species (sulfate and methanesulfonate) in coastal Antarctic aerosol and precipitation, *J. Geophys. Res.,* 103(D9), 10975–10990, doi:10.1029/98JD00249.

Mishra, V. K., K.-H. Kim, S. Hong, and K. Lee (2004), Aerosol composition and its sources at the King Sejong Station, Antarctic peninsula, *Atmospheric Environment*, *38*(24), 4069-4084, doi:10.1016/j.atmosenv.2004.03.052.

Moffet, R. C., H. Furutani, T. C. Rödel, T. R. Henn, P. O. Sprau, A. Laskin, M. Uematsu, and M. K. Gilles (2012), Iron speciation and mixing in single aerosol particles from the Asian continental outflow, *Journal of Geophysical Research: Atmospheres*, *117*(D7), D07204, doi:10.1029/2011JD016746.

Moore, C., M. Mills, K. Arrigo, I. Berman-Frank, L. Bopp, P. Boyd, E. Galbraith, R. Geider, C. Guieu, and S. Jaccard (2013), Processes and patterns of oceanic nutrient limitation, *Nature Geoscience*, *6*(9), 701-710.

Möller, D. (2010), *Chemistry of the Climate System*, Walter de Gruyter, Berlin, 219-222 pp.

Morel, F. M., and N. M. Price (2003), The biogeochemical cycles of trace metals in the oceans, *Science*, *300*(5621), 944-947, doi:10.1126/science.1083545.

Mosher, B. W., R. A. Duce, J. M. Prospero, and D. L. Savoie (1987), Atmospheric selenium: Geographical distribution and ocean to atmosphere flux in the Pacific, *Journal of Geophysical Research: Atmospheres*, *92*(D11), 13277-13287, doi:10.1029/JD092iD11p13277.

Mouri, H., I. Nagao, K. Okada, S. Koga, and H. Tanaka (1997), Elemental compositions of individual aerosol particles collected over the Southern Ocean: A case study, *Atmospheric research*, *43*(2), 183-195.

Murphy, D., J. Anderson, P. Quinn, L. McInnes, F. Brechtel, S. Kreidenweis, A. Middlebrook, M. Posfai, D. Thomson, and P. Buseck (1998), Influence of sea-salt on aerosol radiative properties in the Southern Ocean marine boundary layer, *Nature*, 392(6671), 62-65, doi:10.1038/32138.

Myriokefalitakis, S., K. Tsigaridis, N. Mihalopoulos, J. Sciare, A. Nenes, K. Kawamura, A. Segers, and M. Kanakidou (2011), In-cloud oxalate formation in the global troposphere: a 3-D modeling study, *Atmos. Chem. Phys*, 115761-5782.

Neu, J. L., M. J. Prather, and J. E. Penner (2007), Global atmospheric chemistry: Integrating over fractional cloud cover, *J. Geophys. Res.*, 112, D11306, doi:10.1029/2006JD008007.

Nicol, S., T. Pauly, N. L. Bindoff, S. Wright, D. Thiele, G. W. Hosie, P. G. Strutton, and E. Woehler (2000), Ocean circulation off east Antarctica affects ecosystem structure and sea-ice extent, *Nature*, 406(6795), 504-507, doi: 10.1038/35020053.

Norisuye, K., M. Ezoe, S. Nakatsuka, S. Umetani, and Y. Sohrin (2007), Distribution of bioactive trace metals (Fe, Co, Ni, Cu, Zn and Cd) in the Sulu Sea and its adjacent seas, *Deep Sea Research Part II: Topical Studies in Oceanography*, 54(1–2), 14-37, doi: 10.1016/j.dsr2.2006.04.019.

O'Dowd, C. D., M. H. Smith, I. E. Consterdine, and J. A. Lowe (1997), Marine aerosol, sea-salt, and the marine sulphur cycle: a short review, *Atmos. Environ.*, 31(1), 73-80, doi:10.1016/S1352-2310(96)00106-9.

O'Dowd, C. D., and G. de Leeuw (2007), Marine aerosol production: a review of the current knowledge, *Philos. T. Roy. Soc. A.*, 365(1856), 1753-1774, doi:10.1098/rsta.2007.2043.

Ovadnevaite, J., C. O'Dowd, M. Dall'Osto, D. Ceburnis, D. R. Worsnop, and H. Berresheim (2011), Detecting high contributions of primary organic matter to marine aerosol: A case study, *Geophysical Research Letters*, 38(2), L02807.

Pacyna, J. M., and E. G. Pacyna (2001), An assessment of global and regional emissions of trace metals to the atmosphere from anthropogenic sources worldwide, *Environmental Reviews*, 9(4), 269-298, doi:10.1139/er-9-4-269.

Pakkanen, T. A. (1996), Study of formation of coarse particle nitrate aerosol, *Atmos. Environ.*, 30(14), 2475-2482, doi:10.1016/1352-2310(95)00492-0.

Peter, W. (1988), The growth of atmospheric aerosol particles with relative humidity, *Physica Scripta, 37*(2), 223. doi:10.1088/0031-8949/37/2/008.

Pierce, J. R., and P. J. Adams (2006), Global evaluation of CCN formation by direct emission of sea salt and growth of ultrafine sea salt, *Journal of Geophysical Research: Atmospheres*, *111*(D6), D06203, doi:10.1029/2005JD006186.

Price, N. M., and F. M. M. Morel (1990), Cadmium and cobalt substitution for zinc in a marine diatom, *Nature*, *344*(6267), 658-660.

Price, N. M., and F. M. M. Morel (1991), Colimitation of Phytoplankton Growth by Nickel and Nitrogen, *Limnology and Oceanography*, *36*(6), 1071-1077.

Prospero, J. M., D. L. Savoie, E. S. Saltzman, and R. Larsen (1991), Impact of Oceanic Sources of Biogenic Sulfur on Sulfate Aerosol Concentrations at Mawson, Antarctica, *Nature*, *350*(6315), 221-223, doi:10.1038/350221a0.

Prospero, J. M. (1999), Long-range transport of mineral dust in the global atmosphere: Impact of African dust on the environment of the southeastern United States, *Proceedings of the National Academy of Sciences*, *96*(7), 3396.

Quinn, P. K., D. S. Covert, T. S. Bates, V. N. Kapustin, D.C. Ramsey-Bell, and L. M. Mclnnes (1993), Dimethylsulfide/cloud condensation nuclei/climate system:R elevant size-resolvedm easurementso f the chemical and physical properties of atmospheric aerosol particles, J. Geophy. Res., 98, 10,411-10,427.

Quinn, P. K., V. N. Kapustin, T. S. Bates, and D. S. Covert (1996), Chemical and optical properties of marine boundary layer aerosol particles of the mid-Pacific in relation to sources and meteorological transport, *J. Geophys. Res.,* 101(D3), 6931–6951, doi:10.1029/95JD03444.

Quinn, P., D. Coffman, V. Kapustin, T. Bates, and D. Covert (1998), Aerosol optical properties in the marine boundary layer during the First Aerosol Characterization Experiment (ACE 1) and the underlying chemical and physical aerosol properties, *Journal of Geophysical Research: Atmospheres (1984–2012)*, *103*(D13), 16547-16563.

Quinn, P. K., and T. S. Bates (2011), The case against climate regulation via oceanic phytoplankton sulphur emissions, *Nature*, *480*(7375), 51-56, doi:10.1038/nature10580.

Radhi, M., M. Box, G. Box, R. Mitchell, D. Cohen, E. Stelcer, and M. Keywood (2010), Optical, physical and chemical characteristics of Australian continental aerosols: results from a field experiment, *Atmospheric Chemistry and Physics*, *10*(13), 5925-5942.

Rädlein, N., and K. Heumann (1992), Trace analysis of heavy metals in aerosols over the Atlantic Ocean from Antarctica to Europe, *Int J Environ an Ch*, *48*(2), 127-150.

Rädlein, N., and K. G. Heumann (1995), Size fractionated impactor sampling of aerosol particles over the Atlantic Ocean from Europe to Antarctica as a methodology for source identification of Cd, Pb, Tl, Ni, Cr, and Fe, *Fresenius' journal of analytical chemistry*, *352*(7-8), 748-755.

Rankin, A. M., and E. W. Wolff (2003), A year-long record of size-segregated aerosol composition at Halley, Antarctica, *J. Geophys. Res.,* 108, 4775, doi:10.1029/2003JD003993, D24.

Rankin, A. M., E. W. Wolff, and S. Martin (2002), Frost flowers: Implications for tropospheric chemistry and ice core interpretation, *J. Geophys. Res.,* 107(D23), 4683, doi:10.1029/2002JD002492.

Rastogi, N., and M. M. Sarin (2006), Chemistry of aerosols over a semi-arid region: Evidence for acid neutralization by mineral dust, *Geophys. Res. Lett.,* 33, L23815, doi:10.1029/2006GL027708.

Rea, D. K. (1994), The paleoclimatic record provided by eolian deposition in the deep sea: The geologic history of wind, *Reviews of Geophysics*, *32*(2), 159-196.

Read, K. A., A. C. Lewis, S. Bauguitte, A. M. Rankin, R. A. Salmon, E. W. Wolff, A. Saiz-Lopez, W.J. Bloss, D. E. Heard, J. D. Lee, and J. M. C. Plane (2008), DMS and MSA measurements in the Antarctic Boundary Layer: impact of BrO on MSA production, *Atmos. Chem. Phys.,* 8, 2985-2997, doi:10.5194/acp-8-2985-2008.

Rempillo, O., A. M. Seguin, A.-L. Norman, M. Scarratt, S. Michaud, R. Chang, S. Sjostedt, J. Abbatt, B. Else, T. Papakyriakou, S. Sharma, S. Grasby, and M. Levasseur (2011), Dimethyl sulfide air-sea fluxes and biogenic sulfur as a source of new aerosols in the Arctic fall, *J. Geophys. Res.*, *116*D00S04, doi:10.1029/2011jd016336.

Reid, P. C., A. C. Fischer, E. Lewis-Brown, M. P. Meredith, M. Sparrow, A. J. Andersson, A. Antia, N. R. Bates, U. Bathmann, and G. Beaugrand (2009), Impacts of the oceans on climate change, *Advances in marine biology*, *56*, 1-150.

Revel-Rolland, M., D. De, P., B. Delmonte, P. P. Hesse, J. W. Magee, I. Basile-Doelsch, F. Grousset, and D. Bosch (2006), Eastern Australia: a possible source of dust in East Antarctica interglacial ice, *Earth and Planetary Science Letters*, *249*(1), 1-13.

Riddick, S. N., U. Dragosits, T. D. Blackall, F. Daunt, S. Wanless, and M. A. Sutton (2012), The global distribution of ammonia emissions from seabird colonies, *Atmos. Environ.*, *55*, 319-327, doi:10.1016/j.atmosenv.2012.02.052.

Rinaldi, M., et al. (2011), Evidence of a natural marine source of oxalic acid and a possible link to glyoxal, *Journal of Geophysical Research: Atmospheres*, *116*(D16), D16204, doi:10.1029/2011JD015659.

Saltzman, E. S., I. Dioumaeva, and B. D. Finley (2006), Glacial/interglacial variations in methanesulfonate (MSA) in the Siple Dome ice core, West Antarctica, *Geophys. Res. Lett., 33*, L11811, doi:10.1029/2005GL025629.

Saltzman, E. S., D. L. Savoie, R. G. Zika, and J. M. Prospero (1983), Methane sulfonic acid in the marine atmosphere, *J. Geophys. Res.,* 88(C15), 10897–10902, doi:10.1029/JC088iC15p10897.

Sarmiento, J. L., T. M. C. Hughes, R. J. Stouffer, and S. Manabe (1998), Simulated response of the ocean carbon cycle to anthropogenic climate warming, *Nature, 393*(6682), 245-249, doi:10.1038/30455.

Sarthou, G., E. Bucciarelli, F. Chever, S. P. Hansard, M. González-Dávila, J. M. Santana-Casiano, F. Planchon, and S. Speich (2011), Labile Fe(II) concentrations in the Atlantic sector of the Southern Ocean along a transect from the subtropical domain to the Weddell Sea Gyre, *Biogeosciences*, *8*(9), 2461-2479, doi:10.5194/bg-8-2461-2011.

Savoie, D. L., J. M. Prospero, R. J. Larsen, and E. S. Saltzman (1992), Nitrogen and sulfur species in aerosols at Mawson, Antarctica, and their relationship to natural radionuclides, *J. Atmos. Chem.*, *14*(1-4), 181-204, doi:10.1007/BF00115233.

Savoie, D. L., J. M. Prospero, R. J. Larsen, F. Huang, M. A. Izaguirre, T. Huang, T. H. Snowdon, L. Custals, and C. G. Sanderson (1993), Nitrogen and sulfur species in Antarctic aerosols at Mawson, Palmer Station, and Marsh (King George Island), *J. Atmos. Chem.*, 17(2), 95-122, doi:10.1007/BF00702821.

Saxena, P., L. M. Hildemann, P. H. McMurry, and J. H. Seinfeld (1995), Organics alter hygroscopic behavior of atmospheric particles, *J. Geophys. Res.,* 100(D9), 18755–18770, doi:10.1029/95JD01835.

Saxena, V. K. and F. H. Ruggiero (2013), Aerosol measurements at Palmer Station, Antarctica, In *Contributions to Antarctic Research I* (ed C. R. Bentley), Pp. 50.1-5. American Geophysical Union, Washington, D. C.. doi: 10.1029/AR050p0001.

Schneider, B. (1985), Sources of atmospheric trace metals over the subtropical North Atlantic, *Journal of Geophysical Research: Atmospheres*, *90*(D6), 10744-10746, doi:10.1029/JD090iD06p10744.

Sedwick, P. N., E. R. Sholkovitz, and T. M. Church (2007), Impact of anthropogenic combustion emissions on the fractional solubility of aerosol iron: Evidence from the Sargasso Sea, *Geochemistry, Geophysics, Geosystems*, *8*(10), Q10Q06, doi:10.1029/2007GC001586.

Sedwick, P., A. Bowie, and T. Trull (2008), Dissolved iron in the Australian sector of the Southern Ocean (CLIVAR SR3 section): Meridional and seasonal trends, *Deep Sea*

Research Part I: Oceanographic Research Papers, *55*(8), 911-925.

Seinfeld, J. H. and S. N. Pandis (2006), *Atmospheric Chemistry and Physics: From Air Pollution to Climate Change*, 2nd edition, J. Wiley, New York.

Sholkovitz, E. R., P. N. Sedwick, and T. M. Church (2009), Influence of anthropogenic combustion emissions on the deposition of soluble aerosol iron to the ocean: Empirical estimates for island sites in the North Atlantic, *Geochimica et Cosmochimica Acta*, *73*(14), 3981-4003.

Sholkovitz, E. R., P. N. Sedwick, T. M. Church, A. R. Baker, and C. F. Powell (2012), Fractional solubility of aerosol iron: Synthesis of a global-scale data set, *Geochimica et cosmochimica acta*, *89*, 173-189.

Sievering, H., J. Boatman, J. Galloway, W. Keene, Y. Kim, M. Luria, and J. Ray (1991), Heterogeneous sulfur conversion in sea-salt aerosol particles: the role of aerosol water content and size distribution, *Atmos. Environ. A-Gen.*, *25*(8), 1479-1487, doi:10.1016/0960-1686(91)90007-T.

Simó, R.: The role of marine microbiota in short-term climate regulation (2011), in: *The role of marine biota in the functioning of the biosphere*, edited by: Duarte, C., Fundación BBVA and Rubes Editorial, Bilbao, 107–130 pp.

Smith, W. O.Jr., and J. C. Comiso (2008), Influence of sea ice on primary production in the Southern Ocean: A satellite perspective, *J. Geophys. Res.,* 113, C05S93, doi:10.1029/2007JC004251.

Song, F., and Y. Gao, Size distributions of trace elements associated with ambient particular matter in the affinity of a major highway in the New Jersey-New York metropolitan area (2011), *Atmos. Environ.*, 45, 6714-6723, doi:10.1016/j.atmosenv.2011.08.031.

Sullivan, R. C., and K. A. Prather (2007), Investigations of the diurnal cycle and mixing state of oxalic acid in individual particles in Asian aerosol outflow, *Environmental Science Technology*, *41*(23), 8062-8069.

Tan, S.-C., G.-Y. Shi, and H. Wang (2012), Long-range transport of spring dust storms in Inner Mongolia and impact on the China seas, *Atmospheric Environment*, *46*, 299-308.

Tanaka, T. Y., and M. Chiba (2006), A numerical study of the contributions of dust source regions to the global dust budget, *Global Planet Change*, *52*(1), 88-104.

Tang, I. N., and H. R. Munkelwitz (1984), An investigation of solute nucleation in levitated solution droplets, *Journal of Colloid and Interface Science*, 98(2), 430-438, doi:10.1016/0021-9797(84)90167-X.

Taylor, S. (1964), Abundance of chemical elements in the continental crust: a new table, *Geochimica et Cosmochimica Acta*, *28*(8), 1273-1285.

Teinilä, K., V.-M. Kerminen, and R. Hillamo (2000), A study of size-segregated aerosol chemistry in the Antarctic atmosphere, *J. Geophys. Res.,* 105(D3), 3893–3904, doi:10.1029/1999JD901033.

Trapp, J. M., F. J. Millero, and J. M. Prospero (2010), Trends in the solubility of iron in dust dominated aerosols in the equatorial Atlantic trade winds: Importance of iron speciation and sources, *Geochemistry, Geophysics, Geosystems*, *11*(3), Q03014, doi:10.1029/2009GC002651.

Trevena, A. J., and G. B. Jones (2006), Dimethylsulphide and dimethylsulphoniopropionate in Antarctic sea ice and their release during sea ice melting, *Mar. Chem.*, *98*(2), 210-222, doi: 10.1016/j.marchem.2005.09.005.

Trevena, A., and G. Jones (2012), DMS flux over the Antarctic sea ice zone, *Mar. Chem.*, 134, 47-58, doi:10.1016/j.marchem.2012.03.001.

Turner, J., and J. P. Thomas (1994), Summer season mesoscale cyclones in the bellingshausen weddell region of the antarctic and links with the synoptic scale environment, *Int J Climatol*, *14*(8), 871-894.

Turnipseed, A. A., S. B. Barone, and A. R. Ravishankara (1996), Reaction of OH with Dimethyl Sulfide. 2. Products and Mechanisms, *J. Phys. Chem.*, *100*(35), 14703-14713, doi:10.1021/jp960867c.

Twining, B. S., and S. B. Baines (2013), The trace metal composition of marine phytoplankton, *Annual review of marine science*, *5*, 191-215.

Uematsu, M., H. Hattori, T. Nakamura, Y. Narita, J. Jung, K. Matsumoto, Y. Nakaguchi, and M. D. Kumar (2010), Atmospheric transport and deposition of anthropogenic substances from the Asia to the East China Sea, *Marine Chemistry*, *120*(1), 108-115.

Vallina, S. M., R. Simó, and S. Gassó (2006), What controls CCN seasonality in the Southern Ocean? A statistical analysis based on satellite-derived chlorophyll and CCN and model-estimated OH radical and rainfall, *Global Biogeochem. Cycles*, *20*.

Van Den Broeke, M., Reijmer, C., Van As, D. and Boot, W. (2006), Daily cycle of the surface energy balance in Antarctica and the influence of clouds. *Int. J. Climatol.,* 26: 1587–1605. doi:10.1002/joc.1323.

Virkkula, A., K. Teinilä, R. Hillamo, V. M. Kerminen, S. Saarikoski, M. Aurela, J. Viidanoja, J. Paatero, I. K. Koponen, and M. Kulmala (2006a), Chemical composition

of boundary layer aerosol over the Atlantic Ocean and at an Antarctic site, *Atmos. Chem. Phys., 6*(11), 3407-3421, doi:10.5194/acp-6-3407-2006.

Virkkula, A., K. Teinilä, R. Hillamo, V.-M. Kerminen, S. Saarikoski, M. Aurela, I. K. Koponen, and M. Kulmala (2006b), Chemical size distributions of boundary layer aerosol over the Atlantic Ocean and at an Antarctic site, *J. Geophys. Res.*, 111, D05306, doi:10.1029/2004JD004958.

Wagenbach, D., U. Görlach, K. Moser, and K. O. Münnich (1988), Coastal Antarctic aerosol: the seasonal pattern of its chemical composition and radionuclide content, *Tellus B*, *40*(5), 426-436.

Wagenbach, D. (1996), Coastal Antarctica: Atmospheric chemical composition and atmospheric transport, in *Chemical Exchange Between the Atmosphere and Snow*, edited by E. W. Wolff, and R. C. Bales, *NATO ASI Ser., Ser. 1*, 43, 173–199.

Wagenbach, D., M. Legrand, H. Fischer, F. Pichlmayer, and E. W. Wolff (1998), Atmospheric near-surface nitrate at coastal Antarctic sites, *J. Geophys. Res.,* 103(D9), 11007–11020, doi:10.1029/97JD03364.

Wang, H., K. Kawamura, and K. Yamazaki (2006), Water-Soluble dicarboxylic acids, ketoacids and dicarbonyls in the atmospheric aerosols over the southern ocean and western pacific ocean, *J. Atmos. Chem.*, *53*(1), 43-61, doi:10.1007/s10874-006-1479-4.

Wang, G., M. Xie, S. Hu, S. Gao, E. Tachibana, and K. Kawamura (2010), Dicarboxylic acids, metals and isotopic compositions of C and N in atmospheric aerosols from inland China: implications for dust and coal burning emission and secondary aerosol formation, *Atmospheric Chemistry and Physics*, *10*(13), 6087-6096.

Warneck, P. (2003), In-cloud chemistry opens pathway to the formation of oxalic acid in the marine atmosphere, *Atmospheric Environment*, *37*(17), 2423-2427, doi:10.1016/S1352-2310(03)00136-5.

Weller, R., and D. Wagenbach (2007), Year-round chemical aerosol records in continental Antarctica obtained by automatic samplings, *Tellus B, 59*(4), 755-765, doi: 10.1111/j.1600-0889.2007.00293.x

Weller, R., J. Wöltjen, C. Piel, R. Resenberg, D. Wagenbach, G. KÖNIG LANGLO, and M. Kriews (2008), Seasonal variability of crustal and marine trace elements in the aerosol at Neumayer station, Antarctica, *Tellus B*, *60*(5), 742-752.

Wells, M. L. (2002), Marine colloids and trace metals, *Biogeochemistry of marine dissolved organic matter*, 367-404.

Whitby, K. T. (1978), The physical characteristics of sulfur aerosols, *Atmospheric Environment (1967)*, *12*(1–3), 135-159, doi: 10.1016/0004-6981(78)90196-8.

Whitfield, M. (2001), Interactions between phytoplankton and trace metals in the ocean, *Advances in marine biology*, *41*(1-128), doi: 10.1016/S0065-2881(01)41002-9.

Witt, M., A. R. Baker, and T. D. Jickells (2006), Atmospheric trace metals over the Atlantic and South Indian Oceans: Investigation of metal concentrations and lead isotope ratios in coastal and remote marine aerosols, *Atmospheric Environment*, *40*(28), 5435-5451.

Wolff, E., Nitrate in polar ice (1995), in: *Ice core studies of global biogeochemical cycles*, edited by: Delmas, R., pp. 195-224, Springer-Verlag, New York.

Wolff, E. W., J. S. Hall, R. Mulvaney, E. C. Pasteur, D. Wagenbach, and M. Legrand (1998), Relationship between chemistry of air, fresh snow and firn cores for aerosol species in coastal Antarctica, *J. Geophys. Res*., 103(D9), 11057–11070, doi:10.1029/97JD02613.

Wolff, E. W., H. Fischer, F. Fundel, U. Ruth, B. Twarloh, G. C. Littot, R. Mulvaney, R. Röthlisberger, M. De Angelis, and C. Boutron (2006), Southern Ocean sea-ice extent, productivity and iron flux over the past eight glacial cycles, *Nature, 440*(7083), 491-496, doi:10.1038/nature04614.

Xia, L., and Y. Gao (2010), Chemical composition and size distributions of coastal aerosols observed on the US East Coast, *Mar. Chem.*, *119*(1–4), 77-90, doi:10.1016/j.marchem.2010.01.002.

Xu, G., Y. Gao, Q. Lin, W. Li, and L. Chen (2013), Characteristics of water-soluble inorganic and organic ions in aerosols over the Southern Ocean and coastal East Antarctica during austral summer*, J. Geophys. Res. Atmos., 118*, 13,303–13,318, doi:10.1002/2013JD019496.

Yang, M., B. Huebert, B. Blomquist, S. Howell, L. Shank, C. McNaughton, A. Clarke, L. Hawkins, L. Russell, and D. Covert (2011), Atmospheric sulfur cycling in the southeastern Pacific–longitudinal distribution, vertical profile, and diel variability observed during VOCALS-REx, *Atmospheric Chemistry and Physics*, *11*(10), 5079-5097.

Yang, X., J. A. Pyle, and R. A. Cox (2008), Sea salt aerosol production and bromine release: Role of snow on sea ice, *Geophys. Res. Lett.,* 35, L16815, doi:10.1029/2008GL034536.

Yu, S. (2000), Role of organic acids (formic, acetic, pyruvic and oxalic) in the formation of cloud condensation nuclei (CCN): a review, *Atmos. Res.*, *53*(4), 185-217, doi:10.1016/S0169-8095(00)00037-5.

Yu, J. Z., X.-F. Huang, J. Xu, and M. Hu (2005), When aerosol sulfate goes up, so does oxalate: Implication for the formation mechanisms of oxalate, *Environmental science & technology*, *39*(1), 128-133.

Yuan, W., and J. Zhang (2006), High correlations between Asian dust events and biological productivity in the western North Pacific, *Geophysical research letters*, *33*(7), L07603.

Yum, S. S., J. G. Hudson, and Y. H. Xie (1998), Comparisons of cloud microphysics with cloud condensation nuclei spectra over the summertime Southern Ocean, *Journal of Geophysical Research-Atmospheres*, *103*(D13), 16625-16636.

Zatko, M. C., T. C. Grenfell, B. Alexander, S. J. Doherty, J.L. Thomas, and X. Yang (2013), The influence of snow grain size and impurities on the vertical profiles of actinic flux and associated NO_x emissions on the Antarctic and Greenland ice sheets, *Atmos. Chem. Phys.,* 13, 3547-3567, doi:10.5194/acp-13-3547-2013.

Zeng, J., Zhang, G., Long, S., Liu, K., Cao, L., Bao, L. and Li, Y. (2013), Sea salt deliquescence and crystallization in atmosphere: an *in situ* investigation using x-ray phase contrast imaging. *Surf. Interface Anal.*, 45: 930–936. doi: 10.1002/sia.5184

Zhang, G. S., J. Zhang, and S. M. Liu (2007), Chemical composition of atmospheric wet depositions from the Yellow Sea and East China Sea, *Atmospheric Research*, *85*(1), 84-97, doi:http://dx.doi.org/10.1016/j.atmosres.2006.11.005.

Zhang, H.-H., G.-P. Yang, C.-Y. Liu, and L.-P. Su (2013), Chemical Characteristics of Aerosol Composition over the Yellow Sea and the East China Sea in Autumn*, *Journal of the Atmospheric Sciences*, *70*(6), 1784-1794, doi:10.1175/JAS-D-12-0232.1.

Zhang, L., R. Vet, A. Wiebe, C. Mihele, B. Sukloff, E. Chan, M. D. Moran, and S. Iqbal (2008), Characterization of the size-segregated water-soluble inorganic ions at eight Canadian rural sites, *Atmos. Chem. Phys.,* 8, 7133-7151, doi:10.5194/acp-8-7133-2008.

Zhang, X. Y., S. L. Gong, Z. X. Shen, F. M. Mei, X. X. Xi, L. C. Liu, Z. J. Zhou, D. Wang, Y. Q. Wang, and Y. Cheng (2003), Characterization of soil dust aerosol in China and its transport and distribution during 2001 ACE-Asia: 1. Network observations, *Journal of Geophysical Research: Atmospheres*, *108*(D9), 4261, doi:10.1029/2002JD002632.

Zhao, Y., and Y. Gao (2008a), Mass size distributions of water-soluble inorganic and organic ions in size-segregated aerosols over metropolitan Newark in the US east coast, *Atmos. Environ.*, *42*(18), 4063-4078, doi:10.1016/j.atmosenv.2008.01.032.

Zhao, Y., and Y. Gao (2008b), Acidic species and chloride depletion in coarse aerosol particles in the US east coast, *Sci. Total Environ.*, *407*(1), 541-547, doi:10.1016/j.scitotenv.2008.09.002.

Zhu, R., J. Sun, Y. Liu, Z. Gong and L. Sun (2011), Potential ammonia emissions from penguin guano, ornithogenic soils and seal colony soils in coastal Antarctica: effects of freezing-thawing cycles and selected environmental variables, *Antarct. Sci.*, 23, pp 78-92. doi:10.1017/S0954102010000623.

Zhuang, H., C. K. Chan, M. Fang, and A. S. Wexler (1999), Formation of nitrate and non-sea-salt sulfate on coarse particles, *Atmos. Environ.*, *33*(26), 4223-4233, doi:10.1016/S1352-2310(99)00186-7.

Zoller, W. H., E. S. Gladney, and R. A. Duce (1974), Atmospheric Concentrations and Sources of Trace Metals at the South Pole, *Science, 183*(4121), 198-200, doi:10.1126/science.183.4121.198.

Curriculum Vitae
Guojie Xu

Education:
Ph.D., Environmental Science, Rutgers University, USA, 2015.
M.Sc., Marine Chemistry, Third Institute of Oceanography, China, 2011.
B.Sc., Environmental Science, Shanxi University, China, 2008.

Professional Appointments:
2013-2014: Graduate Teaching Assistant, Department of Earth and Environmental Sciences, Rutgers University.

2011-2012: Graduate Research Assistant, Department of Earth and Environmental Sciences, Rutgers University.

Publications:
Xu, G. and Y. Gao (2015), Characterization of marine aerosol and precipitation through shipboard observations on the transect between 31°N-32°S in the west Pacific, *Atmospheric Pollution Research*, doi:10.5094/APR.2015.018.

Xu, G. and Y. Gao (2014), Atmospheric trace elements in aerosols observed over the Southern Ocean and coastal East Antarctica, *Polar Research,* in press.

Xu, G., Y. Gao, Q. Lin, W. Li, and L. Chen (2013), Characteristics of water-soluble inorganic and organic ions in aerosols over the Southern Ocean and coastal East Antarctica during austral summer, *Journal of Geophysical Research-Atmospheres*, 118, 13,303–13,318, doi:10.1002/2013JD019496.

Gao, Y., **G. Xu**, J. Zhan, J. Zhang, W. Li, Q. Lin, L. Chen, and H. Lin (2013), Spatial and particle size distributions of atmospheric dissolvable iron in aerosols and its input to the Southern Ocean and coastal East Antarctica, *Journal of Geophysical Research-Atmospheres*, 118, 12,634–12,648, doi:10.1002/2013JD020367.

Chen, L., J. Wang, Y. Gao, **G. Xu**, X. Yang, Q. Lin, and Y. Zhang (2012), Latitudinal distributions of atmospheric MSA and MSA/nss-SO_4^{2-} ratios in summer over the high latitude regions of the Southern and Northern Hemispheres, *Journal of Geophysical Research-Atmospheres*, 117, D10306, doi:10.1029/2011JD016559.

Xu, G., L. Chen, Y. Zhang, J. Wang, W. Li, and Q. Lin (2011), Chemical composition of marine aerosols of the 26th Chinese National Antarctic Research Expedition, *Advances in Polar Science*, 22: 165–174, doi: 10.3724/SP.J.1085.2011.00165.

Conference Abstracts:
Xu, G. and Y. Gao. Characterization of atmospheric aerosols over the Southern Ocean and coastal East Antarctica during austral summer. **American Meteorological Society Annual Meeting**, Austin, TX USA, Jan 2013.

Xu, G. and Y. Gao. Particle size distributions of water-soluble species and nutrient elements in aerosols over the Southern Ocean and coastal East Antarctica. **American Geophysics Union Meeting,** San Francisco, CA USA, Dec 2012.